



18 ABSTRACT

19 The mechanisms involved in programmed or damage-induced removal of mitochondria by mitophagy  
20 in response to different stimuli remains elusive. Here, we have screened for regulators of  
21 PRKN-independent mitophagy using an siRNA library targeting 197 proteins containing lipid  
22 interacting domains. We identify Cyclin G-associated kinase (GAK) and Protein Kinase C Delta  
23 (PRKCD) as novel regulators of PRKN-independent mitophagy, with both being dispensable for  
24 PRKN-dependent mitophagy and starvation-induced autophagy. We demonstrate that the kinase  
25 activity of both GAK and PRKCD are required for efficient mitophagy *in vitro*, that PRKCD is present  
26 on mitochondria, and that PRKCD is required for ULK1/ATG13 recruitment to early autophagic  
27 structures. Importantly, we demonstrate *in vivo* relevance for both kinases in the regulation of basal  
28 mitophagy. Knockdown of GAK homologue (*gakh-1*) in *C.elegans* or PRKCD homologues in zebrafish  
29 led to significant inhibition of basal mitophagy, highlighting the evolutionary relevance of these  
30 kinases in mitophagy.

31

## 32 INTRODUCTION

33 The selective degradation of mitochondria by autophagy (mitophagy) is important for cellular  
34 homeostasis and disease prevention. Defective clearance of damaged mitochondria is linked to the  
35 development of neurodegenerative diseases such as Parkinson's disease (PD) and has also been  
36 linked to cancer<sup>1</sup>. Damaged mitochondria have the potential to leak dangerous reactive oxygen  
37 species causing cell damage and ultimately death, so their rapid clearance is favoured. Mitophagy  
38 involves the sequestration of mitochondria into double-membrane structures termed  
39 autophagosomes that transport and deliver material to the lysosome for degradation<sup>2</sup>. Elucidation of  
40 the molecular mechanisms of mitophagy has largely focused upon hereditary forms of PD and the  
41 role of the genetic risk genes *PINK1* and *Parkin* (*PRKN*) in mediating mitophagy in response to  
42 mitochondrial depolarisation<sup>3</sup>. Such studies have shown that selective recognition of damaged  
43 mitochondria involves PINK1-mediated phosphorylation of ubiquitin and PRKN. This further  
44 ubiquitinates outer mitochondrial membrane proteins that are recognised by specific  
45 ubiquitin-binding autophagy receptors that interact with LC3 and GABARAP proteins in the  
46 autophagy membrane to facilitate mitophagosome formation. The relative importance of this  
47 pathway *in vivo* is however not clear, as the vast majority of basal mitophagy occurring *in vivo* seems  
48 largely independent of PINK1/PRKN, as demonstrated in both mice and fly models<sup>4,5</sup>. Consequently,  
49 further characterisation of the mechanisms involved in PRKN-independent basal mitophagy  
50 pathways is needed to understand their role in normal physiology and disease development. One  
51 such pathway is the HIF1 $\alpha$ /hypoxia-dependent pathway that has been particularly well characterised  
52 for the clearance of red blood cell mitochondria that occur via upregulation of the mitophagy  
53 receptor BNIP3<sup>6</sup>. Several small molecules have been identified to stabilise HIF1 $\alpha$  and replicate a  
54 hypoxia-induced mitophagy phenotype without the requirement for hypoxic conditions<sup>7</sup>, including  
55 cobalt chloride, dimethylxaloylglycine (DMOG) and iron chelators, with deferiprone (DFP) found to  
56 be one of the most potent<sup>8,9</sup>.

57 Whilst much progress has been made in our understanding of selective autophagy and the proteins  
58 involved, little is known about the lipids and lipid-binding proteins involved in cargo recognition and  
59 autophagosome biogenesis during selective autophagy. Formation of autophagosomes relies upon a  
60 multitude of trafficking processes to manipulate and deliver lipids to the growing structure and  
61 several proteins containing lipid interaction domains have been found to play important roles in  
62 modulating autophagy<sup>10</sup>. Here we have carried out an imaging-based screen to examine whether  
63 human proteins containing lipid-binding domains have novel roles in HIF1 $\alpha$  dependent mitophagy.  
64 We identify a shortlist of eleven novel and previously unknown candidates that regulate mitophagy.  
65 In particular, we show that the two kinases GAK and PRKCD are specifically required for  
66 HIF1 $\alpha$ -dependent mitophagy without affecting PRKN-dependent mitophagy and that this regulation  
67 is also observed *in vivo* upon basal mitophagy. Therefore, these kinases represent novel targets for  
68 the study and regulation of basal mitophagy.

## 69 RESULTS

### 70 **Induction and verification of mitophagy in U2OS cells**

71 To monitor mitophagy in cultured cells, U2OS cells were stably transfected to express a tandem tag  
72 mitophagy reporter containing EGFP-mCherry fused to the mitochondrial localisation sequence (MLS)  
73 of the mitochondrial matrix protein NIPSNAP1 (hereafter termed inner MLS [IMLS] cells) in a  
74 doxycycline-inducible manner<sup>11</sup>. U2OS cells contain low endogenous PRKN levels that are insufficient  
75 to induce mitophagy in response to mitochondrial membrane depolarisation<sup>12</sup>. However, while a  
76 yellow mitochondrial network is seen under normal conditions, induction of mitophagy with the iron  
77 chelator DFP for 24 h causes movement of mitochondria to lysosomes, where the EGFP signal is  
78 quenched due to the acidic pH, leading to the appearance of red only punctate structures (Fig. 1a,b).  
79 Co-staining for the inner mitochondrial protein TIM23 verified that the EGFP-mCherry tag was  
80 localised to the mitochondrial network (Fig. 1a). To verify that the red only structures represent  
81 autolysosomes/mitolysosomes, the V-ATPase inhibitor Bafilomycin A1 (BafA1) was added for the  
82 final 2 h of DFP treatment to raise lysosomal pH and restore the EGFP signal<sup>13</sup>. As predicted, the  
83 number of red only structures dropped drastically (Fig. 1b). Similarly, siRNA-mediated depletion of  
84 the key autophagy inducer ULK1 before DFP addition significantly reduced the formation of red only  
85 structures (Fig. 1b). The localisation of the IMLS reporter was further validated by correlative light  
86 and electron microscopy (CLEM) following DFP treatment. Indeed, yellow network structures  
87 observed by confocal fluorescence microscopy corresponded to mitochondrial structures by EM,  
88 whereas red only structures demonstrated typical autolysosome morphologies (Fig. 1c).

89 DFP-induced mitophagy could be demonstrated biochemically by measuring the enzymatic activity of  
90 the mitochondrial matrix protein citrate synthase<sup>14</sup>. Treatment with DFP for 24 h reduced citrate  
91 synthase activity by ~40 %, which could be prevented by addition of BafA1 for the final 16 h,  
92 confirming that the reduction was due to lysosomal-mediated degradation (Fig. 1d). Finally, we were  
93 able to demonstrate by proteomic analysis that the addition of DFP for 24 h decreased the

94 abundance of multiple mitochondrial proteins (classified by gene ontology [GO] analysis) compared  
95 to control-treated cells (Fig. 1e). Comparison of different cellular organelles and compartments by  
96 GO annotation highlighted that mitochondrial proteins resident to the inner membrane and matrix  
97 were particularly reduced in response to DFP treatment (Fig. 1f, Supplementary Table 1).  
98 Peroxisomal protein abundance was also slightly reduced, whilst proteins belonging to the ER,  
99 lysosomes or endosomes were generally unaffected (Fig. 1f). In contrast, proteins involved in  
100 processes defined as glycolytic or mitophagy regulation showed increased abundance.

101 Taken together, we show that DFP treatment induces a lysosomal-dependent loss of mitochondrial  
102 proteins in U2OS cells and that mitolysosomes could be quantified by image analysis in U2OS IMLS  
103 cells.

#### 104 **Screening for lipid-binding protein regulators of mitophagy**

105 To uncover the mechanisms involved in selective recognition and turnover of mitochondria in DFP  
106 treated cells we carried out an image-based siRNA screen monitoring the formation of red-only  
107 structures in response to DFP following siRNA mediated knockdown of 197 putative lipid binding  
108 proteins in U2OS IMLS cells. An initial list of proteins containing established lipid interacting protein  
109 domains (FYVE, PX, PH, GRAM, C1, C2, PROPPIN, ENTH) were identified using ExpASY Prosite (see  
110 Methods and Appendix 1). This preliminary target list was cross-examined with several U2OS  
111 proteomic datasets and restricted to proteins validated to be expressed in U2OS cells<sup>15,16</sup>. We  
112 included all FYVE or PX domain containing proteins due to the relevance of phosphatidylinositol  
113 3-phosphate (PtdIns(3)P) binding proteins in autophagy initiation<sup>17</sup>.

114 The primary screen was carried out using a pool containing three different siRNA oligonucleotides  
115 sequences per target. In the absence of DFP treatment, no spontaneous induction of mitophagy was  
116 observed upon gene knockdown (data not shown). In contrast, significant changes were observed  
117 with siRNA treatment in the presence of DFP, which are plotted as fold change relative to  
118 non-targeting (siNT) samples and grouped based upon lipid binding domains (Fig. 2a-e). As previously

119 shown, BafA1 treatment or depletion of ULK1 strongly inhibited DFP-induced formation of red  
120 (mitolysosome) structures (Fig. 1b, Fig. 2a-e red bars). Interestingly, significantly increased levels of  
121 mitophagy were seen following knockdown of HS1BP3 (Fig. 2a), a negative regulator of starvation  
122 induced autophagy that has not previously been examined in mitophagy<sup>18</sup>. It is interesting to note  
123 that relatively few hits from proteins containing a FYVE or PX domain were found compared to C1, C2  
124 or GRAM domain containing proteins (Fig. 2f).

### 125 **GAK and PRKCD identified as DFP mitophagy regulators by siRNA screening**

126 To validate prospective positive and negative regulators that demonstrated significant changes in the  
127 primary screen, we selected 29 candidates for a secondary deconvolution screen where the three  
128 siRNA oligonucleotides used in the primary screen were examined individually in U2OS IMLS cells.  
129 Their effect on DFP-induced mitophagy was analysed and quantified by high-content imaging and the  
130 level of residual target mRNA was quantified by qPCR. The mitophagy phenotype of the individual  
131 siRNA oligos was then correlated to their knock-down efficiencies and compared to the mitophagy  
132 effect of the siRNA pool used in the primary screen (Supplementary Fig. 1a). As the knockdown  
133 efficiencies for some of the targets were disappointing in the secondary screen, we carried out a  
134 tertiary screen for all targets that were found to significantly affect mitophagy in the primary screen,  
135 using individual siRNA oligos at a higher concentration of siRNA (Supplementary Fig. 1b). Based on  
136 the results of the secondary and tertiary screen, we highlighted eleven targets where at least two of  
137 the three oligos had a significant effect on DFP-induced mitophagy (Fig. 3a).

138 To identify candidates with the highest possible relevance for mitophagy, we searched for interacting  
139 proteins for each of these eleven candidate proteins using network analysis of protein interaction  
140 data (see Methods). Interacting proteins were subjected to GO analysis and grouped based upon  
141 compartments of interest, including mitochondria, autophagy and endolysosomal compartments.  
142 The percentage of interacting proteins in each group was compared to the average percentage for all  
143 proteins screened. Of interest, AKAP13 had a high number of interactors linked to mitochondria and

144 autophagy. Additionally, GAK and PRKCD had higher numbers of autophagy and mitochondria linked  
145 proteins respectively than all screened proteins (Fig. 3b and Supplementary Fig. 2a,b). As several  
146 mitophagy receptor proteins involved in HIF1 $\alpha$ -induced mitophagy are regulated by phosphorylation  
147 (including BNIP3 and BNIP3L), whilst the PINK1 kinase is dispensable for PRKN-independent  
148 mitophagy, we decided to further characterise the role of GAK and PRKCD kinases in mitophagy. In  
149 addition, GAK has been linked as a risk factor for PD<sup>19</sup> and PRKCD has been noted to translocate to  
150 mitochondria previously<sup>20</sup>.

151 All three oligonucleotides targeting PRKCD and two of three targeting GAK caused significant  
152 inhibition of DFP-induced mitophagy in the U2OS IMLS cells (Fig. 3a, Supplementary Fig. 3). The level  
153 of citrate synthase activity was significantly decreased in DFP treated control cells, this was not the  
154 case in cells depleted of PRKCD or GAK, further indicating a reduction in mitophagy upon depletion of  
155 these kinases (Fig. 3c). Some loss of citrate synthase was still observed, likely due to incomplete  
156 target knockdown as noted by qPCR in the secondary screen (Supplementary Fig. 1a). To understand  
157 whether GAK or PRKCD localise to mitochondria upon DFP treatment, U2OS cells were treated or not  
158 with DFP and then permeabilised and fractionated by differential centrifugation to enrich for  
159 mitochondria. Successful fractionation was confirmed by enrichment of the mitochondrial proteins  
160 TIM23 and COX-IV in the mitochondrial fraction (Fig. 3d). PRKCD was strongly enriched in  
161 mitochondrial fractions under both control and DFP inducing conditions, while GAK was absent from  
162 the mitochondria fraction (Fig. 3d). Mitochondrial localisation of PRKCD was confirmed by  
163 immunofluorescence staining of endogenous PRKCD in U2OS IMLS cells, showing a striking  
164 co-localisation with the IMLS-EGFP-mCherry reporter both in the presence and absence of DFP  
165 (Fig. 3e). Upon induction of mitophagy by DFP, PRKCD was seen with red only structures, indicating it  
166 follows mitochondria to the lysosome. Indeed, western blotting confirmed the loss of PRKCD in a  
167 DFP-dependent manner that was rescued by BafA1 treatment (Fig. 3f,g). Attempts to identify  
168 endogenous GAK localisation by immunofluorescence were not successful with non-specific staining  
169 observed with all antibodies tested.



170 **The kinase activity of GAK and PRKCD are required for functional mitophagy**

171 As GAK and PRKCD are both serine-threonine protein kinases we next sought to determine whether  
172 their kinase activities are important for DFP-induced mitophagy. We first tested two recently  
173 published kinase inhibitors targeting GAK, IVAP1966 and IVAP1967, with a K<sub>d</sub> of 80nM and 190nM  
174 respectively (Supplementary Fig. 4a)<sup>21</sup>. Concomitant dosing of IMLS cells with DFP and these GAK  
175 inhibitors demonstrated dose-dependent inhibition of mitophagy with IVAP1967, while IVAP1966  
176 had no effect (Supplementary Fig. 4b). Fortunately, we were able to take advantage of a more potent  
177 and specific GAK inhibitor (SGC-GAK-1, termed GAKi here) with a K<sub>d</sub> of 3.1nM and IC<sub>50</sub> of 110nM,  
178 which also has a negative control probe (SGC-GAK-1N, termed GAKc here, GAK IC<sub>50</sub> = >50μM)  
179 (Supplementary Fig. 4a) as well as a second control that accounts for off-target effects of GAKi  
180 (HY-19764, RIPK2 inhibitor)<sup>22</sup>. Using this inhibitor set, we found that DFP-induced mitophagy was  
181 significantly reduced in a dose-dependent manner with GAKi by 40% and 60% at 5 μM and 10 μM,  
182 respectively (Fig. 4a,b). By contrast, neither GAKc nor RIPK2i had an inhibitory effect (Fig. 4a,b),  
183 providing evidence that GAK kinase activity is required for functional DFP mitophagy. The effect of  
184 GAKi on mitophagy was not due to reduced cell growth during DFP treatment (Supplementary Fig.  
185 4c).

186 To investigate a role of the PRKCD kinase activity in mitophagy we utilised the PKC family inhibitors  
187 (PKCi) Enzastaurin (ES) and Sotrastaurin (SS), neither of which is solely specific for PKC Delta due to  
188 isozyme similarity within the PKC family. Both compounds strongly inhibited DFP-induced mitophagy  
189 in a dose-dependent manner (Fig. 4a,b) with Enzastaurin slightly more potent than Sotrastaurin. The  
190 conventional (PRKCA, PRKCB), novel (PRKCD) and atypical (PRKCZ) PKC family members were  
191 included in the primary siRNA screen, with only siPRKCD showing significantly reduced DFP-induced  
192 mitophagy of -57% (Fig. 2c). To further investigate the potential effects of the other PKC isozymes, all  
193 PKC isoforms were depleted in the U2OS IMLS cells, which demonstrated that multiple novel PKC  
194 isoforms decreased DFP-induced mitophagy (Fig. 4c). Novel PKCs do not require calcium, but

195 diacylglycerol (DAG) for regulation of activity, suggesting this may be important for mitophagy. Use  
196 of pan-PKC kinase inhibitors may therefore be beneficial for exploring the role of PKC family  
197 members in DFP-induced mitophagy.

198 To further confirm a role for GAK and PRKCD kinase activities in mitophagy, we determined the level  
199 of citrate synthase activity following treatment with GAKi, GAKc and PKCi. As seen in Figure 4d, GAKi  
200 and PKCi both strongly blocked DFP-induced loss of citrate synthase whilst this was not seen with  
201 DMSO or GAKc control samples. Moreover, addition of GAKi or PKCi both decreased the DFP-induced  
202 loss of inner mitochondrial membrane proteins (MTCO2, COXIV, TIM23) and matrix proteins (PDH,  
203 NIPSNAP1) as examined by western blot analysis, while loss of the outer mitochondrial proteins  
204 FUNDC1 or TOM20 was generally not affected (except that GAKi blocked loss of TOM20) (Fig. 4e).  
205 This is perhaps not surprising as some outer mitochondrial proteins are known to undergo  
206 proteasomal degradation, such as MFN2, upon induction of DFP-induced mitophagy<sup>8</sup>. We further  
207 confirmed the loss of mitochondrial proteins by analysis of whole-cell protein abundance by mass  
208 spectrometry between DMSO and DFP treatments in the presence of GAKi and GAKc. As shown  
209 earlier, DFP treatment caused a loss of mitochondrial proteins (determined by GO Analysis), which  
210 was reduced for cells treated with GAKi, but not for GAKc, indicating that turnover of mitochondria is  
211 hindered when GAK kinase activity is blocked (Fig. 4f).

### 212 **GAK and PRKCD do not regulate the HIF1 $\alpha$ pathway**

213 To understand how depletion or inhibition of GAK or PRKCD prevents DFP-induced mitophagy, we  
214 first examined whether treatment with GAKi or PKCi affected the HIF1 $\alpha$  pathway. HIF1 $\alpha$  stabilization  
215 and expression of the HIF1 $\alpha$  responsive genes BNIP3 and BNIP3L (NIX) are important for driving  
216 mitophagy triggered by iron chelation with DFP<sup>8,23</sup>. As expected, BNIP3/3L mRNA and protein levels  
217 were induced upon DFP treatment with no change in HIF1 $\alpha$  mRNA levels (Fig. 4e and Supplementary  
218 Fig. 5a,b). The expression levels of BNIP3/3L were not significantly affected by treatment with GAKi,  
219 suggesting that GAK does not regulate mitophagy through the HIF1 $\alpha$  response. Furthermore, the

220 PKCi Sotrastaurin had no significant effect on BNIP3/3L expression, although Enzastaurin somewhat  
221 reduced the BNIP3L transcript level (Supplementary Fig. 5a), which may explain the relatively higher  
222 potency of Enzastaurin blocking mitophagy (Fig. 4b). We focused on Sotrastaurin for further  
223 experiments as our data indicated there was an important role for the kinase activity beyond the  
224 decrease in BNIP3L seen with Enzastaurin.

225 BNIP3/3L function as autophagy receptors during HIF1 $\alpha$  induced mitophagy by recruiting ATG8  
226 proteins through specific LC3 interacting regions (LIRs) and phosphorylation promotes their function  
227 in mitophagy<sup>24,25</sup>. To check whether BNIP3/3L are targets for GAK or PRKCD mediated  
228 phosphorylation, cell lysates from U2OS cells treated or not with DFP together with GAKi or PKCi  
229 were analysed using phos-tag acrylamide gels that significantly retard the migration of  
230 phosphorylated proteins<sup>26</sup>. Importantly, neither the protein expression of BNIP3/3L with DFP nor  
231 their migration patterns were changed in GAKi, GAKc and PKCi treated samples (Supplementary Fig.  
232 5b), indicating that neither BNIP3 nor BNIP3L are targets for direct phosphorylation by PRKCD or  
233 GAK.

234 **GAK and PRKCD kinase activities do not regulate PRKN-dependent mitophagy or**  
235 **starvation-induced autophagy**

236 As both GAK and PRKCD regulate DFP-induced mitophagy without affecting the HIF1 $\alpha$  pathway, we  
237 next sought to examine whether these kinases also regulated PRKN-dependent mitophagy. The U2OS  
238 IMLS-EGFP-mCherry cell line was transduced with lentivirus to constitutively overexpress PRKN  
239 (untagged), which permits strong induction of mitophagy in response to mitochondrial depolarisation  
240 such as that induced by the H<sup>+</sup> ionophore CCCP<sup>27,28</sup>. Indeed, treatment with CCCP for 16 h led to  
241 significant induction of mitophagy and near-total loss of mitochondrial network as seen by  
242 accumulation of red only structures (Fig. 5a), reduced citrate synthase activity (Fig. 5b) as well as the  
243 loss of the mitochondrial matrix protein PDH, along with PRKCD that also localises on mitochondria  
244 (Fig. 5c,d). Importantly, we could block PRKN-dependent CCCP-induced mitophagy by co-treatment

245 with the ULK1/2 inhibitor MRT68921 or the lysosomal inhibitor BafA1 (Fig. 5a-d)<sup>13,29</sup>. Co-treatment  
246 with GAKi, GAKc or PKCi had no effect (Fig. 5a-d), suggesting that GAK and PRKCD kinase activities are  
247 dispensable for PRKN-mediated mitophagy under these conditions. We next considered whether  
248 GAKi or PKCi could impair starvation-induced autophagy. Cells were incubated in nutrient starvation  
249 media (EBSS) for 2 h and the autophagic flux examined by immunostaining for endogenous LC3B in  
250 the absence or presence of BafA1, as analysed by fluorescence microscopy (Fig. 5e,f) or  
251 immunoblotting (Fig. 5g). Whilst incubation in EBSS increased LC3 flux relative to the control,  
252 addition of GAKi or GAKc to EBSS treated cells did not significantly inhibit the autophagic flux. PKCi  
253 caused elevated LC3-II levels in the absence of BafA1.

254 Taken together, we show that while GAK and PRKCD kinase activities are required for efficient  
255 DFP-induced mitophagy, but are dispensable for PRKN-dependent mitophagy and starvation-induced  
256 autophagy.

### 257 **PRKCD inhibitors reduce ULK1 initiation complex assembly**

258 To further elucidate how GAK or PRKCD kinase inhibition may block DFP-induced mitophagy, we  
259 examined the recruitment of core autophagy machinery components to mitochondria. U2OS IMLS  
260 cells treated with DMSO or DFP were immunostained for endogenous ATG13, LC3B, ULK1 or WIPI2  
261 and examined by confocal microscopy. In many cases, the early autophagosome structures induced  
262 by DFP treatment were localised at or close to mitochondria, likely representing mitophagosome  
263 start sites (Fig. 6a-d). Using high-content imaging we found that formation of WIPI2, ATG13 or ULK1  
264 puncta were all strongly induced (~5-fold) in response to 24h DFP treatment (Fig. 6e,f,  
265 Supplementary Fig. 6a-d). Treatment with GAKi or GAKc did not affect the number of WIPI2, ATG13  
266 or ULK1 puncta observed following 24 h of DFP treatment (Fig. 6e,f, Supplementary Fig. 6a-d).

267 Moreover, neither GAKi nor GAKc affected phosphorylation of ULK1 at S555 (AMPK site) or S757  
268 (mTOR site) (Supplementary Fig. 6e), suggesting that GAK regulates DFP-induced mitophagy through

269 a different mechanism. Interestingly, control cells treated with GAKi only (no DFP) displayed an  
270 increased number of WIPI2 puncta (Supplementary Fig. 6a,d), but the reason for this is not apparent.  
271 Most importantly, co-treatment of cells with DFP and PKCi caused a dose-responsive decrease in the  
272 number and size of ULK1 and ATG13 puncta (and to a lesser extent WIPI2 though this was not  
273 significant) (Fig. 6e,f and Supplementary Fig. 7d). However, neither the phosphorylation of ATG13 at  
274 S318 (a known ULK1 site)<sup>30</sup> or the phosphorylation of AMPK at T172 (an activation site)<sup>31</sup> that occur  
275 in response to DFP treatment were impaired or altered by co-treatment with GAKi, GAKc or PKCi (Fig.  
276 4e). We thus conclude that the kinase activity of PRKCD is required for successful assembly and  
277 formation of the ULK1 complex during DFP-induced mitophagy, but that it does not affect ULK1  
278 activity directly. As PRKCD is localised to mitochondria, a failure to generate an initiation structure  
279 upon its depletion or inactivation likely explains the reduced level of mitophagy observed.

#### 280 **GAK inhibition alters mitochondrial morphology**

281 As GAK inhibition did not affect HIF1 $\alpha$  signalling, ULK1 activity or ATG13/ULK1 recruitment, we next  
282 examined mitochondrial morphology. IMLS cells co-treated with DFP and siGAK (Supplementary  
283 Fig. 3) or GAKi (Fig. 4a) demonstrated abnormal mitochondrial network structures compared to  
284 control cells. Using live-cell microscopy, we observed a collapsed mitochondrial network with  
285 clumped mitochondrial regions and reduced red structures in IMLS cells co-treated with DFP and  
286 GAKi that were not seen with GAKc (Supplementary Movie 1). Confocal microscopy confirmed this  
287 and by contrast, cells co-treated with DFP and PKCi retained an elongated network (Fig. 7a). Cells  
288 treated with a combination of Oligomycin and Antimycin A (O+A) or CCCP, known to depolarize  
289 mitochondria, caused fragmented network phenotypes (Fig. 7a). In the latter case, little mitophagy is  
290 seen in response to mitochondrial depolarisation as this was carried out in IMLS cells without PRKN  
291 overexpression. To quantify mitochondria morphology, images of U2OS cells depleted of the fission  
292 enzyme DRP1 or the fusion enzyme OPA1 (causing tubulated or fragmented mitochondrial  
293 phenotypes respectively, Supplementary Fig. 7), were applied to train a cell classifier in CellProfiler

294 Analyst. Applying this, we confirmed that GAKi treated cells exhibit a hyper fused mitochondria  
295 phenotype while no morphological differences were detected in GAKc or PKCi treated samples (Fig.  
296 7b). The observed GAKi phenotype was not caused by a general defect in the fission/fusion rate of  
297 the mitochondrial network, as mitochondrial fragmentation could still be induced by co-treatment of  
298 GAKi with DFP and CCCP (Fig. 7c). Importantly, GAKi still prevented the formation of red only  
299 structures under such conditions, indicating that GAK is important for proper uptake of fragmented  
300 mitochondria into autophagosomes.

301 We next examined GAKi treated U2OS IMLS cells by CLEM. Interestingly, this showed condensed  
302 parallel layers of mitochondria that were not fused, but rather stacked closely with one another (Fig.  
303 7d). Additionally, large autolysosome structures were observed, which may indicate lysosomal  
304 defects following GAKi treatment (Fig. 7d). Indeed, an increase in the number of lysosomal  
305 structures was detected in cells stained for the late endosome/lysosome marker LAMP1 following  
306 co-treatment with DFP and GAKi (Fig. 7e,f). As GAKi did not inhibit PRKN-dependent mitophagy  
307 (Fig. 5a-d) or starvation-induced autophagy (Fig. 5e-g) we reasoned that the large autolysosomes  
308 seen in GAKi treated cells retain their acidity and degradative capacity. In line with this, lysotracker  
309 positive structures were detected in cells treated with GAKi or GAKc in the presence or absence of  
310 DFP (Fig. 7g). Thus, we believe that the mitophagy defect induced by GAKi is due to inefficient cargo  
311 loading or delivery to lysosomes rather than a lysosomal defect.

### 312 **Mass Spectrometry with GAKi**

313 To try to identify relevant substrates for GAK kinase-dependent regulation of DFP-induced  
314 mitophagy, we carried out phospho-proteomic analysis of cells treated with DFP in combination with  
315 GAKi or GAKc. GAK is currently defined as an understudied kinase<sup>32</sup> and GAKi was developed by the  
316 SGC consortium to reveal novel understandings of GAK cellular function<sup>22</sup>. Analysis of both the  
317 protein abundance and phospho-sites of interest (Fig. 8a) demonstrated that DFP treatment  
318 increased the abundance of several proteins in a GAKi independent manner, including HIF1 $\alpha$ , BNIP3L,

319 Hexokinase I/II, LAMP1/2 and LC3B. In contrast, SQSTM1 abundance decreased in response to DFP  
320 even with GAKi, further showing that lysosomes are functional in this state. Interestingly,  
321 phosphorylation of RAB7A at S72 was observed in response to DFP treatment. The same RAB7A  
322 modification was recently reported to facilitate a key step in PRKN-dependent mitophagy, suggesting  
323 that similarities exist during DFP mitophagy<sup>33</sup>. RAB14 was also phosphorylated (at S180) in response  
324 to DFP, a change that may be interesting to examine further.

325 GAKi-dependent changes in phosphorylation were also seen, we observed a very specific loss of  
326 clathrin light chain A (CLTA) phosphorylation at S105. This site lies at the interface between the  
327 clathrin heavy and light chains, supporting a previously described role of GAK in clathrin-cage  
328 uncoating. Increased levels of PGK1 S203, PGM1 S117 and PGM2 S165 (established phosphorylation  
329 sites to induce glycolysis) were detected upon GAKi treatment without DFP, suggesting that glycolysis  
330 may be higher at the basal state. We also see higher DRP1 S616 levels with GAKi and DFP, a  
331 modification normally associated with increased fission activity that can be mediated by CDK1<sup>34</sup>.  
332 Moreover, SQSTM1 phosphorylation at S272 is increased with GAKi, also previously noted to be  
333 mediated by CDK1<sup>35</sup>, suggesting that GAKi treatment increases CDK1 activity and may indicate  
334 increased cell numbers in mitosis<sup>36</sup>.

### 335 **GAK and PRKCD modulate mitophagy *in vivo***

336 Knockout of GAK orthologues have been shown to cause embryonic lethality in mice, *C.elegans*  
337 (*dnj-25*) and *D.melanogaster* (*dAux*), which is postulated to occur due to defective  
338 clathrin-dependent endocytosis, as uncoating of clathrin-coated vesicles is mediated by the J-domain  
339 of GAK<sup>37-39</sup>. Indeed, expression of the J-domain alone is able to rescue survival in both mice and  
340 drosophila GAK knockout models<sup>39,40</sup>. *C.elegans* contains two orthologues of GAK, comprising the  
341 kinase domain (*gakh-1*, F46G11.3, 40% overall homology) or the J-domain (*dnj-25*, W07A8.3, 49%  
342 overall homology) (Fig. 8b), where targeting of the latter by RNAi causes lethality during larval  
343 development<sup>38</sup>. As our data indicate a requirement of GAK kinase activity for efficient mitophagy in

344 mammalian cells, we examined the effect of targeting *gakh-1* upon basal mitophagy in a *C.elegans*  
345 reporter line expressing mtRosella GFP-DsRed in body wall muscle cells, following the concept of the  
346 IMLS reporter cell lines. *C.elegans* fed *gakh-1* RNAi demonstrated a significant decrease in the ratio of  
347 GFP to DsRed and more mitophagy events (DSRed only structures, Fig. 8c) compared to the RNAi  
348 control, confirming that GAK kinase activity is important for basal mitophagy *in vivo*.

349 We next sought to examine the role of PRKCD in mitophagy *in vivo* and targeted *Prkcd* in our recently  
350 established transgenic mitophagy reporter zebrafish line, expressing zebrafish *Cox8* fused to  
351 EGFP-mCherry (Abudu et al., 2019). Zebrafish contain paralogues (*prkcda* and *prkcdb*) that are ~80%  
352 similar to one another and ~76% homologous to human PRKCD, with all major domains being highly  
353 conserved (Fig. 9a). We examined the spatio-temporal expression pattern of *prkcda* and *prkcdb*  
354 during zebrafish development up until 5 days post-fertilisation (dpf). Whilst a high level of maternal  
355 *prkcda* mRNA was observed at 2 hours post fertilisation (hpf), possibly indicating a role in early  
356 embryonic signalling events, both genes were expressed at similar levels throughout development  
357 (Fig. 9b). The spatial distribution of *prkcda* and *prkcdb* were analysed by whole-mount *in situ*  
358 hybridisation (WM-ISH) at 5 dpf compared to a sense probe negative control and showed strong  
359 staining in the corpus cerebelli region of the hindbrain for both genes (Fig. 9c, Supplementary Fig.  
360 8a), this is in agreement with ISH data deposited in the ZFIN database (<http://zfin.org>). *prkcda*  
361 expression was also detected in the eyes and the olfactory bulbs (Fig. 9c) whereas *prkcdb* was found  
362 in patches of the retina, optical tectum and the spinal cord (Fig. 9c). We also analysed the spatio-  
363 temporal pattern of *gak* expression across zebrafish development and observed that even though it  
364 is expressed consistently throughout development (Supplementary Fig. 8b), its spatial expression  
365 pattern varies across development with staining of the caudal hindbrain and retina at 2 dpf, the  
366 optical tectum, neurocranium, retina and kidney at 3dpf, the kidney and neurocranium at 4dpf and  
367 the liver, olfactory bulb, optical tectum and retina at 5dpf of the wild type zebrafish larvae, with no  
368 staining of the control probe (Supplementary Fig. 8c).



369 To investigate a possible role for Prkcd in the mitophagy reporter line, we employed CRISPR/Cas9-  
370 mediated genome editing in zebrafish embryos using guide sequences targeting *prkcda* and *prkcdb*  
371 individually or together (Fig. 9d and Supplementary Fig. 8d), with the latter referred to as *prkcd\_ab*  
372 double knock-out (DKO). We verified loss of Prkcd protein levels in DKO embryos by western blot  
373 (Fig. 9d) and therefore used these embryos for *in vivo* mitophagy analysis.

374 To induce mitophagy, zebrafish larvae at 2 dpf were incubated with varying concentrations of DFP  
375 and DMOG for 24 hours. DFP failed to induce mitophagy at all concentrations, however, DMOG  
376 induced mitophagy as shown by reduced levels of Tim23 (Supplementary Fig. 8e,f), in line with a  
377 recent report<sup>41</sup>. We used 100  $\mu$ M DMOG for further experiments, as significant lethality and  
378 morphological defects were present at higher (250  $\mu$ M) concentrations (Supplementary Fig. 8g). As  
379 *prkcd\_a/b* express highly in the hindbrain (Fig. 9c), we examined mitophagy in this region of DKO  
380 larvae compared to control larvae, both at basal (DMSO) and DMOG-treated conditions. Sections of  
381 fixed larva were imaged by confocal microscopy and the number of red puncta in the hindbrain  
382 region quantified. The number of red only puncta was significantly reduced in the hindbrain of DKO  
383 larvae with both basal and DMOG-induced conditions (Fig. 9e,f), showing an important role of  
384 Prkcd\_a/b in regulating mitophagy. Interestingly, we noticed the lack of a properly formed eye-lens  
385 in one of the two eyes of the *prkcd\_ab* DKO, with considerably reduced mitophagy levels when  
386 compared to the control (Supplementary Fig. 8h). We also observed an inconsistent and varied  
387 movement pattern of the DKO larvae, and therefore quantified their locomotor activity. Tracking and  
388 quantification of locomotion was performed in alternating light and dark conditions with a reduced  
389 swimming trend in the dark phase for both Prkcd single KO and DKO larvae compared the WT control  
390 (Fig. 9g). It is likely that this may be related to the observed lens defect or a hindbrain clustered  
391 motor-neuron dependent phenotype.

392 In conclusion, we show that the activity of both GAK and PRKCD is important for regulation of basal  
393 mitophagy *in vivo*, highlighting the evolutionary relevance of these kinases in mitophagy.

## 394 DISCUSSION

395 In this manuscript, we have tested a panel of putative lipid-binding proteins for their ability to  
396 regulate DFP-induced mitophagy. We have identified eleven candidate proteins that demonstrate  
397 significant modulation of DFP-induced mitophagy and explored two of these, GAK and PRKCD, in  
398 further detail. In both cases, we show that functional kinase activity is required for their positive  
399 regulation of DFP-induced mitophagy and we have identified putative mechanisms for how each  
400 function in mitophagy regulation. Importantly, neither GAK nor PRKCD are required for  
401 PRKN-dependent mitophagy or starvation-induced autophagy, offering novel targets for the specific  
402 modulation of PRKN-independent mitophagy. Critically, we find that both of these targets identified  
403 *in vitro* are also relevant targets *in vivo* for the regulation of basal mitophagy in *C.elegans* and *D.rario*,  
404 demonstrating their conserved function in mitophagy.

405 The linkage of GAK to mitophagy is of particular relevance to neurodegenerative disease as SNPs in  
406 GAK have previously been identified as a risk factor for familial PD<sup>19</sup> and expression changes in GAK  
407 are observed in the substantia nigra of PD patients<sup>42</sup>. Knockout of the drosophila homologue of GAK  
408 (Auxilin) also demonstrates Parkinsonian like mobility defects and loss of dopaminergic neurons<sup>43</sup>.  
409 Further work has shown that the commonly mutated PD gene, LRRK2, can phosphorylate Auxilin<sup>44</sup>.  
410 Studies of GAK have to date, however, been hindered by the limited availability of chemical tools  
411 alongside the inherent difficulty of modulating embryonic lethal genes to dissect their function.  
412 *C.elegans* presents a unique opportunity for the *in vivo* study of GAK kinase function due to the  
413 presence of two orthologues of human GAK, with the homologous kinase domain within a separate  
414 protein (gakh-1) than that of the developmentally essential J-domain (dnj-25)<sup>38</sup>. By knockdown of  
415 gakh-1, we were able to see >50% reduction in basal mitophagy in muscle-cell wall highlighting the  
416 importance of GAK for mitophagy. Further investigation is required to mechanistically ascertain how  
417 this functional effect is mediated, as Hif1 $\alpha$  induction and subsequent recruitment of ULK1/ATG13 to  
418 mitophagosomes in response to DFP stimulation appears normal in cells with GAK kinase activity

419 inhibited. However, we observed a significant disruption of mitochondrial network morphology  
420 which may modulate the ability of mitochondria to be loaded correctly into mitophagosomes.  
421 Artificially inducing mitochondrial fragmentation with CCCP, however, was not sufficient to rescue  
422 mitochondrial degradation. Moreover, enlarged lysosomes were observed, though these still possess  
423 degradative potential to mediate starvation-induced or PRKN-dependent mitophagy. Mass  
424 spectrometry analysis indicates that several glycolytic enzymes are activated in response to GAKi  
425 treatment, which may indicate that more fundamental metabolic changes are occurring that alter the  
426 cellular degradation of mitochondria.

427 PRKCD is a member of the large PKC kinase family and belongs to the subgroup of novel PKCs (nPKCs)  
428 including PRKCE, PRKCH and PRKCQ that are all activated with DAG independent of  $Ca^{2+}$ . Whilst we  
429 have primarily focused upon PRKCD due to its prominent mitochondrial localisation, it is interesting  
430 to note that all nPKCs reduced DFP-induced mitophagy to varying extents, suggesting DAG and PKCs  
431 play a prominent role in the regulation of mitophagy. Usage of a pan-PKC inhibitor consistently gave  
432 a stronger and more robust inhibition of DFP-induced mitophagy, indicating that several isoforms  
433 could play a role or serve redundant functions with one another. Treatment with the PKC inhibitor  
434 sotrastaurin led to a significant inhibition in the recruitment of early autophagy markers, thereby  
435 reducing mitophagosome formation.

436 Formation of mitochondrial DAG has previously been observed during oxidative stress induced by  
437  $H_2O_2$ , which resulted in the recruitment of Protein Kinase D1 (PKD1) to mitochondria<sup>45</sup>. Recent data  
438 in mice have also implicated PKD1 in the regulation of mitochondrial depolarisation and is itself  
439 regulated by PRKCD in the activation loop at S738/S742, it is tempting to speculate that PKD1 might  
440 also be involved in DFP-induced mitophagy<sup>46</sup>. Another intriguing detail is that PKD1 can bind to  
441 AKAP13, another identified regulator of mitophagy in our screen<sup>47</sup>. The formation of mitochondrial  
442 DAG could therefore be a key step in the regulation of DFP-dependent mitophagy. DAG can be  
443 formed from phosphatidic acid by phosphatidic acid phosphohydrolases, such as the Lipin family of

444 proteins. Interestingly, Lipin-1 deficiency is associated with accumulation of mitochondria combined  
445 with morphological abnormalities<sup>48</sup>. Additionally, Lipin-1 depletion was found to reduce the level of  
446 PKD1 phosphorylation with a subsequent decrease in VPS34 mediated PtdIns(3)P formation<sup>48</sup>.

447 Further examination of PKD1 regulation may therefore be important for studying the role of PKCs in  
448 DFP-induced mitophagy.

449 Interestingly, neither GAK nor PRKCD inhibition was able to modulate PRKN-mediated mitophagy.

450 This adds further evidence that the machinery required for PRKN-dependent and independent

451 mitophagy pathways are fundamentally different. Tantalisingly, both *c.elegans* and *d.rario* models

452 indicate that basal mitophagy (along with DMOG-stimulated in zebrafish experiments) can be

453 regulated by these kinases as opposed to stress-induced mitophagy, such as that regulated by PRKN.

454 By looking at the hindbrain region of zebrafish, showing the highest expression of Prkcd, we observed

455 a significant reduction in the level of mitophagy upon depletion of prkcda and prkcdb and

456 impairment of locomotory responses. This may be due to deterioration of hindbrain locomotory

457 neurons as a consequence of impaired mitophagy or may be associated with an anxiety-like response

458 (thought to be triggered in zebrafish due to light changes) noted previously in mice to be impaired

459 with PRKCD depletion<sup>49</sup>.

460 To conclude, this initial screen of lipid-binding proteins in DFP-induced mitophagy identified two

461 lipid-binding kinases that have been validated by functional characterisation and confirmation in

462 higher organisms. This highlights the importance of protein-lipid interactions and provides a strong

463 initial basis for further investigation into the molecular mechanisms of mitophagy.

464

## 465 Materials and Methods

### 466 **Materials**

467 LysoTracker Red DND-99 (L7528) was from ThermoFisher Scientific. Antimycin A (A8674), DFP  
468 (379409), DMOG (D3695), SGC-GAK-1 (GAKi, SML2202), SGC-GAK-1N (GAKc, SML2203) and Q-VD-  
469 OPh (SML0063) were from Sigma Aldrich. Bafilomycin A1 (BML-CM110), CCCP (BML-CM124) were  
470 from Enzo Life Sciences. Enzastaurin (S1055), Oligomycin A (S1478), and Sotrastaurin (S2791) were  
471 from Selleckchem. MRT68921 (1190379-70-4) and VPS34-IN1 (1383716-33-3) were from Cayman  
472 Chemical. IVAP1966 (12g) and IVAP1966 (12i) were gratefully received from the lab of Prof. Piet  
473 Herdewijn <sup>21</sup>. HY-19764 was gratefully received from the structural genomics consortium <sup>22</sup>. Bradford  
474 reagent dye (#5000006) was from Bio-Rad. 1,4-dithiothreitol (DTT, #441496P) was from VWR.  
475 Complete EDTA-free protease inhibitors (#05056489001) and phosphatase inhibitors  
476 (#04906837001) were from Roche.

### 477 **Cell Lines, Maintenance and Induction of Mitophagy**

478 U2OS FlpIN TRex cells with stable dox-inducible expression of MLS-EGFP-mCherry (referred to as  
479 IMLS cells) <sup>11</sup> were grown and maintained in a complete medium of Dulbecco's Modified Eagle  
480 Medium (DMEM – Lonza 12-741F) supplemented with 10% v/v foetal bovine serum (FBS – Sigma  
481 Aldrich #F7524) and 100 U/ml Penicillin + 100 µg/ml Streptomycin (ThermoFisher Scientific  
482 #15140122) in a humidified incubator at 37°C with 5% CO<sub>2</sub>. U2OS IMLS cells with stable expression of  
483 PRKN were generated by cloning of PRKN into a pLenti-III-PGK viral expression vector that was  
484 co-transfected into 293FT cells with psPAX2 and pCMV-VSVG to generate lentiviral particles, which  
485 were transduced into U2OS IMLS cells and positive cells selected with puromycin (Sigma #P7255).  
486 Mitophagy was typically induced utilising 1 mM DFP by addition to cell culture media for 24 h. In the  
487 case of PRKN overexpression, CCCP was used at 20 µM for 16 h or a combination of Oligomycin and  
488 Antimycin A (10µM and 1µM respectively) for 16 h. In the case of PRKN-dependent mitophagy

489 experiments, the pan-caspase inhibitor Q-VD-OPh<sup>50</sup> was included to reduce cell death and improve  
490 imaging quality, in accordance with previous papers studying PRKN-dependent mitophagy<sup>51</sup>.

#### 491 **Imaging and Image Analysis**

492 The initial siRNA screen, secondary siRNA screen and other experiments where indicated were  
493 carried out utilising an AxioObserver widefield microscope (Zen Blue 2.3, Zeiss) with a 20x objective  
494 (NA 0.5). Relevant channels were imaged using a solid-state light source (Colibri 7) and multi-  
495 bandpass filter (BP425/30, 524/50, 688/145) or individual filters. The tertiary siRNA screen was  
496 carried out utilising an ImageXpress Micro Confocal (Molecular Devices) using a 20x objective (NA  
497 0.45). Confocal images were taken with a LSM710 microscope or LSM800 (Zebrafish experiments)  
498 microscope (Zen Black 2012 SP5 FP3, Zeiss) utilising a 63x oil objective (NA 1.4) combined with a laser  
499 diode (405nm), Ar-Laser Multiline (458/488/514nm), DPSS (561nm) and HeNe-laser (633nm) for  
500 relevant fluorophore acquisition.

501 Identification of relevant structures by image analysis was determined using CellProfiler software  
502 (v2.8.0, The Broad Institute)<sup>52</sup>. In the case of IMLS cell analysis for mitophagy, red only structures  
503 were identified by dividing the red signal by green signal per pixel following background noise  
504 reduction and weighting of the red signal to match that of the green signal in non-mitophagy  
505 inducing controls. By this method a value of ~1 indicates “yellow” networked mitochondria and  
506 values <1 represent mitochondria that have a stronger red signal than green signal. Values of <0.5  
507 were taken to represent true red structures, regions that are therefore twice as bright for red than  
508 green.

#### 509 **Zebrafish Maintenance and *in situ* hybridisation (ISH)**

510 Wild-type zebrafish (AB strain) and transgenic tandem-tagged mitofish (TT-mitofish)<sup>11</sup> were housed at  
511 the zebrafish facility at the Centre for Molecular Medicine Norway (AVD.172) using standard practices.  
512 Embryos were incubated in egg water (0.06 g/L salt (Red Sea)) or E3 medium (5 mM NaCl, 0.17 mM  
513 KCl, 0.33 mM CaCl<sub>2</sub>, 0.33 mM MgSO<sub>4</sub>, equilibrated to pH 7.0). Embryos were held at 28 °C in an

514 incubator following collection. Experimental procedures followed the recommendations of the  
515 Norwegian Regulation on Animal Experimentation (“Forskrift om forsøk med dyr” from 15.jan.1996).  
516 All experiments conducted on wild-type zebrafish and transgenic tandem-tagged mitofish larvae were  
517 done at 5 dpf or earlier.

518 Whole-mount ISH for *prkcda* and *prkcdb* were performed as previously described using digoxigenin-  
519 labelled riboprobes<sup>53</sup>. Primer sequences for sense and antisense probes are described in  
520 Oligonucleotide Primers/Probes

521 Appendix 2.

## 522 **Screening Library**

523 Human targets for the siRNA library were identified by using the ExpASY PROSITE sequence motif  
524 database identifier for human proteins containing true-positive identified lipid binding domains.  
525 These included C1 domains (ID: PS50081), C2 domains (ID: PS50004), ENTH (ID: PS50942), PH Domain  
526 (ID: PS50003), PX Domain (ID: PS50195), FYVE domain (PS50178), GRAM or PROPPIN (SVP1 family)  
527 domains (No ID). This list was cross-checked against several previously published U2OS cell line  
528 proteomes (determined by mass spectrometry) and proteins not observed to be expressed in U2OS  
529 cells were removed<sup>15,16</sup>. See Appendix 1 for a full list of siRNA targets.

## 530 **siRNA knockdown**

531 The primary screen was carried out using a pooled siRNA approach with three Silencer Select siRNA  
532 oligonucleotides targeting each gene at 2.5nM final concentration each (7.5nM final). For  
533 transfection, 125µl of OptiMEM (Thermofisher Scientific #31985070) containing 100 ng/ml  
534 Doxycycline (Clontech #631311) and 0.1 µl RNAiMAX per pmol siRNA (Thermofisher Scientific  
535 #13778150) was added to each well of an Ibidi 96-well µ-plate (Ibidi #89626). After 5 mins at room  
536 temperature (RT), 25 µl of 75 nM siRNA (pooled) diluted in OptiMEM was added per well and  
537 incubated a further 15 mins at RT. U2OS IMLS cells were trypsinised and resuspended in complete  
538 media before centrifugation at 300 x g for 5 mins at RT. Media was removed and cells resuspended in

539 OptiMEM to  $2 \times 10^5$  cells/ml. 100  $\mu$ l of cells were added per well and samples were incubated for 16 h  
540 at 37°C. The media was then removed and changed to complete media for a further 24 h before the  
541 media again was changed to complete media  $\pm$  1mM DFP and incubated for 24h to induce  
542 mitophagy. Control wells with BafA1 treatment were dosed 2h prior to fixation. At the end of the  
543 experiment, samples were washed once in PBS and then fixed in 3.7% PFA, 200 mM HEPES pH 7 for  
544 15mins /37°C. PFA was then quenched by washing twice and incubating a further 15mins in DMEM +  
545 10mM HEPES pH 7. Wells were then washed twice with PBS and then incubated in PBS + 2  $\mu$ g/ml  
546 Hoechst to stain nuclei for a minimum of 1h prior to imaging. Images were obtained on a Zeiss  
547 AxioObserver widefield microscope with a 20x objective acquiring a minimum of 35 fields of view per  
548 treatment. Analysis of red only punctate structures was carried out utilizing CellProfiler from a  
549 minimum of 1000 cells per condition per replicate.

#### 550 **Identification and plotting of protein-protein interactome (PPI) networks**

551 PPI represents the physical interaction among a set of proteins. PPI was obtained from Biological  
552 General Repository for interaction Datasets (BioGRID) version BIOGRID-ORGANISM-3.5.185.mitab<sup>54</sup>  
553 (compiled April 25<sup>th</sup> 2020) containing non-redundant and curated interactions. The networks were  
554 visualized using Cytoscape (v3.8.0)<sup>55</sup>, we considered only the connected component of these seed  
555 networks for statistical and functional analysis. Functional and pathway analysis of connected  
556 components of interaction network was performed by ShinyGO<sup>56</sup>. We only considered GO terms for  
557 cellular component, molecular functions and biological process with significant p-value and  
558 enrichment values. Graphs were plotted using R package ggplots.

#### 559 **RNA Isolation, cDNA synthesis and qPCR**

560 For quantifying knockdown in the secondary deconvolution siRNA screen, RNA was isolated and  
561 cDNA generated from transfected U2OS cells using *Power SYBR Green Cells-to-C<sub>T</sub>* kit (ThermoFisher  
562 Scientific #4402955) as per manufacturer's instructions.



563 For other experiments, RNA was isolated from cells or zebrafish (~50 embryos per sample) using  
564 Trizol reagent (ThermoFisher Scientific #15596026). cDNA was synthesised from RNA using  
565 Superscript III reverse transcriptase (ThermoFisher Scientific #18080085) according to  
566 manufacturer's instructions. Amplification was performed with KAPA SYBR FAST qPCR Kit using a  
567 CFX96 real-time PCR system (Bio-Rad) using primers designed to amplify target genes as indicated in  
568 Oligonucleotide Primers/Probes

569 Appendix 2 following normalisation of transcript levels to TATA-box-binding protein (TBP – cell  
570 samples) or  $\beta$ -actin (zebrafish samples) using the  $2^{-\Delta\Delta Ct}$  method.

### 571 **Western Blotting**

572 For western blotting experiments, cells were treated as indicated in figure legends prior to moving  
573 onto ice and washing twice with cold PBS. Cells were lysed on ice in NP-40 lysis buffer [50mM HEPES  
574 pH 7.4, 150mM NaCl, 1mM EDTA, 10% (v/v) Glycerol, 0.5% (v/v) NP-40 + 1mM DTT, 1x Phosphatase  
575 inhibitors and 1x Protease inhibitors fresh] and incubated 5 mins prior to collecting. For zebrafish  
576 samples, embryos were collected at 3 dpf and lysed in RIPA buffer [50 mM Tris-HCl pH 8, 150 mM  
577 NaCl, 5 mM EDTA, 1 % NP-40, 0.5 % Sodium deoxycholate, 0.1 % SDS, 1x protease inhibitor cocktail],  
578 approximately 20-30 embryos were used per gel lane.

579 Samples were clarified by centrifugation at 21000 x g / 4 °C / 10 mins and supernatant retained.  
580 Protein levels were quantified by Bradford assay (Bio-Rad #5000006) relative to a BSA standard.  
581 Samples were normalised and added to loading sample [1x = 62.5mM Tris pH 6.8, 10% (v/v) Glycerol,  
582 2% (w/v) SDS, 0.005% (w/v) Bromophenol Blue] to achieve 30 $\mu$ g-50 $\mu$ g of protein per lane. Samples  
583 were ran by acrylamide gel and transferred to PVDF (350mA/50mins). Samples were blocked in TBS  
584 Odyssey Blocking Buffer (Li-Cor #927-50000) for 30mins/RT before incubation overnight at 4°C with  
585 primary antibodies (TBS blocking buffer + 0.2% Tween). Membranes were washed 3x10 mins in TBST  
586 before secondary antibody incubation (TBS blocking buffer + 0.2% Tween + 0.01% SDS) for 1h.

587 Membranes were washed 3x 10min with TBST before a final wash in TBS only and membrane  
588 imaging.

### 589 **Antibodies**

590 Primary antibodies targeting ATG13 (#13468, Clone E1Y9V), AMPK P-T172 (#2535),  $\beta$ -Actin (#3700,  
591 Clone 8H10D10), BNIP3 (#44060, Clone D7U1T), BNIP3L (#12396, Clone D4R4B), COXIV (#4850, Clone  
592 3E11), PDH (#2784), PRKCD (#9616, D10E2), PRKCD P-S663 (#9376), LC3B (Western blotting only,  
593 #3868, Clone D11), ULK1 (#8054), ULK1 P-S555 (#5869), ULK1 P-S757 (#6888, Clone D1H4) were from  
594 Cell Signaling Technology. FUNDC1 (#Ab74834), GAK (#Ab115179, Clone 1C2), NIPSNAP1 (#Ab67302),  
595 MTCO2 (#Ab110258, Clone 12C4F12) and WIPI2 (#Ab105459, Clone 2A2) were from Abcam. ATG13  
596 P-S318 (#600-401-C49S) was from Rockland. HIF1 $\alpha$  (MAB1536-SP, Clone 241809) was from R&D  
597 Systems. LAMP1 (sc-20011, Clone H4A3) was from Santa Cruz Biotechnology.  $\alpha$ -Tubulin (T5168, Clone  
598 B-5-1-2) was from Sigma Aldrich.

599 Secondary antibodies for western blotting are indicated in the source data file, these included  
600 anti-rabbit (Starbright Blue, Bio-Rad, 12004161) (DyLight 800, ThermoFisher Scientific, SA5-10044)  
601 (DyLight 680, ThermoFisher Scientific, SA5-10042) or anti-mouse (Starbright Blue, Bio-Rad,12004158)  
602 (DyLight 680, ThermoFisher Scientific, SA5-10170) or anti-tubulin (hFAB Rhodamine, Bio Rad,  
603 12004166). Secondary antibodies for immunofluorescence were anti-rabbit Alexa Fluor-594  
604 (Invitrogen, A11058), Alexa Fluor-647 (ThermoFisher Scientific, A21245) or anti-mouse Alexa Fluor-  
605 647 (ThermoFisher Scientific, A21236).

### 606 **Phos-Tag Gels**

607 Phos-tag acrylamide gels were prepared in line with manufacturer's instructions. Briefly, 8% resolving  
608 poly-acrylamide gels were prepared containing 25 $\mu$ M Phos-tag reagent (Wako Chemicals #AAL-107)  
609 and 50 $\mu$ M MnCl<sub>2</sub><sup>26</sup>. Samples to be ran for analysis were diluted in loading sample containing 10 mM  
610 MnCl<sub>2</sub>. Acrylamide gels were ran at 40 mA until complete and washed 3x10 min/RT in 1x transfer  
611 buffer (48mM Tris, 39mM Glycine, 0.0375% (w/v) SDS) + 10mM EDTA followed by 1x10min in 1x

612 transfer buffer. Samples were then transferred to PVDF at 350mA / 50min and treated as noted earlier  
613 for western blot samples.

#### 614 **PFA Fixation, antibody staining and imaging**

615 Cells to be imaged were seeded onto glass coverslips 16h prior to treatments as indicated in figure  
616 legends. Following treatment, cells were washed once with PBS prior to addition of warmed fixation  
617 buffer (3.7% (w/v) PFA, 200mM HEPES pH 7.4) or for double tag IMLS cells (3.7% (w/v) PFA, 200mM  
618 HEPES pH 7) and incubated 15 mins at 37°C. Coverslips were washed twice and incubated 1x15 mins  
619 with DMEM + 10mM HEPES pH7.4 (IMLS = pH 7). Cells were then washed once with PBS and then  
620 permeabilised by incubation for 5 mins with permeabilisation buffer (0.2% (v/v) NP-40 in PBS). Cells  
621 were washed twice and then incubated 20 mins with IF blocking buffer (PBS + 1% (w/v) BSA) to block  
622 the samples. Coverslips were then incubated 1 h / 37 °C with primary antibodies diluted in IF blocking  
623 buffer before washing 3x10 mins in IF blocking buffer. Coverslips were then incubated 30 mins / RT  
624 with appropriate secondary antibodies. Finally, samples were washed 3x10 mins in IF blocking buffer  
625 prior to mounting on to coverslips with ProLong Diamond Antifade Mountant with DAPI  
626 (ThermoFisher Scientific #P36962). Slides were allowed to cure overnight before imaging with either  
627 a Zeiss AxioObserver widefield microscope (20x) or Zeiss LSM 800 confocal microscope (60x).

#### 628 **Citrate Synthase Assay**

629 To biochemically quantify mitochondrial abundance, we assayed citrate synthase activity from cell  
630 lysates. Briefly, U2OS cells were grown and subject to treatments as described in figure legends, cells  
631 were then washed twice with PBS on ice before lysis [50 mM HEPES pH 7.4, 150 mM NaCl, 1 mM  
632 EDTA, 10 % Glycerol, 0.5 % NP-40, 1 mM DTT, 1x Phosphatase inhibitors, 1x Protease inhibitors]. Cell  
633 lysates were clarified by centrifugation at 21000 x g / 10 min / 4 °C and supernatants retained.  
634 Protein concentration was determined by Bradford assay. To determine citrate synthase activity 1 µl  
635 of protein lysate was added to 197 µl of CS assay buffer [100 mM Tris pH 8, 0.1 % Triton X-100,  
636 0.1 mM Acetyl CoA, 0.2 mM DTNB [5,5'Dithiobis(2-nitrobenzoic acid)]] in a multi well plate. At the

637 assay start point, 2  $\mu$ l of 20 mM Iodoacetamide was added per well and incubated at 32 °C and  
638 reactions monitored at  $\lambda_{\text{Abs}}=420$  nm for 30 min in a FLUOstar OPTIMA (v2.20R2, BMG Labtech) plate  
639 reader and compared to iodoacetamide null controls. The  $\Delta \lambda_{\text{Abs}}$  was plotted and the reaction rate  
640 determined across the linear range before saturation. The reaction rate was then normalised to the  
641 protein concentration and plotted relative to the control.

#### 642 **Correlative Light Electron Microscopy (CLEM)**

643 For CLEM, U2OS IMLS cells were grown on photo-etched coverslips (Electron Microscopy Sciences,  
644 Hatfield, USA). The next day, cells were treated with DFP (1mM)  $\pm$  GAKi (10  $\mu$ M) for 24 h. Cells were  
645 then fixed in 4 % formaldehyde, 0.1 % glutaraldehyde/0.1 M PHEM (60 mM PIPES, 25 mM HEPES, 2  
646 mM  $\text{MgCl}_2$ , 10 mM EGTA, pH 6.9), for 1 h. The cells were mounted with Mowiol containing 2  $\mu$ g/ml  
647 Hoechst 33342 (Sigma-Aldrich). Mounted coverslips were examined with a Zeiss LSM710 confocal  
648 microscope with a Zeiss plan-Apochromat 63x/1.4 Oil DIC III objective. Cells of interest were  
649 identified by fluorescence microscopy and a Z-stack was acquired. The relative positioning of the cells  
650 on the photo-etched coverslips was determined by taking a DIC image. The coverslips were removed  
651 from the object glass, washed with 0.1 M PHEM buffer and fixed in 2 % glutaraldehyde/0.1 M PHEM  
652 for 1h. Cells were post fixed in osmium tetroxide and uranyl acetate, stained with tannic acid,  
653 dehydrated stepwise to 100% ethanol and flat-embedded in Epon. Serial sections ( $\sim$ 100-200nm)  
654 were cut on an Ultracut UCT ultramicrotome (Leica, Germany), collected on formvar coated slot-  
655 grids. Samples were observed in a Thermo Scientific™ Talos™ F200C microscope and images were  
656 recorded with a Ceta 16M camera. For tomograms, single-tilt image series were recorded between -  
657 60° and 60° tilt angle with 2° increment. Single axis tomograms were computed using weighted back  
658 projection and, using the IMOD software package version 4.9<sup>57</sup>.

#### 659 **Mitochondrial Enrichment**

660 Cells to be enriched for mitochondria were grown and treated as noted in figure legends. Cells were  
661 then moved to ice and washed twice with ice cold PBS. 1 ml of mito fractionation buffer (5 mM Tris-

662 HCl pH 7.5, 210 mM Mannitol, 70 mM Sucrose, 1 mM EDTA pH 7.5, 1 mM DTT, 1x protease and  
663 phosphatase inhibitors) was added per 10 cm dish and scraped to collect cells. A “cell homogenizer”  
664 (Isobiotec) was utilised with a 16 µm clearance ball and prepared by passing through 1 ml of mito  
665 fractionation buffer. Cell solution was collected in a 1 ml syringe and passed through the cell  
666 homogenizer 9 times. The resulting mix was centrifuged 500 x g / 4°C / 5 mins to pellet unbroken  
667 cells and nuclei. The supernatant was taken, and a small sample retained as post nuclear  
668 supernatant, the remaining was centrifuged at 10000 x g/4°C/ 10 mins to pellet mitochondria. The  
669 supernatant was removed to waste, and the pellet resuspended in 500 µl mito fractionation buffer  
670 and 10000 x g/4 °C/10 mins centrifugation step repeated. The supernatant was removed once more,  
671 the pellet represents enriched mitochondria that could be added directly to protein loading sample  
672 for downstream western blotting.

### 673 **Mitochondrial Classifier**

674 Cellular mitochondria were classified as tubular or fragmented by implementing an image classified  
675 utilising CellProfiler Analyst (v2.2.1, The Broad Institute). Classifications were determined by using  
676 siDRP1 and siOPA1 treated cells as positive controls for fragmented and hyperfused phenotypes  
677 respectively. Classifier was trained on the EGFP fluorescent images and with a confusion matrix of  
678 >0.90 for each phenotype.

### 679 **Crystal Violet Staining**

680 U2OS cells were seeded into 96-well plates in triplicate at  $2 \times 10^4$  cells per well and incubated  
681 overnight in complete media. Cells were then treated for 24 h with indicated compounds and doses,  
682 utilising puromycin as a positive control. Following treatment, cell media was removed and cells  
683 washed twice with a gentle stream of water. This was then removed and 100 µl of staining solution  
684 (0.5% (w/v) crystal violet, 20% methanol) added and incubated 20 min / RT with gentle rocking. Wells  
685 were washed 4x with water, all liquid removed and left overnight to air dry. Then 200µl per well of  
686 100% methanol for 20min/RT was added with gentle rocking and sample absorbance read at OD<sub>570</sub>.

687 Sample values were adjusted by no-well control (blank) wells and viability determined by  
688 normalisation to an untreated control.

### 689 **Quantification of mitophagy in *C. elegans*.**

690 The strain used to monitor mitophagy process in *C. elegans* was IR2539:

691 *unc-119(ed3);Ex<sub>[p<sub>myo-3</sub>TOMM-20::Rosella;unc-119(+)]</sub>*. Standard procedures for *C. elegans* strain

692 maintenance were followed. Nematode rearing temperature was kept at 20°C. For RNAi experiments

693 worms were placed on NGM plates containing 2 mM IPTG and seeded with HT115(DE3) bacteria

694 transformed with either the pL4440 vector or the *gakh-1* RNA construct for two generations.

695 Synchronous animal populations were generated by hypochlorite treatment of gravid adults to

696 obtain tightly synchronized embryos that were allowed to develop into adulthood under appropriate,

697 defined conditions. Progeny of these adults were tested on adult day 2. We performed imaging of

698 mitophagy process in *C. elegans* based on the methods we had established<sup>58-60</sup>. Briefly, worms were

699 immobilized with levamisole before mounting on 2% agarose pads for microscopic examination using

700 EVOS Imaging System. Images were acquired as Z-stacks under the same exposure. Average pixel

701 intensity values and frequency of GFP/DsRed puncta were calculated by sampling images of different

702 animals. The calculated mean pixel intensity for each animal in these images was obtained using FIJI.

### 703 **CRISPR/Cas9 genome editing in zebrafish and microinjections**

704 To generate *prkcd*a and *prkcd*b knock-out embryos, we utilised CRISPR/Cas9 as described earlier (Jao

705 et al., 2013). Potential gRNA target sites were identified using the online web tool CRISPR Design

706 (<http://CRISPR.mit.edu>) or CHOPCHOP (<http://chopchop.cbu.uib.no/index.php>) (Montague et al.,

707 2014). Genomic DNA sequences retrieved from Ensembl GRCz10 or z11

708 ([http://uswest.ensembl.org/Danio\\_reio/Info/Index](http://uswest.ensembl.org/Danio_reio/Info/Index)) were used for the target site searches. Three

709 guide RNAs were designed each for *prkcd*a and *prkcd*b respectively, based on predictions from the

710 aforementioned web programs. All sgRNAs were prepared by *in vitro* transcription of double-stranded

711 deoxyoligonucleotide templates as described previously<sup>61</sup>. Cas9 nuclease (EnGen Cas9 NLS, NEB) was

712 combined with an equimolar mixture of 3x sgRNA's (or 6x for *prkcd\_ab* DKO) and incubated for 5-6  
713 minutes at room temperature. After incubation, the mixture was immediately placed back on ice, until  
714 pipetted into the capillary needle used for microinjection and then approximately 1 nl of 5  $\mu$ M  
715 sgRNA:Cas9 complex was microinjected into the cytoplasm of one celled stage zebrafish embryo.

716 Oligonucleotides used for sgRNA synthesis are listed in Oligonucleotide Primers/Probes

717 Appendix 2, a universal primer was used with individual sgRNA primers  
718 (5'AAAAGCACCGACTCGGTGCCACTTTTTCAAGTTGATAACGGACTAGCCTTA  
719 TTTAACTTGCTATTCTAGCTCTAAAAC'3).

### 720 **Zebrafish Locomotor Assay**

721 Larval motility was monitored using the ZebraBox and Viewpoint software (v3.10.0.42, Viewpoint Life  
722 Sciences Inc) under infrared light. At 5 days post fertilization (dpf), larvae were singly placed in  
723 48-well plates with 300  $\mu$ l of fish water per well, followed by incubation at 28.5  $^{\circ}$ C on a normal light  
724 cycle overnight. All experiments were completed in a quiet room at 5 dpf between 10 AM and 2 PM.  
725 Larvae were allowed to acclimate in the ZebraBox measurement apparatus for 2 h before recording.  
726 Larvae were then exposed to alternating cycles of infrared light and dark, every 30 min as  
727 described<sup>63</sup>. Larval locomotion was tracked with the Viewpoint software. Motility was defined as  
728 tracks moving less than 10 cm/s, but more than 0.1 cm/s.

### 729 **Zebrafish Mitophagy cryosectioning and confocal microscopy**

730 Zebrafish mitophagy experiments were conducted on *tt-mitofish* with relevant *prkcd\_a/b* KO lines as  
731 described above. To examine mitophagy, zebrafish larvae were treated with DMOG or control for 24 h.  
732 At experimental end-points, larvae were washed once in embryo water and fixed with 3.7% PFA (in  
733 HEPES, pH 7-7.2) at 4  $^{\circ}$ C overnight. Post fixation, larvae were washed three times in PBS. The larvae  
734 were then cryopreserved in a 2 mL tube in increasing amounts of sucrose in 0.1 M PBS with 0.01 %  
735 sodium azide. Cryopreservation was done first in 15 % sucrose solution for 1 hour at RT or up until the  
736 larvae drops to the bottom of the tube and then in 30% sucrose solution at 4  $^{\circ}$ C overnight with gentle

737 shaking. Cryopreserved larvae were oriented in a cryomold (Tissue-Tek Cryomold, Sakura, Ref: 4565)  
738 with optimal cutting temperature compound (OCT compound) (Tissue-Tek Sakura, Ref: 4583). Larvae  
739 were oriented with the ventral side down and additional OCT was added to fill the mold and frozen  
740 down on dry ice. A solid block of OCT with couple of larvae oriented in the desired way, was taken out  
741 from the mold and 12  $\mu\text{m}$  coronal slices were sectioned on the cryostat (Thermo Scientific). Sections  
742 were collected on Superfrost Plus glass slides (Thermo Scientific, Ref: J1800AMNZ) and kept at RT for  
743 at least 2 h to firmly tether slices onto the glass slide.

744 The pH of all solutions and buffers used were 7-7.2. Slides were rehydrated three times in PBST (0.1 %  
745 Tween 20 in 1X PBS) at room temperature for 3 minutes each. Area of interest was circled by a  
746 hydrophobic PAP pen (Abcam, ab2601) and the slides were placed in a humidified chamber to avoid  
747 drying out. 100-200  $\mu\text{l}$  of 1  $\mu\text{g}/\text{ml}$  Hoechst solution was gently pipetted onto the slides and incubated  
748 for 30 mins at RT. Post incubation, slides were washed 3 times in PBST for 5 minutes each and mounted  
749 using ProLong Diamond Antifade Mountant (Invitrogen, P3696). Coverslips were carefully placed over  
750 the sections. Confocal images were obtained using an Aplanachromat 20x/0.8 or 63x/1.2 oil DIC objective  
751 on an LSM 800 microscope (Zeiss). Red puncta were counted manually from hind-brain regions.

## 752 **Mass Spectrometry**

### 753 Sample Preparation

754 Cells were dissolved in RIPA buffer and further homogenized with a sonicator (30 sec x 3 times with 30  
755 sec interval) and insoluble material was removed by centrifugation. Protein concentrations were  
756 estimated by BCA assay (Pierce). For each replicate, 600  $\mu\text{g}$  of protein samples for phosphoproteomics  
757 and 30  $\mu\text{g}$  for whole cell lysate proteomics were reduced and alkylated and further digested with  
758 trypsin by FASP (Filter aided sample preparation) method. Digested peptides were transferred to a  
759 new tube, acidified and the peptides were de-salted using Oasis cartridges for STY peptides  
760 enrichments. Phosphorylated peptides enrichment was performed based on  $\text{TiO}_2$ <sup>64</sup>. Enriched peptides  
761 fractions were de-salted by  $\text{C}_{18}$  stage tips.



762 LC-MS/MS:

763 Peptide samples were dissolved in 10  $\mu$ l 0.1 % formic buffer and 3  $\mu$ l were loaded for MS analysis. The  
764 Ultimate 3000 nano-UHPLC system (Dionex, Sunnyvale, CA, USA) connected to a Q Exactive mass  
765 spectrometer (ThermoElectron, Bremen, Germany) equipped with a nano electrospray ion source was  
766 used for analysis. For liquid chromatography separation, an Acclaim PepMap 100 column (C18, 3  $\mu$ m  
767 beads, 100  $\text{\AA}$ , 75  $\mu$ m inner diameter) (Dionex, Sunnyvale CA, USA) capillary of 50 cm bed length was  
768 used. A flow rate of 300 nL/min was employed with a solvent gradient of 3-35 % B in 220 mins, to 50 %  
769 B in 20 min and then to 80 % B in 2 min. Solvent A was 0.1 % formic acid and solvent B was 0.1 % formic  
770 acid/90% acetonitrile.

771 The mass spectrometer was operated in the data-dependent mode to automatically switch between  
772 MS and MS/MS acquisition. Survey full scan MS spectra (from m/z 400 to 2000) were acquired with  
773 the resolution  $R = 70,000$  at m/z 200, after accumulation to a target of  $1e6$ . The maximum allowed ion  
774 accumulation times were 100 ms. The method used allowed sequential isolation of up to the ten most  
775 intense ions, depending on signal intensity (intensity threshold  $1.7e4$ ), for fragmentation using higher  
776 collision induced dissociation (HCD) at a target value of 10,000 charges and a resolution  $R = 17,500$ .  
777 Target ions already selected for MS/MS were dynamically excluded for 30 sec. The isolation window  
778 was  $m/z = 2$  without offset. The maximum allowed ion accumulation for the MS/MS spectrum was  
779 60 ms. For accurate mass measurements, the lock mass option was enabled in MS mode and the  
780 polydimethylcyclosiloxane ions generated in the electrospray process from ambient air were used for  
781 internal recalibration during the analysis.

782 Data Analysis:

783 Raw files from the LC-MS/MS analyses were submitted to MaxQuant (v1.6.1.0) software for  
784 peptide/protein identification<sup>65</sup>. Parameters were set as follow: Carbamidomethyl (C) was set as a fixed  
785 modification; protein N-acetylation and methionine oxidation as variable modifications and PTY. A first  
786 search error window of 20 ppm and mains search error of 6 ppm was used. Minimal unique peptides

787 were set to one, and FDR allowed was 0.01 (1 %) for peptide and protein identification. The Uniprot  
788 human database was used. Generation of reversed sequences was selected to assign FDR rates.  
789 MaxQuant output files (proteinGroups.txt for proteomic data and STY(sites).txt for phosphoproteomic  
790 data) were loaded into the Perseus software<sup>66</sup>. Identifications from potential contaminants and  
791 reversed sequences were removed and intensities were transformed to log<sub>2</sub>. Identified  
792 phosphorylation sites were filtered only for those that were confidently localized (class I, localization  
793 probability  $\geq 0.75$ ). Next, proteins identified in two out three replicates were considered for further  
794 analysis. All zero intensity values were replaced using noise values of the normal distribution of each  
795 sample. Protein or STY abundances were compared using LFQ intensity values and a two-sample  
796 Student's T-test (permutation-based FDR correction (250 randomizations), FDR cut-off: 0.05, S0: 0.1).  
797 The complete datasets have been uploaded to ProteomXchange.

## 798 **Statistics and Significance**

799 Experimental values were used for statistical analysis using Prism (v8.0.1) where indicated using  
800 analyses and post-hoc tests as indicated in figure legends. All data values come from distinct  
801 samples. Where shown \*\*\*\* =  $p > 0.0001$ , \*\*\* =  $p > 0.001$ , \*\* =  $p > 0.01$ , \* =  $p > 0.05$  or n.s = not  
802 significant.

803

## 804 **ACKNOWLEDGEMENTS**

805 We would like to thank Coen Campersteijn for assistance with live cell imaging. We would also like to  
806 thank the Simonsen lab for their support and critical discussion throughout.

807 This work was supported by the Norwegian Cancer Society (Project: 171318) and the Research  
808 Council of Norway through its Centres of Excellence funding scheme (Project: 262652) and FRIPRO  
809 grant (Project: 221831).

## 810 AUTHOR CONTRIBUTIONS

811 Experimental planning, data analysis and writing of the manuscript were performed by M.J.M and A.S  
812 with input from all authors. B.J.M carried out *D.rario* experiments, Seb.S carried out CLEM  
813 experiments. Y.A and E.F carried out *C.elegans* experiments. Sac.S and J.W prepared and ran samples  
814 for MS analysis. Sak.S carried out analysis of interaction networks. A.H.L generated the IMLS cell line.  
815 M.J.M, L.T.M, M.Y.W.N.G and L.R.dIB performed all remaining experiments.

## 816 AUTHOR DECLARATIONS

817 M.J.M is now an employee of AstraZeneca plc.

## 818 DATA AVAILABILITY

819 All data is available upon reasonable request. Source data for quantitative figures and supplementary  
820 figures is provided as supplementary information. Proteomics Data has been uploaded to PRIDE.

APPENDICES

**siRNA Targets List**

**Appendix 1 – siRNA Targets**

| Gene Name       | RefSeq    | Lipid Binding Domain(s) | Sense siRNA            |                        |                        | siRNA ID |         |         | Primary Screen |      |
|-----------------|-----------|-------------------------|------------------------|------------------------|------------------------|----------|---------|---------|----------------|------|
|                 |           |                         | Oligo #1               | Oligo #2               | Oligo #3               | Oligo 1  | Oligo 2 | Oligo 3 | Average (fold) | SEM  |
| <b>ABR</b>      | NM_001092 | PH, C2                  | GCGAAGAGAUCUACAUAAtt   | CGGCUAUUUUGUCAGCAAAtt  | CGGACGUGAUUGAGAUAAtt   | s876     | s877    | s878    | -0.14          | 0.09 |
| <b>AKAP13</b>   | NM_006738 | PH, C1                  | GCAUUAUUGCUUGUAACUCAtt | GGAAGAAGCUUGUACGUGAtt  | GGAUAAUAGACAGCAAGUAtt  | s680     | s681    | s682    | -0.74          | 0.04 |
| <b>ANKFY1</b>   | NM_016376 | FYVE                    | GGACUUAUUUGAUGAGAAtt   | GAAACUAGCAAUCGGUUAtt   | GUACAGCGAUCUGAAGAUAtt  | s28198   | s28199  | s28200  | +0.15          | 0.10 |
| <b>ARAF</b>     | NM_001654 | C1                      | CGAGAUCUCAAGUCUAACAtt  | GUGUUGACAUGAGUACCAAtt  | UGCACAAUUUUGUACGGAAtt  | s575     | s576    | s577    | +0.78          | 0.12 |
| <b>ARHGAP29</b> | NM_004815 | C1                      | GCAUAGGUGUUUGUAUCAtt   | GACCAAGGCUAAAACGAAAtt  | GGUCAACUCUCUACUGAUAtt  | s484     | s485    | s486    | +0.09          | 0.05 |
| <b>Arhgap33</b> | NM_178252 | PX (atypical)           | GGAAGACAUCUUUGUCUCUAtt | GAGGUUCUGUUCAGCGAUAtt  | GGCAUGAGUUUGAUAGUGAtt  | s107439  | s107440 | s107441 | +0.22          | 0.05 |
| <b>ARHGEF2</b>  | NM_004723 | PH, C1                  | GGAUCUACCGUCACUACUAtt  | CCAAGUACCCGUUACUCAAtt  | GCUUACCGCGGCGAAUUAtt   | s17545   | s17546  | s17547  | -0.37          | 0.02 |
| <b>Arhgef28</b> | NM_012026 | PH, C1                  | CGAUUUGGAUAUCAUAUAtt   | CCGACUGCGUCUUAACGAAtt  | GCUUCGCGUCUUUCGUGAtt   | s99834   | s99835  | s99836  | +0.10          | 0.05 |
| <b>BRAF</b>     | NM_004333 | C1                      | CAGAGGAUUUJAGUCUAUAtt  | GCAUAAUCCACCAUCAUAtt   | CAGUUGUCUGGAUCCAUUAtt  | s2080    | s2081   | s2082   | +0.01          | 0.05 |
| <b>C2CD5</b>    | NM_014802 | C2                      | GCUCGGAUGAAGUACAGAtt   | GGAAAUUCCGGAAUCGUAtt   | GCCUCAACCGACUAAUCAAtt  | s19053   | s19054  | s19055  | +0.11          | 0.08 |
| <b>CDC42BPA</b> | NM_014826 | PH, C1                  | GAUGGAAGAUGGAACGGUAtt  | CCGCAAUCAUAGAUCAUGAtt  | CCAUAUCUCUCGGUGUACAtt  | s16098   | s16096  | s16097  | -0.10          | 0.08 |
| <b>CDC42BPB</b> | NM_006035 | PH, C1                  | CGAGAACGGCAUAACGAGAtt  | CACUCAACUCCAUCGAAUAtt  | GGCUGAUCCUUUGCUAUGAtt  | s18401   | s18402  | s18403  | +0.41          | 0.14 |
| <b>CDC42BPG</b> | NM_017525 | PH, C1                  | GCAAGAUCAUGAACACGAtt   | GGAUGUGAACGGGCACAUAtt  | CAACUCCUGAUUCCCUAtt    | s30983   | s30984  | s30985  | -0.13          | 0.07 |
| <b>CHN1</b>     | NM_001822 | C1                      | CAUUGAAUGAUUACGGUAtt   | CAUUUAUCACUGGUGCACUAtt | CUCUCUAUAUUGAAACCAAtt  | s3016    | s3017   | s3018   | -0.48          | 0.06 |
| <b>CIT</b>      | NM_007174 | PH, C1                  | GGAAGGUGAUGACCGUCUAtt  | CGUGGAUUCUACGGAAGAtt   | GAUUCUACGGAAGACGUAtt   | s21910   | s21911  | s21912  | +0.12          | 0.06 |
| <b>CLINT1</b>   | NM_014666 | ENTH                    | GCUCUAGCUUACCUCAUAtt   | GCACAAUUGAUGACACCAUAtt | GAAUGUUAAAAGACAACAAtt  | s18644   | s18645  | s18646  | +0.53          | 0.12 |
| <b>CPNE1</b>    | NM_152925 | C2 x2                   | GAAUCUAUGACAUAGACAAtt  | CCAUGUCAGUGAUCAUUGUAtt | GCUACGCUUUGGAAUCUAUAtt | s17023   | s17024  | s17025  | +0.77          | 0.12 |
| <b>CPNE2</b>    | NM_152727 | C2 x2                   | GGACUGAGGUGAUCAAGUAtt  | UGUUCACCGUUGGAAUAGAtt  | CUACUGGACCGGAUGUUAtt   | s47982   | s47983  | s47984  | +1.32          | 0.15 |
| <b>CPNE3</b>    | NM_003909 | C2 x2                   | CCAUAAGGUGGAGUGUUAtt   | GGAAUAUAGGAUCUAUUAtt   | GCAUUAAGAUUUCAGCUGAtt  | s17005   | s17006  | s17007  | +0.30          | 0.08 |

|                |              |                |                        |                        |                        |        |         |         |       |      |
|----------------|--------------|----------------|------------------------|------------------------|------------------------|--------|---------|---------|-------|------|
| <b>CPNE7</b>   | NM_153636    | C2 x2          | GGAUUACGACUCUCGAGGAtt  | AGUAUGAGGUGUCCCAUGAtt  | CAGCCGAACGAGUACCUGAtt  | s25879 | s25880  | s25881  | +1.04 | 0.16 |
| <b>DAB2IP</b>  | NM_138709    | PH, C2         | CGAUCUUUCCGGUCUGAUAtt  | GCUUGGACUCCAACAGAtt    | GAGCAUGAGUGGACCAACAtt  | s237   | s238    | s239    | +0.97 | 0.11 |
| <b>DGKA</b>    | NM_201554    | C1 x2          | GGAUUCGUAUUUAGCAAAtt   | GCAUCGCAGUGCUAAACAAtt  | CCGGAGAAGUUAACAGCAtt   | s3911  | s3912   | s3913   | +0.26 | 0.10 |
| <b>DYSF</b>    | NM_003494    | C2 x7          | GCGUGAACCCUGUAUGGAAtt  | GGACCUCCUUCAACAUCAtt   | GGGUCGACCUUUUCCGAAtt   | s15788 | s15789  | s15790  | +0.64 | 0.10 |
| <b>EEA1</b>    | NM_003566    | FYVE           | GCUAAGUUGCAUUCGAAAtt   | GCUGGAUAAUACAACUGCAtt  | GCAAUCUAGUCAACGGAGAtt  | s15969 | s15970  | s15971  | -0.06 | 0.07 |
| <b>ENTHD1</b>  | NM_152512    | ENTH           | GCACAUAGAUGAAGCUGGAtt  | CGAUCGCUAGAUUACAUGAtt  | GAUUCAUGGUUGGAAAUCAtt  | s45419 | s45420  | s45421  | +0.20 | 0.14 |
| <b>EPN1</b>    | NM_013333    | ENTH           | AAUCCUUGGUGAUGAUUUAtt  | GACUUUGACCGACUCCGAtt   | CAUCGUCCACAACUACUCAtt  | s26712 | s26713  | s26714  | -0.32 | 0.04 |
| <b>EPN2</b>    | NM_148921    | ENTH           | CGCUGUUGGAUUUAAUGGAtt  | GGAAAACACCGAGUCCUAtt   | AGAGCGAGCUUUAAAACUAtt  | s22639 | s230616 | s230617 | -0.15 | 0.06 |
| <b>EPN3</b>    | NM_017957    | ENTH           | GACUCUCUGAGGUAGAAAAtt  | CGUGUACAAGGCUCUAAAtt   | CAACUACUCCGAGGCAGAAAtt | s30052 | s30053  | s30054  | +0.26 | 0.05 |
| <b>ESYT1</b>   | NM_015292    | C2 x5          | GGACUUGAACAUACGCUAAtt  | CCAUGAUAUGGACUCCAUAtt  | GGGAAGGUGUUAACAGGCUAtt | s23605 | s23606  | s23607  | +0.02 | 0.06 |
| <b>Esyt2</b>   | NM_028731    | C2 x3          | GGAAACCACUUUAGAGAAtt   | GAGUAAGAUUCGAUACAAAtt  | CAAAUCCUCUUGUCCAGAUAtt | s78925 | s78926  | s78927  | -0.37 | 0.05 |
| <b>FAM148C</b> | XM_065166    | C2             | GUGUCUCUGCUCAAAGGUAtt  | GCAAUGUGUUGACGCCGAtt   | GGAGGUGACAAGUCUUGGAtt  | s43053 | s195676 | s195677 | -0.34 | 0.05 |
| <b>FGD1</b>    | NM_004463    | FYVE, PHx2     | CCUUGGUGCUGUAUAUCUAtt  | CAAGAUGUAUGGUGAGUAAtt  | GCAAAAGGUGUUUCACAUAtt  | s5121  | s5122   | s5123   | +0.19 | 0.20 |
| <b>FGD2</b>    | NM_173558    | FYVE, PHx2     | AGAAGAAGAUUCGUCCAGGAtt | UCGGUGACGUGAUCCAGAAtt  | GGGCCGAACUGAAAUCGAtt   | s48057 | s48058  | s48059  | +0.35 | 0.20 |
| <b>FGD3</b>    | NM_033086    | FYVE, PHx2     | GAACUUGACCGAGCCGUAtt   | UCAUGGGCAUAUUCUCUAtt   | AGAGCUGAGUGGUAGCUUAtt  | s40147 | s40148  | s40149  | +0.49 | 0.14 |
| <b>FGD4</b>    | NM_139241    | FYVE, PHx2     | GAAGGAGACUAAUGAGCAAtt  | CAACCACCCUCAACAAAAtt   | GAAAGGAUUUGAUAAUGCAtt  | s42476 | s42477  | s42478  | +0.18 | 0.09 |
| <b>FGD5</b>    | NM_152536    | FYVE, PHx2     | GGAGGACAGUGCUUCAAGAtt  | CGAAAGGUUUAGAAUCAGAtt  | GACUAAUUAAAACAACCUUAtt | s45682 | s45683  | s45684  | +0.08 | 0.11 |
| <b>FGD6</b>    | NM_018351    | FYVE, PHx2     | GUCUGUACCCGUUUCGUCAtt  | GAUGAGACUUUGACUAUAAtt  | GAAGUUACCUAUCCUUAUAtt  | s31503 | s31504  | s31505  | -0.18 | 0.08 |
| <b>FYCO1</b>   | NM_024513    | FYVE           | CCUGCAAUUUGAUCAGAAAtt  | GAGGCACAGUUAGACGAUAtt  | CACUGACCGUGGAAAAGGAtt  | s35794 | s35795  | s35796  | +0.16 | 0.12 |
| <b>GAK</b>     | XM_001127411 | C2-tensin type | GUCGUCGCUAUUUAUGCAtt   | CACCAGAAAUCAUAGACUAtt  | CGAGGAUACAACACCAAAtt   | s5527  | s5528   | s5529   | -0.55 | 0.02 |
| <b>GRAMD1A</b> | NM_020895    | GRAM           | GGAGCGGCAUUGAAGACUAtt  | GAAGUGACAUGUCUGAAGAtt  | GAGGAGCUAUUGACAGACAtt  | s33529 | s33530  | s33531  | +0.20 | 0.06 |
| <b>GRAMD1B</b> | NM_020716    | GRAM           | GAGAGUGAAUGUUACGUGAtt  | CCAGUGCUAUUGGGAACGAAtt | CUCUUGAGUCCCAACAAAtt   | s33112 | s33113  | s33114  | +0.68 | 0.11 |
| <b>GRAMD1C</b> | NM_017577    | GRAM           | CUGCUCGACUCAUCCAAAAtt  | GAUUACUUCUAUACCGUGAtt  | CCUACACUAUAGUCCUUAAtt  | s29399 | s29400  | s29401  | +0.74 | 0.07 |
| <b>GRAMD2</b>  | NM_001012642 | GRAM           | GGAUGUUCUUGGAGGAAtt    | CAAAGAAUGCUGUCUAUGAtt  | CGAGAAGGGUAACACUGAtt   | s47069 | s47070  | s47071  | -0.18 | 0.03 |
| <b>GRAMD3</b>  | NM_023927    | GRAM           | GGACACCCAUAAUCUGAAtt   | CGACCUUCUACAUGAGAUAtt  | GAAAGCUCUUGUAUCAGAtt   | s35302 | s35303  | s35304  | -0.23 | 0.04 |
| <b>GRAMD4</b>  | NM_015124    | GRAM           | GAAAUUGCCUUAUUGGAAAtt  | CCUCCAAAGGAAGACUGAtt   | CCCAGAACCUUUUCGGGAAtt  | s23148 | s23149  | s23150  | +0.52 | 0.03 |
| <b>HECW1</b>   | NM_015052    | C2             | GGACAGCUGCAAUCCGAUAtt  | GCUCCGAAUUUCUACAGAtt   | GAUGAGGUCUUGUCCGAAAtt  | s22968 | s22969  | s22970  | +0.06 | 0.07 |
| <b>HGS</b>     | NM_004712    | FYVE           | CGUCUUCCAGAAUUCAAAtt   | UGGAAUCUGUGGUAAGAAtt   | CACGGUAUCUCAACCGGAAtt  | s17480 | s17481  | s17482  | +0.55 | 0.22 |
| <b>HIP1</b>    | NM_005338    | ENTH           | CCACUAAUUGAGCGACUAtt   | GCAAUACACAGAUCGAAGAtt  | GAGCCUGUCUGAGAUAGAAtt  | s6542  | s6543   | s6544   | -0.10 | 0.04 |

|               |              |                   |                        |                        |                        |         |         |         |              |      |
|---------------|--------------|-------------------|------------------------|------------------------|------------------------|---------|---------|---------|--------------|------|
| <b>HIP1R</b>  | NM_003959    | ENTH              | GGACCGAUGUCAACAACAAtt  | GCAGGAAUGUUCUCGCACAtt  | GAUUGUGAGCUGAAGCUUAtt  | s17203  | s17204  | s17205  | <b>+0.24</b> | 0.06 |
| <b>HS1BP3</b> | NM_022460    | PX                | AGAUGGACAUCUUGCAGUAtt  | UGAGGAGUUUUACCAGAAAtt  | GGUGAUACCCAGAAAACAtt   | s34647  | s34648  | s34649  | <b>+0.46</b> | 0.09 |
| <b>ITCH</b>   | NM_031483    | C2                | CGGGCGAGUUUACUUAUGUAtt | GGAACUCGUGCAUUAGAUAtt  | GGAAUACAUCAGAAUGGUAtt  | s38163  | s38164  | s38165  | <b>-0.38</b> | 0.05 |
| <b>ITSN1</b>  | NM_003024    | PH, C2            | GCUCAACAUCUGUAGAUAtt   | CAAGAACUUAUCUUUAGCAtt  | GAACGAAAGAUCAUAGAAUAtt | s12793  | s12794  | s12795  | <b>-0.47</b> | 0.04 |
| <b>ITSN2</b>  | NM_147152    | PH, C2            | CAACGUAAGGUAAGGAUAtt   | GGAGUGAAGUAAAACGGGAtt  | CUGGAUCUGUAUCACCUAAtt  | s27052  | s27053  | s27054  | <b>+0.66</b> | 0.12 |
| <b>KIF16B</b> | NM_024704    | PX                | CAACUGCGUUUCUUCGAAUAtt | GAAUUUUGGUGACGUAGAAtt  | CCAAUUGUUUCGUUUUAAtt   | s31080  | s31081  | s31082  | <b>+0.24</b> | 0.06 |
| <b>LRBA</b>   | NM_006726    | PH-Beach          | GGCGGUUAUUCUCCAGUAAtt  | GCUCGUUCUGAGUCAUUAAtt  | GGUUACGUGUUUAUCACAAtt  | s2735   | s2736   | s2737   | <b>-0.25</b> | 0.07 |
| <b>LYST</b>   | NM_000081    | PH-Beach          | CCAAAUGACUUAUCGAAAtt   | GCAACGGUGUUUCAUCACAtt  | GCAUUAGCAGUCGAGUUAtt   | s3028   | s3029   | s3030   | <b>-0.40</b> | 0.02 |
| <b>MTM1</b>   | NM_000252    | GRAM              | CAUUGAAGGGUUCGAAAUAtt  | GGUACUUUCUUUAUUAACUAtt | CUGUGAAUCUGCUCGAGAAtt  | s9041   | s9042   | s9043   | <b>+0.54</b> | 0.05 |
| <b>MTMR1</b>  | NM_003828    | GRAM              | GCUUAUAGCUGCUACAUAUAtt | GUUACUACAGGACCAUUAAtt  | GGAUACCUUUUAUAGCUGUAtt | s16718  | s16717  | s16719  | <b>+0.00</b> | 0.07 |
| <b>MTMR2</b>  | NM_016156    | GRAM              | GGACAUCGAAUUCAACUAAtt  | CUCUGACUGUCACGAAUUAtt  | GAGAGAAUCAAUACGAAAAtt  | s17014  | s17015  | s17016  | <b>-0.20</b> | 0.11 |
| <b>MTMR3</b>  | NM_153050    | FYVE              | GCUGGACCCUUAUUACCGAtt  | GGAAAUUCCUGUGCAACAtt   | GGUUGGGUUUUGAUUAUGAAtt | s17011  | s17012  | s17013  | <b>+0.02</b> | 0.09 |
| <b>MTMR4</b>  | NM_004687    | FYVE              | CGUACAUCGAGUACCCUAtt   | GGAUUUUGGGCACAAGUUUAtt | GCAACACCUCUGAUCCUGAtt  | s17383  | s17384  | s17385  | <b>+0.07</b> | 0.07 |
| <b>MYO9A</b>  | NM_006901    | C1 x2             | GGAUAGUUUUUCGAAUUAAtt  | GCUCUUACUUUGGAUAUCAtt  | GUAUAGAGAGUAAUUCGAAtt  | s9220   | s9221   | s9222   | <b>-0.03</b> | 0.05 |
| <b>MYO9B</b>  | NM_004145    | C1                | CGAUGUACUCUGUCCGAAtt   | GGAAUACCCAGAUCCGGAAtt  | GAAAACCGGUGACCGUCAAtt  | s715    | s716    | s717    | <b>+0.32</b> | 0.06 |
| <b>MYOF</b>   | NM_133337    | C2 x5             | CGAACAACUCUGUAUCGUUAtt | GGGACAUCGUUAUCGAAUAtt  | GGUUGGACAUGAUUCCGGAtt  | s25476  | s25477  | s25478  | <b>+0.02</b> | 0.03 |
| <b>NBEA</b>   | NM_015678    | PH-Beach          | GGAGACGAUUUGUUCGCAAtt  | GGAUUGAAAGCGAUAGUAtt   | CGGACUACAAGUUUCGUAtt   | s25649  | s25650  | s25651  | <b>+0.02</b> | 0.08 |
| <b>NBEAL1</b> | XM_001134432 | PH-Beach          | GGAUUAACAGCUAGAGUAtt   | CUAGUGCCUUGAGAGUAUAtt  | CUAUGGUACUCACUAUUCAtt  | s35186  | s35187  | s35188  | <b>+0.00</b> | 0.02 |
| <b>NBEAL2</b> | XM_941211    | PH-Beach          | CCAUGACAAGUUCACUAAtt   | GCUACUCCAUGUCCUUAAtt   | CCAUACUGCUGUUACGUCUAtt | s23313  | s23314  | s23315  | <b>-0.25</b> | 0.03 |
| <b>NCF1</b>   | NM_000265    | PX                | CGAGUUCCAUAAAACCUUAtt  | AGGGCACACUUAACCGAGUAtt | AGACAUACUUGAUGCCCAAtt  | s57647  | s57648  | s57649  | <b>+0.45</b> | 0.12 |
| <b>NCF4</b>   | NM_000631    | PX                | AAGUCUACGUGGGUGUGAAtt  | GGAGGAUCCAAGUACCUCAAtt | CCUCAGUCGGAUCAACAAAtt  | s9306   | s9307   | s9308   | <b>+0.49</b> | 0.18 |
| <b>NEDD4L</b> | NM_015277    | C2                | CAGUAACCCUGAAUGACAtt   | GGACAUCGCGAGUACCUAAtt  | CCUUUGAAGAUUUACGAGAtt  | s23569  | s23570  | s23571  | <b>-0.15</b> | 0.04 |
| <b>NISCH</b>  | NM_007184    | PX                | GCCCAUCCUCUCUAACCAAtt  | GAAUCAUGUUCGUUCAGGAtt  | GGAUCCGACAGAUUGGAGGAtt | s22092  | s22093  | s22094  | <b>+0.45</b> | 0.08 |
| <b>NOXO1</b>  | NM_144603    | PX                | CAAGAGGCCUCAAACGUUAtt  | UGCGCGUGUUGGAAACGUAtt  | GGAGUUUGGACGAAUUCAGAtt | s195651 | s195652 | s195653 | <b>+0.90</b> | 0.20 |
| <b>NSMAF</b>  | NM_003580    | PH-Beach,<br>GRAM | CAACGGAAUUUAAAAGAGUAtt | GGUGUAGACUUGAACAGCAtt  | GCAAGCACACUGUUAGUUAtt  | s16015  | s16016  | s16017  | <b>+0.47</b> | 0.08 |
| <b>OXR1</b>   | NM_181354    | GRAM              | CUAACGAACUUGUUCAAUAtt  | GGAUUCUUUGAAUAGCAUAtt  | CAAUUGAGGAUUCUAGUAAtt  | s30111  | s30112  | s30113  | <b>+0.05</b> | 0.08 |
| <b>PCLO</b>   | XM_940805    | C2 x2             | CCACUAGUGAAACAACCAAtt  | GGAUUACCGUUAACAAGAAtt  | GGAGGACUUCAUUCGAAAAtt  | s26249  | s26250  | s26251  | <b>-0.28</b> | 0.04 |
| <b>PDZD8</b>  | NM_173791    | C1                | GCAUAUCCAUAUACAACAAtt  | CAAUACUAGUUCUCGUUUAtt  | GAGUUCUAUUUAGACGGUAtt  | s42265  | s42266  | s42267  | <b>+0.04</b> | 0.09 |

|                  |              |                |                        |                        |                        |        |        |        |       |      |
|------------------|--------------|----------------|------------------------|------------------------|------------------------|--------|--------|--------|-------|------|
| <b>PICALM</b>    | NM_001008660 | ENTH           | GGAAUUGACAUGUCUACAAtt  | GGCAAGCACUGGUCUAUCAtt  | CCACCUAGCAAGUUAGUAUAtt | s15799 | s15800 | s15801 | -0.09 | 0.05 |
| <b>PIK3C2A</b>   | NM_002645    | PX, C2, C2     | GCCUACAACUUGAUAGAAtt   | GGAUCUUUUAAAACCUAUAtt  | GGCUUUGAGUUGUCAAGCAtt  | s10508 | s10509 | s10510 | -0.04 | 0.11 |
| <b>PIK3C2B</b>   | NM_002646    | PX, C2         | GCUCUGAUCCUACCCUUAAtt  | CCUACAACCUAUUCGCAAtt   | CGGAAAACCUAGCAUCCUAtt  | s10511 | s10512 | s10513 | -0.02 | 0.11 |
| <b>PIK3C2G</b>   | NM_004570    | PX, C2         | CCAUCUACCAGCUAAUCAAtt  | GUAGCAUUCUCCAACAAAtt   | GCUACUGGGUGGGAGUAUAtt  | s10514 | s10515 | s10516 | +0.28 | 0.14 |
| <b>PIKFYVE</b>   | NM_152671    | FYVE           | CACUGAGGAUGAACGCAAtt   | GGAAAUCUCCUGCUGAAAtt   | CACCGCUACUGGUUGAGAAtt  | s47254 | s47255 | s47256 | +0.23 | 0.11 |
| <b>PLA2G4A</b>   | NM_024420    | C2             | GGGCUUGAAUCUCAAUACAtt  | GAAUUUAGUCCAUCGAAAtt   | CCGUAUCCCUUGAUACUGAtt  | s10592 | s10593 | s10594 | -0.42 | 0.03 |
| <b>PLCB3</b>     | NM_000932    | C2             | GCAUAACACCUAUUCACUAtt  | CGUCCUUUGUGGAGACCAAtt  | GGCUGCUCAUCGAAAAGUAtt  | s10619 | s10620 | s10621 | -0.32 | 0.05 |
| <b>PLCD1</b>     | NM_006225    | PH, C2         | CAACAAGAAUAAGAAUUCAtt  | GGACCAGCGCAAUACACUAtt  | GGAGUUUGCGUUUGAGGUAtt  | s10625 | s10626 | s10627 | +0.60 | 0.12 |
| <b>PLCD3</b>     | NM_133373    | C2             | UGGUCAACGUGGACAUGAAtt  | GCAGCUCAUUCAGACCUAAtt  | GGUUUGUGGUGGAGAAUAtt   | s41418 | s41419 | s41420 | +0.39 | 0.11 |
| <b>PLCG1</b>     | NM_182811    | PH x2, C2      | GGGUGAAAAAGAUCCGUGAtt  | GAAUCGUGAGGAUCGUUAtt   | GGACUUUGAUUCGUUCAAtt   | s10631 | s10632 | s10633 | +0.22 | 0.06 |
| <b>PLCG2</b>     | NM_002661    | PH, C2         | GGAUCUCCUCGUCACAUAAAtt | CAAUUAGGAAAGAGAUUAtt   | GGGAUUCUUAUGACCAGAAtt  | s10634 | s10635 | s10636 | +0.11 | 0.12 |
| <b>PLCH1</b>     | NM_014996    | PH, C2         | GGACGAAUGAUGCAGUUAAtt  | CCAGUGUAUUAGUAAGUAtt   | GCAUAGAAGGCUUCACGAAtt  | s22817 | s22818 | s22819 | -0.02 | 0.07 |
| <b>PLCL2</b>     | NM_015184    | PH, C2         | GCCGGAGUGUUGAAUJAGAtt  | GGACUGCGGUACCUAAUUAtt  | CCGUGGAUGAGGUUUUCAAtt  | s23334 | s23335 | s23336 | +1.01 | 0.29 |
| <b>PLD1</b>      | NM_002662    | PX, PH         | GCACUAUAUCUAUAUCGAAtt  | CACUAUAUCUAUAUCGAAAtt  | GGCACUAUAUCUAUAUCGAtt  | s10637 | s10638 | s10639 | -0.15 | 0.07 |
| <b>PLD2</b>      | NM_002663    | PX, PH         | CCAUGUCUUUCUAUCGCAAtt  | GUGUGAUUCUUGGAGCAAtt   | GAAGAAUACCGUAUUUUAtt   | s10640 | s10641 | s10642 | -0.01 | 0.09 |
| <b>PLEKHF1</b>   | NM_024310    | FYVE, PH       | CACAGGUCUUGGUAACAAAtt  | CCAGCUGUCUCAUGCCUUAtt  | CCUUUUUGCUGGACACUGAtt  | s35643 | s35644 | s35645 | -0.07 | 0.09 |
| <b>PLEKHF2</b>   | NM_024613    | FYVE, PH       | CUAAAUCUUUUGCAGUUUAtt  | GUAAUAGUAUAGUGGAAAtt   | GGAGAAGGAGUAUUGACUAtt  | s36049 | s36050 | s36051 | +0.23 | 0.11 |
| <b>PLEKHM1</b>   | NM_014798    | PH x2, C1      | GCAGAUCCGCUUCUCCUUAtt  | GCACCUCAUUGGGAGGAGAtt  | GGAUCAUCCACAACUGGGAtt  | s19041 | s19042 | s19043 | +0.07 | 0.12 |
| <b>PRKCA</b>     | NM_002737    | C2, C1 x2      | CAACGUACCAUUCGGAAAtt   | GGCUGUACUUCGUCAUGGAtt  | GCUCCACACUAAAUCGCAAtt  | s11092 | s11094 | s11093 | +0.23 | 0.04 |
| <b>PRKCB</b>     | NM_212535    | C2, C1 x2      | GGUCUGUUCUUCUACAGAtt   | GGAUGAAACUGACCGAUUAtt  | GAAUCGGACAAAGACAGAAtt  | s11095 | s11096 | s11097 | +0.30 | 0.10 |
| <b>PRKCD</b>     | NM_212539    | C2, C1 x2      | GGGACACUAUAUCCAGAAtt   | GGAUUAAAGUGUGAAGACUAtt | GGAGUGACCGGAAACAUCAtt  | s11099 | s11098 | s11100 | -0.57 | 0.04 |
| <b>PRKCI</b>     | NM_002740    | C1             | GAGACCUAAUGUUUCAUAtt   | GGAUAUGAUGGAGCAAAAAtt  | GUAAUCCAUUAUAAUCCUAtt  | s11110 | s11111 | s11112 | -0.24 | 0.07 |
| <b>PRK CZ</b>    | NM_002744    | C1             | CGUUCGACAUCAUCACGAtt   | GGACUUUGACCUAAUCAGAtt  | CGAGGAUUAUGACUGGGUAtt  | s11128 | s11129 | s11130 | +0.42 | 0.08 |
| <b>PRKD2</b>     | NM_016457    | PH, C1 x2      | CAGUGGGCGUGAUCAUGUAtt  | GAACAACACGACCAACAGAtt  | AGAUGAUCCUGUCCAGUGAtt  | s24644 | s24645 | s24646 | -0.08 | 0.10 |
| <b>PTEN</b>      | NM_000314    | C2-tensin type | GCAUACGAUUUAAGCGGAtt   | CACCGCAUAUUAACCGUAtt   | GGUUUUCGAGUCCUAAUAtt   | s325   | s326   | s327   | +0.18 | 0.10 |
| <b>PXK</b>       | NM_017771    | PX             | CGGAAUUAUUAUUCGAGUAtt  | GGAUCUGAUCUACAAGCAtt   | GACAUAGGUUGGAGAAUAtt   | s29710 | s29711 | s29712 | +0.24 | 0.08 |
| <b>RAB11FIP1</b> | NM_001002814 | C2             | ACGAUGAGCGUAUUCAGCAtt  | CGAGCUGGAAGACUACUAtt   | AGAAGGAAACGAUAAGCAAtt  | s37090 | s37091 | s37092 | +0.89 | 0.09 |
| <b>RAB11FIP2</b> | NM_014904    | C2             | GCGCAUUCAAUGUCUGAUUAtt | GGUUUAGAUUAGAAUCCAAtt  | CGAGCUACCUUGGAUUGCUAtt | s22475 | s22476 | s22477 | +0.56 | 0.02 |
| <b>RAB11FIP5</b> | NM_015470    | C2             | GGAACGCGCGGAGAUUGAAtt  | GAAGAAGUAUGAUCUGGAAtt  | GGCCGCGAGAAGUACAGUAtt  | s25026 | s25027 | s25028 | +0.05 | 0.08 |

|                           |              |             |                        |                        |                        |         |        |        |       |      |
|---------------------------|--------------|-------------|------------------------|------------------------|------------------------|---------|--------|--------|-------|------|
| <b>RACGAP1</b>            | NM_013277    | C1          | CAGUGACUGUCCCAAUGAtt   | CAACUAAGCGAGGAGCAAAtt  | GCGAAAAGCUGGAACGACAtt  | s26550  | s26551 | s26552 | +0.67 | 0.09 |
| <b>RAF1</b>               | NM_002880    | C1          | GGAACUGUUUUAAGGGUAtt   | GGAUUUCGAUGUCAGACUUt   | CGUGUUUCUUGCCGAACAtt   | s11749  | s11750 | s11751 | +0.91 | 0.06 |
| <b>RASA1</b>              | NM_002890    | PH, C2      | CAUAGAUCACUAUCGAAAAtt  | GAAUCGUUGUUGUUAUGCAtt  | CCACGGAUGUCAAUAUCAtt   | s11820  | s11819 | s11821 | -0.28 | 0.07 |
| <b>RASA3</b>              | NM_007368    | PH, C2 x2   | CUCUUCAACUUGUACAUGAtt  | GAAUUUACCUACCACAAAAtt  | GCCCAUCUGUCUAAAAGAAtt  | s355    | s357   | s356   | +0.37 | 0.12 |
| <b>RASAL2</b>             | NM_170692    | PH, C2 x2   | GGAUCAUGCUGAGAUGCAAtt  | GCAGGACAGUUAACCUAAtt   | CUAGUGAACUGAUAGACCAtt  | s18125  | s18126 | s18127 | -0.11 | 0.06 |
| <b>Rbsn</b>               | NM_030081    | FYVE        | GAAAGUAUAUGAGCUAAUAtt  | GGAUUAUGAAUCAUUCAGUUt  | GGAAGAUCGUGAUGUCAAAAtt | s95445  | s95446 | s95447 | +0.41 | 0.19 |
| <b>RIMS1</b>              | NM_014989    | FYVE, C2 x2 | GUGCAUCGAUUUAAGCAGAtt  | GCAUUCACCAGAACGAGAAtt  | GGCUAUAGGUCUAGUGCUAtt  | s22808  | s22809 | s22810 | -0.04 | 0.10 |
| <b>RIMS2</b>              | NM_014677    | FYVE, C2 x2 | CUACCGAAGUGAUCCGAUUt   | GCGAAUACCUGAUAGCACAtt  | CCAACACGGAGGUUGCAAAtt  | s18683  | s18684 | s18685 | +0.35 | 0.10 |
| <b>ROCK1</b>              | NM_005406    | PH, C1      | GGUUAGAACAAGAGGUAAAtt  | CGGUUAGAACAAGAGGUAAAtt | GCUUGUAGGUGAUACACCUAtt | s12097  | s12098 | s12099 | -0.19 | 0.06 |
| <b>ROCK2</b>              | NM_004850    | PH, C1      | GGAGAUUACCUUACGGAAAAtt | GAGAUUACCUUACGGAAAAtt  | GGAUCGAACCUAUGGAUCAtt  | s18161  | s18162 | s18163 | +0.34 | 0.10 |
| <b>RPH3A</b>              | NM_014954    | FYVE, C2 x2 | GAGUUUUUCUUAUGACAUCAtt | CGAAUUCAAUGAGGAGUUUt   | CCUUGAAUCCCGAAUUCAAAtt | s22610  | s22611 | s22612 | +0.01 | 0.10 |
| <b>RPH3AL</b>             | NM_006987    | FYVE        | GCUCGUCGGUUGUCGAAtt    | GGACCGGAAAGGCGACAAAtt  | GAUAGUGACUCGGAUCUUAtt  | s18218  | s18219 | s18220 | +0.03 | 0.09 |
| <b>RPS6KC1</b>            | NM_012424    | PX          | GGAAUGGUGUUGAUACAAAtt  | GGCAAACUGUGGUCAUUAAtt  | CAAUCCUUAUGUAUAACAtt   | s25624  | s25625 | s25626 | +0.19 | 0.06 |
| <b>RUFY1</b>              | NM_001040451 | FYVE        | CGACUAGUGUCAGAAAUCUAtt | GGAAAACCAACCAAGUUAtt   | GAAUUCAGUAGUCCUUGAtt   | s37102  | s37103 | s37104 | +0.07 | 0.08 |
| <b>RUFY2</b>              | NM_017987    | FYVE        | GAGCUAGCAGUACAAGUUAtt  | GGAUUGAAGAAUGAGCUAtt   | GAUUGAAGAGUUAAGCAUAtt  | s31236  | s31237 | s31238 | +0.27 | 0.12 |
| <b>RUFY4</b>              | NM_198483    | FYVE        | GCAACAAAGGAAGACUCUAtt  | AGAAGAUCGCCAGCCGAUAtt  | GAAAGUCCAGGAAACAUAtt   | s49837  | s49838 | s49839 | -0.13 | 0.09 |
| <b>SBF1</b>               | NM_002972    | PH, GRAM    | CUAAGACUGUGGACGAGAAtt  | ACACGGAGGUGUUCAGGAAtt  | GCACUGCUGUUCCUCUCAtt   | s12482  | s12483 | s12484 | +0.57 | 0.07 |
| <b>SBF2</b>               | NM_030962    | PH, GRAM    | GAUGAUGAAUUGUACUCUAtt  | GCACUAUUAAAAUCCCGAtt   | GGACUGGGAUGAUACACCUAtt | s37818  | s37819 | s37820 | +0.36 | 0.08 |
| <b>SGK3</b>               | NM_001033578 | PX          | GAGCAUCCUUCAAAUGGAtt   | GAGCAGGACUAAACGAAUUt   | CAUUUUCUCCAAACAAtt     | s24316  | s24317 | s24318 | +0.03 | 0.05 |
| <b>SH3PXD2A</b>           | NM_014631    | PX          | GCUGGUGGUUAUCAGAUAtt   | GAAGGCUGGUGGUUAUAtt    | CCAUGAUCCUGGAACAGUAtt  | s18542  | s18543 | s18544 | +0.32 | 0.11 |
| <b>SH3PXD2B</b>           | NM_001017995 | PX          | AGGUCGAGGUGAUCGAGAAtt  | GCACAUUGGGAAAAAGAAAtt  | CCAUGGAAGGAGGACAGAAtt  | s49972  | s49973 | s49974 | +0.22 | 0.12 |
| <b>Non-target control</b> |              |             | AGUACUGCUUACGAUACGGtt  | UAACGACGCGACGACGUAAtt  | UCGUAAAGUAAGCGCAACCCtt | s229084 | s813   | s814   | +0.04 | 0.05 |
| <b>SMURF1</b>             | NM_020429    | C2          | CCUGCCAGAGAUACGAAAAtt  | GCAUGAACUGAAACCAAUUt   | CCAUAUGAGUCCUUAUGAGAtt | s32796  | s32797 | s32798 | +0.34 | 0.06 |
| <b>SMURF2</b>             | NM_022739    | C2          | CACACUUGCUUCAACGAAtt   | CACUUGCUUCAAUCCGAUAtt  | CCGGAACAUUUUCCUUAUUt   | s34857  | s34858 | s34859 | -0.38 | 0.07 |
| <b>SNAP91</b>             | NM_014841    | ENTH        | GGAUUUCUGGUACCACAAtt   | CAAACGAUUUCUACUAGAtt   | GUUUUAACUUAUCUGAAAtt   | s19161  | s19162 | s19163 | +0.10 | 0.06 |
| <b>SNX1</b>               | NM_003099    | PX          | GGGCCGCUUAGAAAGGUAtt   | GCCUCAUAGGGAUGACAAAtt  | CAACAGUGGUCCGAAAAGAtt  | s13255  | s13256 | s13257 | +0.26 | 0.07 |
| <b>SNX10</b>              | NM_013322    | PX          | GGCAGAGACUCCAAAGUAAtt  | GAUAUGUAUUCUACUAAUUt   | GCACUUUUGCUUUCAGAUAtt  | s26643  | s26644 | s26645 | +0.55 | 0.08 |
| <b>SNX11</b>              | NM_152244    | PX          | CUCCAGUUGUUGACUCUGAtt  | CCUCCAUACCAACGACAAAtt  | AGAUUUCUCCAUACCAAtt    | s26697  | s26698 | s26699 | -0.05 | 0.06 |



|                |              |        |                        |                         |                        |        |         |         |              |      |
|----------------|--------------|--------|------------------------|-------------------------|------------------------|--------|---------|---------|--------------|------|
| <b>SNX12</b>   | NM_013346    | PX     | UGAGGAGUCUUUCAUCGAAtt  | CCACCUAUGAGGUUCGCAUtt   | CUACCUAUCUUCAAGCUAAtt  | s26739 | s26740  | s26741  | <b>+0.14</b> | 0.12 |
| <b>SNX13</b>   | NM_015132    | PX     | GGAUGAAGUAUUCGACUUAAtt | GAGUAGCAGGAAAAACGAAtt   | CGGCUCAACUUGACGAUAAtt  | s23163 | s23164  | s23165  | <b>-0.07</b> | 0.06 |
| <b>SNX14</b>   | NM_020468    | PX     | GAAAUUUGCAGAACCUAGAtt  | CGUUUGGUCUCACUCAUAAtt   | GAACAUUGGUCUGUCUAUAtt  | s32927 | s32928  | s32929  | <b>+0.01</b> | 0.06 |
| <b>SNX15</b>   | NM_013306    | PX     | CCGCGCAGUUCAUCUCAAAtt  | AGGAAGGUGUGAGAAGAAtt    | UCGCUUCACUGUGCACAUAAtt | s26682 | s26683  | s26684  | <b>+0.43</b> | 0.14 |
| <b>SNX16</b>   | NM_022133    | PX     | GGGUCCAUUUGAUAGCCUAAtt | GAUAGACCAUCUACACCUAAtt  | CACUUGAGGUUGAUCAAGAtt  | s34409 | s34410  | s34411  | <b>+0.34</b> | 0.07 |
| <b>SNX17</b>   | NM_014748    | PX     | GCUUUUUGCUCAGACGGUAAtt | GGGAGUCUAUGGUCAAACUtt   | GUCUAUUCUUGAUUCGAGAtt  | s18903 | s18904  | s18905  | <b>-0.03</b> | 0.06 |
| <b>SNX18</b>   | NM_052870    | PX     | AGGUGACCGCUUCAAAAAtt   | CAUCAUCCAGUUCAGAAAtt    | GCAGCGAUGAUGACUGGGAtt  | s41342 | s229521 | s229522 | <b>+0.15</b> | 0.08 |
| <b>SNX19</b>   | NM_014758    | PX     | CACAUGCAAUGUAUCUUUAAtt | CACUGUGAAUCGUCGCUAAtt   | GUUUUGCCUUUGUCAAGAAtt  | s53225 | s53226  | s53227  | <b>-0.05</b> | 0.07 |
| <b>SNX2</b>    | NM_003100    | PX     | GCGACUUUCUUGGUUUGCAtt  | GAACAGAUUUCUAAAACGAtt   | GCAUUAUGAGUAACAACAAtt  | s13258 | s13259  | s13260  | <b>+0.34</b> | 0.10 |
| <b>SNX20</b>   | NM_182854    | PX     | GCAUCGAGGAGAGAAAAGUtt  | AGUUUGUGGUGUACCAAUtt    | GCAUGGGACCUUAACCCAtt   | s42740 | s42741  | s42742  | <b>-0.19</b> | 0.07 |
| <b>SNX21</b>   | NM_152897    | PX     | GAACGAGUCUUGUUUCUCUtt  | GCCGUUACUCGGACUUUGAtt   | UGGUAAUUCAGUAAAAAUtt   | s40288 | s40289  | s40290  | <b>+0.04</b> | 0.06 |
| <b>SNX22</b>   | NM_024798    | PX     | GAAUUUGUAUGCUCUUAAGAtt | GCUUCCAUGUGGAUCCUAtt    | GGCAGGGUCAAGAAGUAUAtt  | s36495 | s36496  | s36497  | <b>-0.04</b> | 0.08 |
| <b>SNX24</b>   | NM_014035    | PX     | CGACGACAAGGCUUGGAAAtt  | GGCAGAAAGUUGUGGAUCUtt   | CUUCUAAACAUGUUAGGAAtt  | s26312 | s26313  | s26314  | <b>+0.10</b> | 0.06 |
| <b>SNX25</b>   | NM_031953    | PX     | GUCUCUCAGCUUACGUUAUAtt | GGAUGAAAUAUCCUAAUAtt    | GCGAGUUUCAGAAUUUACAtt  | s38290 | s38291  | s38292  | <b>+0.13</b> | 0.06 |
| <b>SNX27</b>   | NM_030918    | PX     | GAACAGUACUACAGACCAAtt  | GGAACAACGGUUAACAGUCAAtt | GCAUUUGAAUGGGAUGAGAtt  | s37695 | s37696  | s37697  | <b>-0.20</b> | 0.06 |
| <b>SNX29</b>   | XM_001131890 | PX     | GAGUUUGUCGGAUUUUGAAtt  | GAAUAUUUAUCGCCGUAUtt    | AGACGAUGAAUGGAAUUAUtt  | s40838 | s40839  | s40840  | <b>+0.33</b> | 0.08 |
| <b>SNX3</b>    | NM_003795    | PX     | GCUCGGAAGUGAAUUAGAAtt  | GAAUCUACUGUUAAGAAGAAtt  | AGACAAAUCUCCUUAUUUtt   | s16618 | s16619  | s16620  | <b>+0.41</b> | 0.11 |
| <b>SNX30</b>   | XM_376902    | PX     | CAGCUUCGGUGACAAGGAUtt  | CCAGCCACUCAUCUCAUtt     | GGGAACCAUUGAUCGAAUAtt  | s53639 | s53640  | s53641  | <b>-0.12</b> | 0.08 |
| <b>SNX31</b>   | NM_152628    | PX     | GCAGAUUGAAGUUCCGGAAtt  | GAACUCUGCUGGAUACGGAtt   | CCAUGGACCCAACGUGUtt    | s46737 | s46738  | s46739  | <b>-0.20</b> | 0.10 |
| <b>SNX32</b>   | NM_152760    | PX     | GCACCCUGAUUCUCCGGAAtt  | AGGUGAAAUCACUGUUCAtt    | GAAAUUCACUGUCAAACAtt   | s48495 | s48496  | s48497  | <b>-0.02</b> | 0.07 |
| <b>SNX33</b>   | NM_153271    | PX     | CAACCGUUUCUCAUGCUUtt   | CAAAUUCAAGGGCAUCAAAtt   | GGCCGUAACCUCAACCGUtt   | s48887 | s48888  | s48889  | <b>+0.17</b> | 0.10 |
| <b>SNX4</b>    | NM_003794    | PX     | CAAGCUCUUUGGUCAAGAAtt  | GCGACGGAUUGGUUUAAGAAtt  | GCUACCUUUUAGUUUACUAtt  | s16615 | s16616  | s16617  | <b>-0.01</b> | 0.07 |
| <b>SNX5</b>    | NM_152227    | PX     | GAGUUAAGGAGGUAGAUGAtt  | CUGUAUCUGUGGACCUGAAtt   | CGAUACUACAUGCUCAAACAtt | s25876 | s25877  | s25878  | <b>+0.26</b> | 0.07 |
| <b>SNX6</b>    | NM_152233    | PX     | GGUCACUAGUGGAUUUAUGAtt | GCAGAUGGAGUAAUCGUUtt    | GGAGAAGGGUCAUAGCAGAtt  | s33937 | s33938  | s33939  | <b>-0.22</b> | 0.07 |
| <b>SNX7</b>    | NM_015976    | PX     | CAAUGAUAAACAAAUCAAtt   | GAAACUUUCAUUAACGUUAAtt  | CCGAAUUGCUGAUCAUCCAtt  | s28045 | s28046  | s28047  | <b>+0.54</b> | 0.15 |
| <b>SNX8</b>    | NM_013321    | PX     | CAAUAGCUUUCACAAGCUtt   | GAUCUUCUCAUUAUCGGGAtt   | CGUCAACUCUCAGAUCCAAtt  | s26640 | s26641  | s26642  | <b>+0.09</b> | 0.09 |
| <b>SNX9</b>    | NM_016224    | PX     | CAGUCGUGCUAGUUCUCAAtt  | GCAUCAUGUCUACGCGUtt     | GCAGUCCUAAAUUCCGAtt    | s28123 | s28124  | s28125  | <b>-0.10</b> | 0.06 |
| <b>SYNGAP1</b> | NM_006772    | PH, C2 | CGAACGAAGUCACAACCCAtt  | GCACCGAACCCAAUACGUtt    | GCACGUUACAGACAAUGAtt   | s16846 | s16847  | s16848  | <b>+0.83</b> | 0.20 |
| <b>SYT7</b>    | NM_004200    | C2 x2  | CCAUCAUCGUGAACAUCAUtt  | UCCAAGUCCUGGACUAUGAtt   | AGAAGACGGUGACGAUGAAtt  | s17291 | s17292  | s17293  | <b>-0.05</b> | 0.11 |

|                |              |                    |                        |                        |                        |         |         |         |       |      |
|----------------|--------------|--------------------|------------------------|------------------------|------------------------|---------|---------|---------|-------|------|
| <b>SYTL1</b>   | NM_032872    | C2 x2              | CCUGGGUCGCAACAUCUUUtt  | GAAGGACUGUUGACCUCAtt   | ACAUCUUUCUGGGCGAAGUtt  | s39754  | s39755  | s39756  | +0.77 | 0.09 |
| <b>SYTL2</b>   | NM_032379    | C2 x2              | GGACUCUACUUCAGAGGAAtt  | GGGAUACAUUUUAGCGCAAtt  | GGACUGAAGUGGACUGGAUtt  | s29567  | s29568  | s29569  | +0.95 | 0.08 |
| <b>SYTL4</b>   | NM_080737    | C2 x2, FYVE-type   | GCGGGACACUAAUUAUCCAtt  | GAGUUACUGGAGAUAAAAAtt  | GGAAAUAGAGUUGAAGAAAtt  | s230068 | s230069 | s230070 | -0.05 | 0.10 |
| <b>SYTL5</b>   | NM_138780    | C2 x2, FYVE-type   | GGUUUGUGCUUCAACCCAAtt  | CUCUUAGAAGCAAACGUAtt   | CAACAAGCGUAAGACCAAAtt  | s41275  | s41276  | s41277  | -0.26 | 0.09 |
| <b>TBC1D8</b>  | NM_001102426 | GRAM x2            | GAACGAAACGGGAAUUGCUtt  | CUCUACGACUUAUUAAGAtt   | CUAUUAUACAGGCUUCAUAtt  | s230654 | s230655 | s230656 | +0.34 | 0.05 |
| <b>TBC1D8B</b> | NM_198881    | GRAM x2            | GGACUCUACUGCUAAAGUAtt  | CUACUAAUCCUGACUUAUAtt  | GGCAAUCAGUGUAGUGUAAtt  | s29674  | s29675  | s29676  | +0.02 | 0.06 |
| <b>TBC1D9</b>  | NM_015130    | GRAM x2            | GCGAUGAUGUGGAACCUUAtt  | CUAUUAUCUUGCAGCUAUtt   | GGAUUUUGAACAAGAUCGAUtt | s23160  | s23161  | s23162  | +0.23 | 0.06 |
| <b>TBC1D9B</b> | NM_198868    | GRAM x2            | CGUGAUUUUCUUGGUGCAGAtt | CAGAUGCGGUUUAAACAGAtt  | GAGUGGACAUUGGACUCAAtt  | s22941  | s22942  | s22943  | +0.14 | 0.05 |
| <b>TNS1</b>    | NM_022648    | C2-tensin type     | GUUCCGCUCUCAAUCCUUUtt  | CCAGGACACUUCUUAAGUAtt  | CCAUCAUGCAGCAGAAUAAtt  | s14299  | s14300  | s14301  | +0.24 | 0.12 |
| <b>Tns2</b>    | NM_153533    | C1, C2-tensin type | CCUGAGCUGUUGACAAGCAAtt | CCCAUGUGCUUCAAUCCAAtt  | GAACACCCUUUACAAGAGAtt  | s102008 | s102009 | s102010 | -0.09 | 0.04 |
| <b>TNS3</b>    | NM_022748    | C2-tensin type     | GCUCAUUCAUUGUUCGAGAtt  | CUUACGAAGCUUAACCCAAtt  | GGAUUCGCAUCGCUAUCGAtt  | s34875  | s34876  | s34877  | +0.24 | 0.11 |
| <b>TPTE</b>    | NM_199261    | C2-tensin type     | CGUUAUGUACGUGAUUAAtt   | GAAAAUGUUCGGUACUUGAtt  | AGAAGAGAUUAGUUGCAUAtt  | s14361  | s14362  | s14363  | +0.73 | 0.11 |
| <b>ULK1</b>    | XM_001133335 | None               | GCAUCGGCACCAUCGUCUAtt  | GCAUCGGCACCAUCGUCUAtt  | GCAUCGGCACCAUCGUCUAtt  | s15963  | s15963  | s15963  | -0.93 | 0.02 |
| <b>UNC13A</b>  | NM_001080421 | C2 x3, C1          | GGUCCAAGCUGAUUACCCUtt  | GCAUACCUUUCUUCGGAUtt   | CAAUGAGUAUGUGACGGAAtt  | s22857  | s22858  | s22859  | +0.07 | 0.09 |
| <b>UNC13B</b>  | NM_006377    | C2 x3, C1          | GAAGCGUACCAAGACCAUtt   | GGAUUGCGCUGAAGACUAtt   | GCACUUCUCUUAAGGACGAtt  | s20574  | s20575  | s20576  | -0.38 | 0.02 |
| <b>UNC13D</b>  | NM_199242    | C2 x2              | ACUGAAUGGUUCCACCGUAtt  | GGGACAAGAUUCUCCACAAtt  | GAGCUUUGCUACAUGAACAtt  | s47356  | s47357  | s47358  | -0.52 | 0.07 |
| <b>VAV2</b>    | NM_003371    | PH, C1             | CGUUUGACAAGACCACCAAtt  | GCCUGCAAAAUGUUCUCAAtt  | CAGCAUCGCGCAGAACAAAtt  | s14753  | s14754  | s14755  | +0.73 | 0.08 |
| <b>VPS36</b>   | NM_016075    | GLUE               | CAGUUACCAGAGAAACCUAtt  | GCCCAUUCAGAGUAGUAAtt   | CCCAGUCAUUACAAACAAAtt  | s27276  | s27277  | s27278  | +0.41 | 0.08 |
| <b>WBP2</b>    | NM_012478    | GRAM               | CCGUUUUGGUGCAACUAtt    | AGAGCAUCCUAAUGUCCUAtt  | GCAUCCUAAUGUCCUUAUGAtt | s24092  | s24093  | s24094  | +0.76 | 0.04 |
| <b>WBP2NL</b>  | NM_152613    | GRAM               | GCCCGAGGAUUUCCACUAtt   | CUUCAUUAAGGGAACUUAUtt  | UCAGCUCUUAUGGGAUUUAtt  | s46539  | s46540  | s46541  | -0.45 | 0.04 |
| <b>WDFY1</b>   | NM_020830    | FYVE               | GGGUGUCUGCGAUUAUCUtt   | GCUCUCAGUGGUUGGAAAtt   | AGAUGAAGAUCCGACUUCUtt  | s33388  | s33389  | s33390  | -0.02 | 0.08 |
| <b>WDFY2</b>   | NM_052950    | FYVE               | GCAUGUCUUUUAAACCGGAtt  | GGAACUGACAAGGUUAUUAAtt | GACUGUCCAUAGGUCUAGAtt  | s41881  | s41882  | s41883  | +0.03 | 0.04 |
| <b>WDFY3</b>   | NM_014991    | FYVE, PH-Beac      | GCUUAAAAUUAUUAACCUUGtt | UGGUUAAUCUGUAACUUCtt   | GCACAUAGACUCAGAAGGAAtt | s200499 | s200500 | s200501 | +0.19 | 0.07 |
| <b>WDFY4</b>   | NM_020945    | PH-Beach           | GGAAGACUGAGGAUGUGAAtt  | GACAAGUUAUUUACAAGAtt   | GGUUUAAAGAAGUUGAGAAtt  | s229872 | s229873 | s229874 | +0.24 | 0.06 |
| <b>WDR45</b>   | NM_007075    | PROPPIN            | UCCCAGAAGGGUACCCUUAAtt | AGAUCGUGAUCGUGCUGAAtt  | CGCUUCCAGUGUAAGGGUtt   | s21995  | s21996  | s21997  | -0.47 | 0.04 |
| <b>WDR45B</b>  | NM_019613    | PROPPIN            | GCUGCAACUAAUUAGCUUtt   | CUAUAACACUGAUCCACUAtt  | GGAAUAAACAGUCCAGUUtt   | s32117  | s32118  | s32119  | -0.16 | 0.07 |
| <b>WIPI1</b>   | NM_017983    | PROPPIN            | GCACUAAUUGCUGCCCAUGAtt | GAAACUCCUGAAAACAGUtt   | CCCUCUACGAUCCAGAAtt    | s30081  | s30082  | s30083  | +0.46 | 0.07 |

|                |              |               |                       |                       |                        |        |        |        |              |      |
|----------------|--------------|---------------|-----------------------|-----------------------|------------------------|--------|--------|--------|--------------|------|
| <b>WIPI2</b>   | NM_016003    | PROPPIN       | GCAGGUCUUCGAUACCAUUt  | GUCUGGAAACGACCAUGAtt  | UGACGCAAGUGGAACUAAAtt  | s25100 | s25101 | s25102 | <b>+0.07</b> | 0.03 |
| <b>WWP1</b>    | NM_007013    | C2            | CAGUAGUUCUUCUAAUCCAtt | GGUUCGGAACAGCAAUUAtt  | GCACGAAUGGAAUAGAUAAAtt | s21788 | s21789 | s21790 | <b>+0.52</b> | 0.05 |
| <b>ZFYVE1</b>  | NM_178441    | FYVE x2       | GGAUGGGUCUCGAAAAUAtt  | GGAUGUAAGAAAAGCAUGAtt | CACUAGGUCUGGUAAAGGAtt  | s28712 | s28713 | s28714 | <b>-0.08</b> | 0.11 |
| <b>ZFYVE16</b> | NM_014733    | FYVE          | GGUGGAUCUAGUUUCGUAAtt | GCGGCUAGCUUACGAGAAtt  | CCUUCGAAAUUACCAGUAUtt  | s18852 | s18853 | s18854 | <b>+0.41</b> | 0.13 |
| <b>ZFYVE19</b> | NM_001077268 | FYVE          | GGAGUACGGCUGUAAGAAUtt | AGUUCACCCUCUUCAAGAAtt | CCUUUGAGCUUAAAGAGCAtt  | s39700 | s39701 | s39702 | <b>+0.02</b> | 0.07 |
| <b>ZFYVE21</b> | NM_024071    | FYVE, PH-like | GGACAAGGAGUGUCGGAGAtt | CUAUGAAAUCGAAAUUGUAtt | GACUUGUCGUCUUUCCAAUtt  | s35465 | s35466 | s35467 | <b>+0.34</b> | 0.11 |
| <b>ZFYVE26</b> | NM_015346    | FYVE          | GAAUGGUGUUUACUCUAUtt  | CCUUGCAAGAUGACGAUUAtt | GGAUGUGGUUGAGUACCUAtt  | s23943 | s23944 | s23945 | <b>+0.48</b> | 0.10 |
| <b>ZFYVE27</b> | NM_001002262 | FYVE          | CAGGUGAUGGUGUUCGAUAtt | CAGCAGAGGAUGAACCCAAtt | GAGCUGCAGUAAUUGUGGAtt  | s42248 | s42249 | s42250 | <b>+0.00</b> | 0.07 |
| <b>ZFYVE28</b> | NM_020972    | FYVE          | CUCUGAACUUGGACCGCAAtt | GAGAAGUAUUCUAAAACAtt  | GCAUUUCCAAGACGUGGAtt   | s33699 | s33700 | s33701 | <b>-0.06</b> | 0.07 |
| <b>ZFYVE9</b>  | NM_004799    | FYVE          | GGACUGAAUCUAAAUCCAtt  | CGAUUACAAGUUUACGGUtt  | GGACAUUACAAAACGAUUUtt  | s17931 | s17932 | s17933 | <b>-0.03</b> | 0.07 |

## Oligonucleotide Primers/Probes

### Appendix 2 – Oligonucleotide primers/probes

| Target                | Usage              | Forward (5' -> 3')                                      | Reverse (5' -> 3')       |
|-----------------------|--------------------|---|--------------------------|
| <b>AKAP13</b>         | qPCR               | GCAGAGCCCAGAATGTGAGA                                    | CCATGTCATCACTGGGTGAGT    |
| <b>ARHGEF2</b>        | qPCR               | TTCTCAGGTCTTAGTGCGGA                                    | CGGGTCACTTTCCGGATGAA     |
| <b><i>β-actin</i></b> | ZF, qPCR           | CGAACGACCAACCTAAACCTCTCG                                | ATGCGCCATACAGAGCAGAAGC   |
| <b>BNIP3</b>          | qPCR               | GGCCATCGGATTGGGGATCT                                    | GGCCACCCAGGATCTAACA      |
| <b>BNIP3L</b>         | qPCR               | TCCACCCAAGGAGTTCCACT                                    | GTGTGCTCAGTCGCTTTCCA     |
| <b>CHN1</b>           | qPCR               | CTAAAGAGAGTGACCCCTCCACG                                 | GGGTGGGTCCAAAAGACGATT    |
| <b>CPNE2</b>          | qPCR               | GTGTGCTCAGTCGCTTTCCA                                    | AGGATGAAGTACTGCGTGCC     |
| <b>CPNE7</b>          | qPCR               | AGGATGAAGTACTGCGTGCC                                    | AGGCCTCTGTGGCTGTAGTA     |
| <b>GAK</b>            | qPCR               | GTGGAGGAAGAGATCACGAGG                                   | AGATATCCTGCTTCTCGCCG     |
| <b>GRAMD1C</b>        | qPCR               | GCAACTGCTCCAGCAGAATA                                    | CTTCTTCCTGGACTTCTTGGCT   |
| <b>HIF1α</b>          | qPCR               | CTTCTTCCTGGACTTCTTGGCT                                  | GCAGGGTCAGCACTACTTCCG    |
| <b>HS1BP3</b>         | qPCR               | Qiagen - QT00094899                                     |                          |
| <b>ITSN1</b>          | qPCR               | CGGAGATGAGGCGTCGATTA                                    | ACTGCTGATCATGCTTCGCT     |
| <b>ITSN2</b>          | qPCR               | GGCTCAGTTTCCCACAGCTA                                    | ACGTGCTTGATCACCTGTTATGT  |
| <b>LYST</b>           | qPCR               | Qiagen - QT00094906                                     |                          |
| <b>PRKCD</b>          | qPCR               | GCAGGGTCAGCACTACTTCCG                                   | GCAGGGTCAGCACTACTTCCG    |
| <b><i>prkcd</i></b>   | ZF, qPCR           | TTGGCGTATCTGTGTTGGCT                                    | ATGACGACACACTGAGCCTG     |
| <b><i>prkcd</i></b>   | ZF, qPCR           | ACAAAAATGTGCCAGCGGAC                                    | ACGCGAAGTGTGGAGACAAT     |
| <b><i>prkcd</i></b>   | 5'UTR ISH Probe    | GCTCTGCCTGAGGGGTTGCCATGGC                               | GAGGCCTGTTTGACAAGACCC    |
| <b><i>prkcd</i></b>   | ORF ISH Probe      | CTGCTGGCAGAAGCTCTTACTCAAG                               | GAAGGTTGTGGCCGATTGTCTCC  |
| <b><i>prkcd</i></b>   | sgRNA #1 (Exon 2)  | taatacgactcactataGGGGCCATGGCAACCCCTCgtttttagagctagaa    |                          |
| <b><i>prkcd</i></b>   | sgRNA #2 (Exon 11) | taatacgactcactataGGGTGGGTGATTCGAGATGGgtttttagagctagaa   |                          |
| <b><i>prkcd</i></b>   | sgRNA #3 (Exon 15) | taatacgactcactataGGGAGTTCCGCAGAAGGTTGgtttttagagctagaa   |                          |
| <b><i>prkcd</i></b>   | 5'UTR ISH Probe    | GAAGCTGTGATCTCTCACCATG                                  | CCGAGAGGTTGGCAACCTTTG    |
| <b><i>prkcd</i></b>   | ORF ISH Probe      | CGGAGGGCTCTCAGTATGGG                                    | GGACGTCCATGCGGATGGAG     |
| <b><i>prkcd</i></b>   | sgRNA #1 (Exon 2)  | taatacgactcactataGGTCACCATGGCTCCGTTCTTGgtttttagagctagaa |                          |
| <b><i>prkcd</i></b>   | sgRNA #2 (Exon 8)  | taatacgactcactataGGTAGCCTGGTACGCGGTTTgtttttagagctagaa   |                          |
| <b><i>prkcd</i></b>   | sgRNA #3 (Exon 14) | taatacgactcactataGGGCCTCTTTGGTGATCCAGgtttttagagctagaa   |                          |
| <b>RAB11FIP1</b>      | qPCR               | GCAGGGTCAGCACTACTTCCG                                   | GCAGGGTCAGCACTACTTCCG    |
| <b>SMURF1</b>         | qPCR               | TACCGGATACCAGCGTTTGG                                    | ACCACTATCTGGCCACGAAC     |
| <b>SMURF2</b>         | qPCR               | CATGTCTAACCCCGGAGGC                                     | CAAATGGATCAGGAAGTCGGAAAA |
| <b>SYTL2</b>          | qPCR               | CTGTCCATTTGGCATCGGGA                                    | GTGCTGTCTTCGCTTCAGA      |
| <b>SYTL4</b>          | qPCR               | ATGTGCCTGGAAGTACTGT                                     | ACTGATCCCAGTGCCAACAC     |
| <b>SYTL5</b>          | qPCR               | GTGACAAAATCGCGCAGCTA                                    | GGACAACATCAGTGCCGAGA     |
| <b>SNX10</b>          | qPCR               | CAGAAAGTTCATCCTCTGGGCT                                  | CAGAAAGTTCATCCTCTGGGCT   |
| <b>SNX15</b>          | qPCR               | GATGACTTCTGCGGCACTA                                     | ACCACCACCTCTTTGACATCC    |
| <b>TBP</b>            | qPCR               | CAGAAAGTTCATCCTCTGGGCT                                  | TATATTCGGGTTTCGGGCA      |

|                |      |                        |                        |
|----------------|------|------------------------|------------------------|
| <b>UNC13B</b>  | qPCR | CTCTGCGTGCGCGTTAAAAG   | GGAAGGCTGATCACCACGAA   |
| <b>UNC13D</b>  | qPCR | CTCAAGGCAGAACAGCAGGA   | GAAGACAGAGCGGAACCTCC   |
| <b>WIPI1</b>   | qPCR | CCATAAGGCTGAACCGGCA    | CATAGACCTGTTGGGTTTGCAG |
| <b>WIPI2</b>   | qPCR | TGCTCGCTAGCCACAATTCA   | TGCTTCATCAGGGCACACTC   |
| <b>WDR45B</b>  | qPCR | GCCGAAATACCCTCCCAACA   | CCACAATTCTATCTCGCCGC   |
| <b>WDR45</b>   | qPCR | TCTGTCATTGCCATCTGCGT   | CACGTCGAAAGCCTCTCTGT   |
| <b>zFYVE21</b> | qPCR | GTCATGTCCTCCGAGGTGTC   | CATCTCCGACACTCCTTGTC   |
| <b>zFYVE26</b> | qPCR | CCTCAGAGGGAGAAACGATCAG | TACTGGAGATACCAGGAGGAGC |

## REFERENCES

1. Evans, C. S. & Holzbaur, E. L. F. Quality Control in Neurons: Mitophagy and Other Selective Autophagy Mechanisms. *J. Mol. Biol.* **432**, 240–260 (2020).
2. Montava-Garriga, L. & Ganley, I. G. Outstanding Questions in Mitophagy: What We Do and Do Not Know. *J. Mol. Biol.* (2019). doi:10.1016/j.jmb.2019.06.032
3. Wang, X. Le *et al.* Parkin, an E3 Ubiquitin Ligase, Plays an Essential Role in Mitochondrial Quality Control in Parkinson's Disease. *Cell. Mol. Neurobiol.* (2020). doi:10.1007/s10571-020-00914-2
4. McWilliams, T. G. *et al.* Basal Mitophagy Occurs Independently of PINK1 in Mouse Tissues of High Metabolic Demand. *Cell Metab.* **27**, 439-449.e5 (2018).
5. Lee, J. J. *et al.* Basal mitophagy is widespread in *Drosophila* but minimally affected by loss of Pink1 or parkin. *J. Cell Biol.* **217**, 1613–1622 (2018).
6. Bruick, R. K. Expression of the gene encoding the proapoptotic Nip3 protein is induced by hypoxia. *Proc. Natl. Acad. Sci. U. S. A.* **97**, 9082–7 (2000).
7. Jaakkola, P. *et al.* Targeting of HIF- $\alpha$  to the von Hippel-Lindau ubiquitylation complex by O<sub>2</sub>-regulated prolyl hydroxylation. *Science (80-. ).* **292**, 468–472 (2001).
8. Allen, G. F. G., Toth, R., James, J. & Ganley, I. G. Loss of iron triggers PINK1/Parkin-independent mitophagy. *EMBO Rep.* **14**, 1127–35 (2013).
9. Zhao, J.-F., Rodger, C. E., Allen, G. F. G., Weidlich, S. & Ganley, I. G. HIF1 $\alpha$ -dependent mitophagy facilitates cardiomyoblast differentiation. **4**, 99–113 (2020).
10. de la Ballina, L. R., Munson, M. J. & Simonsen, A. Lipids and lipid-binding proteins in

- selective autophagy. *J. Mol. Biol.* (2019). doi:10.1016/j.jmb.2019.05.051
11. Princely Abudu, Y. *et al.* NIPSNAP1 and NIPSNAP2 Act as ‘Eat Me’ Signals for Mitophagy. *Dev. Cell* **49**, 509-525.e12 (2019).
  12. Tang, M. Y. *et al.* Structure-guided mutagenesis reveals a hierarchical mechanism of Parkin activation. *Nat. Commun.* **8**, (2017).
  13. Yoshimori, T., Yamamoto, A., Moriyama, Y., Futai, M. & Tashiro, Y. Bafilomycin A1, a specific inhibitor of vacuolar-type H(+)-ATPase, inhibits acidification and protein degradation in lysosomes of cultured cells. *J. Biol. Chem.* **266**, 17707–12 (1991).
  14. Shepherd, D. & Garland, P. B. The kinetic properties of citrate synthase from rat liver mitochondria. *Biochem. J.* **114**, 597–610 (1969).
  15. Kirkwood, K. J., Ahmad, Y., Larance, M. & Lamond, A. I. Characterization of native protein complexes and protein isoform variation using sizefractionation- based quantitative proteomics. *Mol. Cell. Proteomics* **12**, 3851–3873 (2013).
  16. Larance, M., Ahmad, Y., Kirkwood, K. J., Ly, T. & Lamond, A. I. Global subcellular characterization of protein degradation using quantitative proteomics. *Mol. Cell. Proteomics* **12**, 638–650 (2013).
  17. Nascimbeni, A. C., Codogno, P. & Morel, E. Phosphatidylinositol-3-phosphate in the regulation of autophagy membrane dynamics. *FEBS J.* **284**, 1267–1278 (2017).
  18. Holland, P. *et al.* HS1BP3 negatively regulates autophagy by modulation of phosphatidic acid levels. *Nat. Commun.* **7**, (2016).
  19. Pankratz, N. *et al.* Genomewide association study for susceptibility genes contributing

- to familial Parkinson disease. *Hum. Genet.* **124**, 593–605 (2009).
20. Liu, J., Chen, J., Dai, Q. & Lee, R. M. Phospholipid scramblase 3 is the mitochondrial target of protein kinase C delta-induced apoptosis. *Cancer Res.* **63**, 1153–6 (2003).
  21. Pu, S. Y. *et al.* Optimization of Isothiazolo[4,3- b]pyridine-Based Inhibitors of Cyclin G Associated Kinase (GAK) with Broad-Spectrum Antiviral Activity. *J. Med. Chem.* **61**, 6178–6192 (2018).
  22. Asquith, C. R. M. *et al.* SGC-GAK-1: A Chemical Probe for Cyclin G Associated Kinase (GAK). *J. Med. Chem.* **62**, 2830–2836 (2019).
  23. Zhang, J. & Ney, P. A. Role of BNIP3 and NIX in cell death, autophagy, and mitophagy. *Cell Death Differ.* **16**, 939–46 (2009).
  24. Johansen, T. & Lamark, T. Selective Autophagy: ATG8 Family Proteins, LIR Motifs and Cargo Receptors. *J. Mol. Biol.* **432**, 80–103 (2020).
  25. Marinković, M., Šprung, M. & Novak, I. Dimerization of mitophagy receptor BNIP3L/NIX is essential for recruitment of autophagic machinery. *Autophagy* (2020).  
doi:10.1080/15548627.2020.1755120
  26. Kinoshita, E., Kinoshita-Kikuta, E., Takiyama, K. & Koike, T. Phosphate-binding tag, a new tool to visualize phosphorylated proteins. *Mol. Cell. Proteomics* **5**, 749–57 (2006).
  27. Scaduto, R. C. & Grotyohann, L. W. Measurement of mitochondrial membrane potential using fluorescent rhodamine derivatives. *Biophys. J.* **76**, 469–477 (1999).
  28. Matsuda, N. *et al.* PINK1 stabilized by mitochondrial depolarization recruits Parkin to damaged mitochondria and activates latent Parkin for mitophagy. *J. Cell Biol.* **189**,



- 211–221 (2010).
29. Petherick, K. J. *et al.* Pharmacological inhibition of ULK1 kinase blocks mammalian target of rapamycin (mTOR)-dependent autophagy. *J. Biol. Chem.* **290**, 11376–11383 (2015).
  30. Joo, J. H. *et al.* Hsp90-Cdc37 chaperone complex regulates Ulk1- and Atg13-mediated mitophagy. *Mol. Cell* **43**, 572–85 (2011).
  31. Stein, S. C., Woods, A., Jones, N. A., Davison, M. D. & Carling, D. The regulation of AMP-activated protein kinase by phosphorylation. *Biochem. J.* **345 Pt 3**, 437–43 (2000).
  32. Knapp, S. *et al.* A public-private partnership to unlock the untargeted kinome. *Nat. Chem. Biol.* **9**, 3–6 (2013).
  33. Heo, J. M. *et al.* RAB7A phosphorylation by TBK1 promotes mitophagy via the PINK-PARKIN pathway. *Sci. Adv.* **4**, 1–17 (2018).
  34. Kashatus, D. F. *et al.* RALA and RALBP1 regulate mitochondrial fission at mitosis. *Nat. Cell Biol.* **13**, 1108–1117 (2011).
  35. Linares, J. F., Amanchy, R., Diaz-Meco, M. T. & Moscat, J. Phosphorylation of p62 by cdk1 Controls the Timely Transit of Cells through Mitosis and Tumor Cell Proliferation. *Mol. Cell. Biol.* **31**, 105–117 (2011).
  36. Gavet, O. & Pines, J. Progressive Activation of CyclinB1-Cdk1 Coordinates Entry to Mitosis. *Dev. Cell* **18**, 533–543 (2010).
  37. Lee, D.-W., Zhao, X., Yim, Y.-I., Eisenberg, E. & Greene, L. E. Essential role of cyclin-G-

- associated kinase (Auxilin-2) in developing and mature mice. *Mol. Biol. Cell* **19**, 2766–76 (2008).
38. Greener, T. *et al.* Caenorhabditis elegans auxilin: A J-domain protein essential for clathrin-mediated endocytosis in vivo. *Nat. Cell Biol.* **3**, 215–219 (2001).
39. Kandachar, V., Bai, T. & Chang, H. C. The clathrin-binding motif and the J-domain of Drosophila Auxilin are essential for facilitating Notch ligand endocytosis. *BMC Dev. Biol.* **8**, 1–15 (2008).
40. Park, B. C. *et al.* The clathrin-binding and J-domains of GAK support the uncoating and chaperoning of clathrin by Hsc70 in the brain. *J. Cell Sci.* **128**, 3811–3821 (2015).
41. Wrighton, P. Quantitative intravital imaging reveals in vivo dynamics of physiological-stress induced mitophagy. 1–45 (2020).  
doi:<https://doi.org/10.1101/2020.03.26.010405>
42. Grünblatt, E. *et al.* Gene expression profiling of parkinsonian substantia nigra pars compacta; alterations in ubiquitin-proteasome, heat shock protein, iron and oxidative stress regulated proteins, cell adhesion/cellular matrix and vesicle trafficking genes. *J. Neural Transm.* **111**, 1543–73 (2004).
43. Song, L. *et al.* Auxilin Underlies Progressive Locomotor Deficits and Dopaminergic Neuron Loss in a Drosophila Model of Parkinson’s Disease. *Cell Rep.* **18**, 1132–1143 (2017).
44. Nguyen, M. & Krainc, D. LRRK2 phosphorylation of auxilin mediates synaptic defects in dopaminergic neurons from patients with Parkinson’s disease. *Proc. Natl. Acad. Sci. U. S. A.* **115**, 5576–5581 (2018).

45. Cowell, C. F. *et al.* Mitochondrial diacylglycerol initiates protein-kinase D1-mediated ROS signaling. *J. Cell Sci.* **122**, 919–28 (2009).
46. Zhang, T., Sell, P., Braun, U. & Leitges, M. PKD1 protein is involved in reactive oxygen species-mediated mitochondrial depolarization in cooperation with protein kinase C $\delta$  (PKC $\delta$ ). *J. Biol. Chem.* **290**, 10472–85 (2015).
47. Caso, S., Maric, D., Arambasic, M., Cotecchia, S. & Diviani, D. AKAP-Lbc mediates protection against doxorubicin-induced cardiomyocyte toxicity. *Biochim. Biophys. Acta - Mol. Cell Res.* **1864**, 2336–2346 (2017).
48. Zhang, P., Verity, M. A. & Reue, K. Lipin-1 regulates autophagy clearance and intersects with statin drug effects in skeletal muscle. *Cell Metab.* **20**, 267–279 (2014).
49. Botta, P. *et al.* Regulating anxiety with extrasynaptic inhibition. *Nat. Neurosci.* **18**, 1493–1500 (2015).
50. Caserta, T. M., Smith, A. N., Gultice, A. D., Reedy, M. A. & Brown, T. L. Q-VD-OPh, a broad spectrum caspase inhibitor with potent antiapoptotic properties. *Apoptosis* **8**, 345–52 (2003).
51. Lazarou, M. *et al.* The ubiquitin kinase PINK1 recruits autophagy receptors to induce mitophagy. *Nature* **524**, 309–314 (2015).
52. Carpenter, A. E. *et al.* CellProfiler: image analysis software for identifying and quantifying cell phenotypes. *Genome Biol.* **7**, R100 (2006).
53. Thisse, C. & Thisse, B. High-resolution in situ hybridization to whole-mount zebrafish embryos. *Nat. Protoc.* **3**, 59–69 (2008).

54. Stark, C. *et al.* BioGRID: a general repository for interaction datasets. *Nucleic Acids Res.* **34**, (2006).
55. Cline, M. S. *et al.* Integration of biological networks and gene expression data using cytoscape. *Nat. Protoc.* **2**, 2366–2382 (2007).
56. Ge, S. X., Jung, D., Jung, D. & Yao, R. ShinyGO: A graphical gene-set enrichment tool for animals and plants. *Bioinformatics* **36**, 2628–2629 (2020).
57. Kremer, J. R., Mastronarde, D. N. & McIntosh, J. R. Computer visualization of three-dimensional image data using IMOD. *J. Struct. Biol.* **116**, 71–76 (1996).
58. Fang, E. F. *et al.* In vitro and in vivo detection of mitophagy in human cells, *C. Elegans*, and mice. *J. Vis. Exp.* **2017**, 1–9 (2017).
59. Fang, E. F. *et al.* Mitophagy inhibits amyloid- $\beta$  and tau pathology and reverses cognitive deficits in models of Alzheimer’s disease. *Nat. Neurosci.* **22**, 401–412 (2019).
60. Palikaras, K., Lionaki, E. & Tavernarakis, N. Coordination of mitophagy and mitochondrial biogenesis during ageing in *C. elegans*. *Nature* **521**, 525–528 (2015).
61. Jao, L.-E., Wente, S. R. & Chen, W. Efficient multiplex biallelic zebrafish genome editing using a CRISPR nuclease system. *Proc. Natl. Acad. Sci. U. S. A.* **110**, 13904–9 (2013).
62. Montague, T. G., Cruz, J. M., Gagnon, J. A., Church, G. M. & Valen, E. CHOPCHOP: A CRISPR/Cas9 and TALEN web tool for genome editing. *Nucleic Acids Res.* **42**, 401–407 (2014).
63. Emran, F., Rihel, J. & Dowling, J. E. A behavioral assay to measure responsiveness of

Zebrafish to changes in light intensities. *J. Vis. Exp.* 1–6 (2008). doi:10.3791/923

64. Casado, P. *et al.* Kinase-substrate enrichment analysis provides insights into the heterogeneity of signaling pathway activation in leukemia cells. *Sci. Signal.* **6**, 1–14 (2013).
65. Cox, J. & Mann, M. MaxQuant enables high peptide identification rates, individualized p.p.b.-range mass accuracies and proteome-wide protein quantification. *Nat. Biotechnol.* **26**, 1367–1372 (2008).
66. Tyanova, S. *et al.* The Perseus computational platform for comprehensive analysis of (prote)omics data. *Nat. Methods* **13**, 731–740 (2016).

# Figure 1

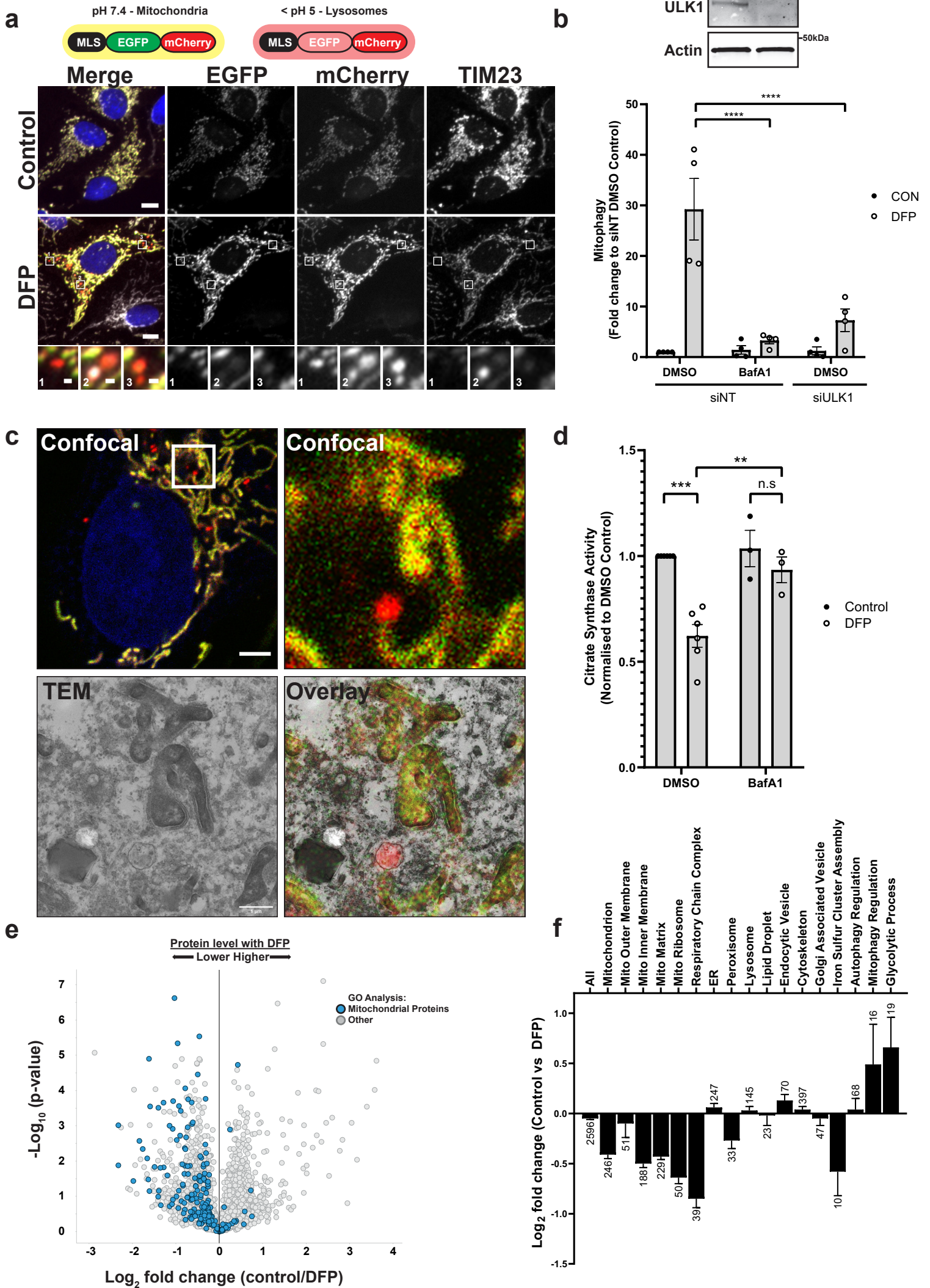


## Figure 1 - Measuring DFP-induced mitophagy in vitro

**a** U2OS cells stably expressing an internal MLS-EGFP-mCherry (IMLS) reporter that is pH responsive (yellow at neutral, red at acidic pH) were incubated for 24 h  $\pm$  1mM DFP followed by PFA fixation, antibody staining for TIM23 (Alexa Fluor-647) and widefield microscopy. Scale bar = 10  $\mu$ m, inset = 0.5  $\mu$ m. **b** U2OS IMLS cells were transfected with 7.5 nM siRNA non-targeting control (siNT) or siULK1 for 48 h prior to 24 h treatment  $\pm$  1 mM DFP in the presence or absence of 50 nM BafA1 for the final 2 h. Western blot from cell lysates shows representative ULK1 knockdown level. Graph represents the mean red only area per cell from fluorescence images normalised to control DMSO siNT cells  $\pm$  SEM from n=4 independent experiments. Significance was determined by two-way ANOVA followed by Tukey's multiple comparison test. **c** U2OS IMLS cells treated with 1 mM DFP as in **a** and fixed for CLEM analysis. Inset of cell area in white box is shown by confocal analysis and EM section along with EM overlay. Scale bar = 5 $\mu$ m, inset = 1 $\mu$ m **d** Citrate synthase activity from U2OS cells treated for 24 h  $\pm$  1 mM DFP with final 16 h in the presence of 50 nM BafA1 or DMSO, values are normalised to DMSO control from n=6 (DMSO) or n=3 (+BafA1) independent experiments  $\pm$  SEM. Significance was determined by two-way ANOVA followed by Sidak's multiple comparisons test. **e** U2OS whole cell protein abundance was determined by mass spectrometry following treatment  $\pm$  1 mM DFP 24 h. Mitochondrial proteins identified by GO analysis (Term = Mitochondrion) are highlighted in blue. **f** Mean T-test difference between Control and DFP samples for peptides identified in **e** matching GO terms related to cellular organelles. Bars represent Log<sub>2</sub> fold change (Control vs DFP)  $\pm$  SEM, number on bars indicate how many protein targets are included in GO analysis. \*\* = p < 0.01, \*\*\* = p < 0.001, \*\*\*\* = p < 0.0001 and n.s = not significant in all relevant panels.

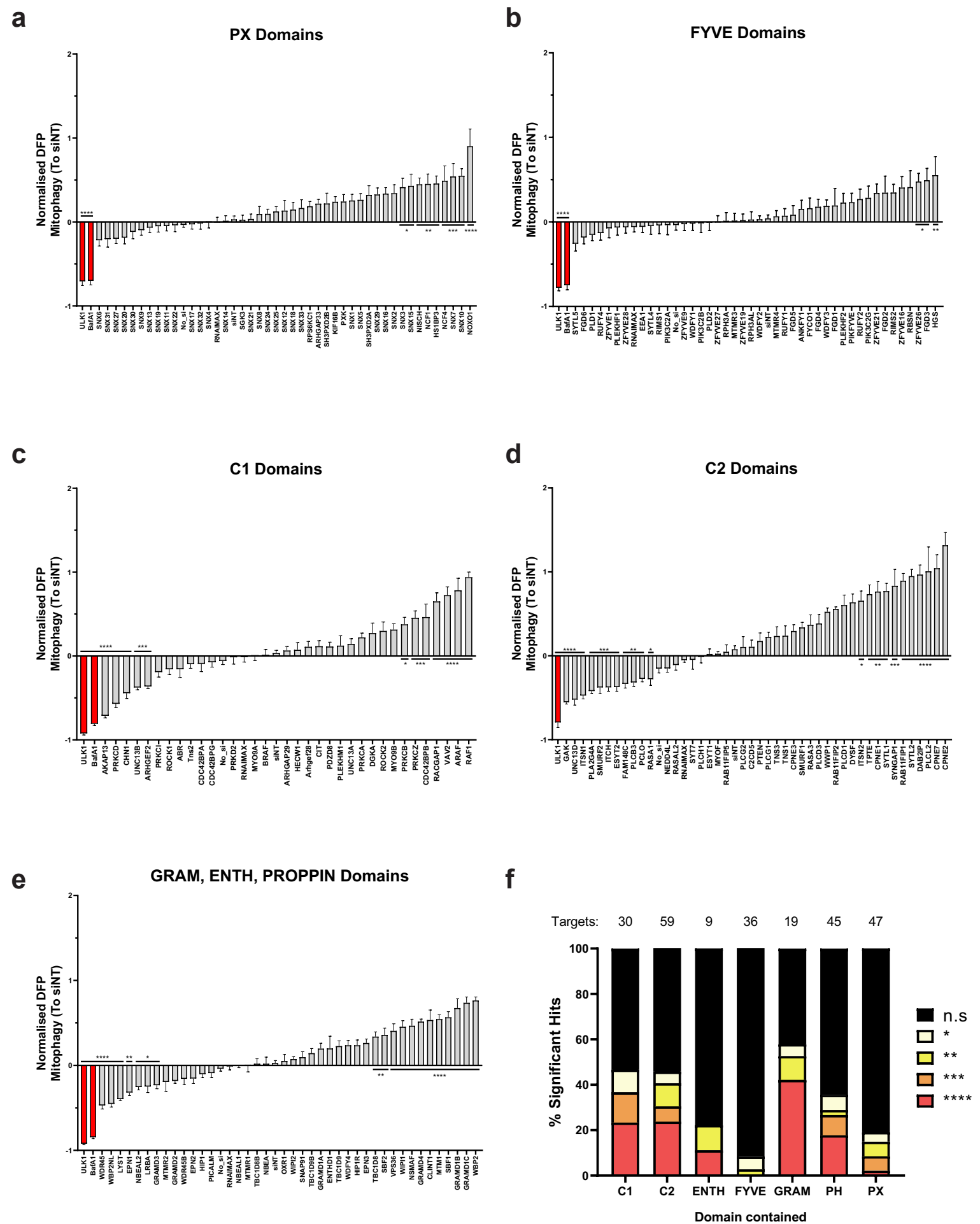




## Figure 2 – siRNA screen for lipid binding proteins involved in DFP-induced mitophagy.

**a-e** Primary siRNA screen data. U2OS cells were transfected with a pool of 3 sequence variable siRNA oligonucleotides per gene target (2.5 nM per oligo) for 48 h before addition of 1 mM DFP for 24 h. Cells were PFA fixed and imaged using a 20x objective (35 fields of view per well). The red area per cell was normalised to the average of siNT controls and adjusted so that the DFP siNT control was 0 from n= 14 plates (**a,b**) or n=6 plates (**c-e**)  $\pm$  SEM. siULK1 and BafA1 (red bars) are negative controls. siRNA targets containing similar lipid binding domains were assayed and plotted together as shown for **a** PX domains, **b** FYVE domains **c** C1 domains **d** C2 domains **e** GRAM, ENTH, PROPPIN domains. **f** Summary of significance of different lipid binding domains relative to the total tested from a e, proteins containing more than one type of domain are represented in each category. Significance was determined by one-way ANOVA followed by Dunnett's multiple comparison test to the siNT control where \* =  $p < 0.05$ , \*\* =  $p < 0.01$ , \*\*\* =  $p < 0.001$ , \*\*\*\* =  $p < 0.0001$  and n.s = not significant in all relevant panels.

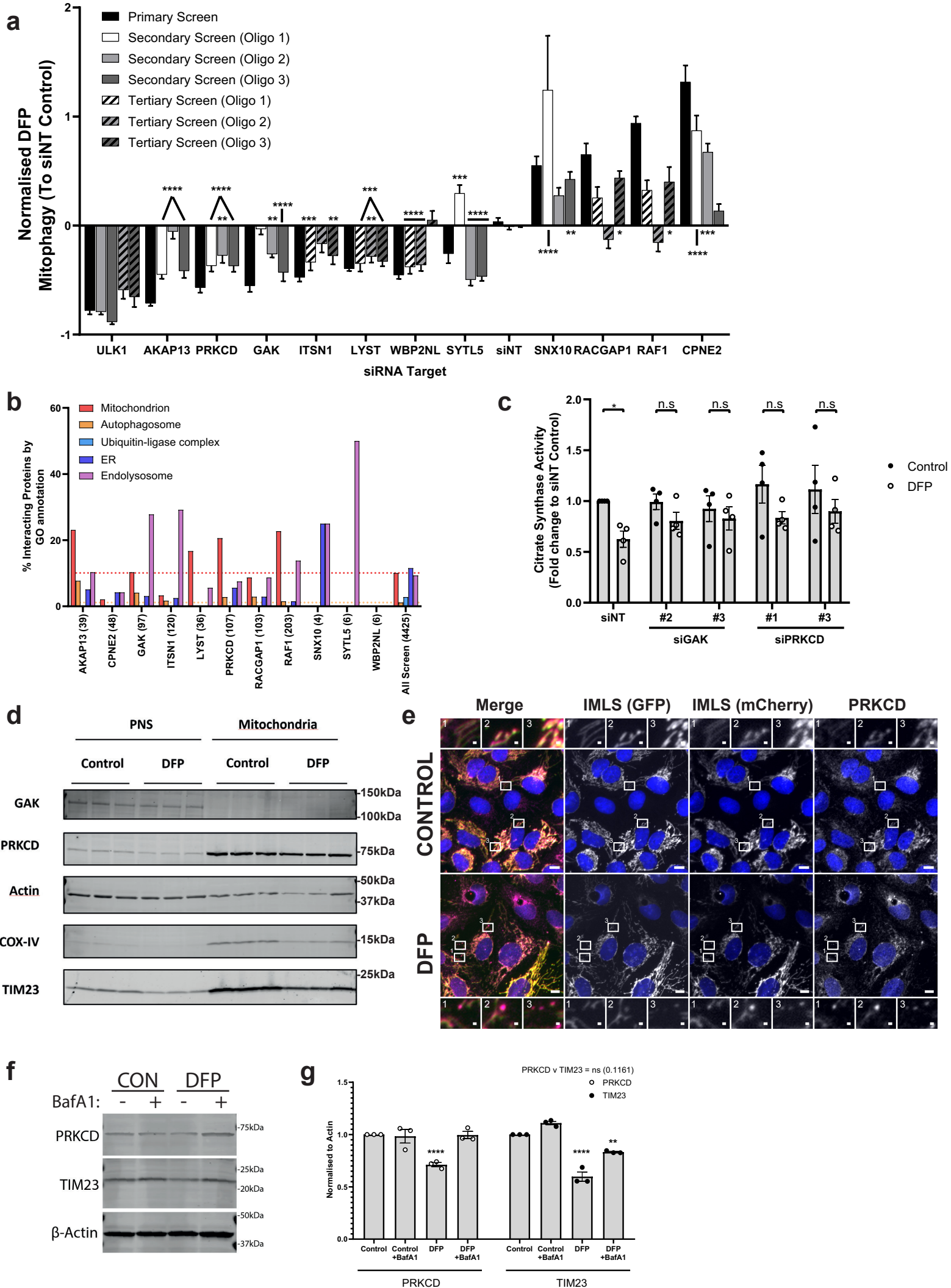


**Figure 3 - GAK and PRKCD are regulators of DFP mediated mitophagy.**

**a** Summary of significant targets identified across primary, secondary (7.5 nM individual siRNA oligos) and tertiary screen (15 nM each oligo) siRNA screens. Cells were transfected for 48 h prior to 24 h of 1 mM DFP treatment. Bars represent mean fold change in mitophagy relative to the siNT controls  $\pm$  SEM. Significance was determined by one-way ANOVA followed by Dunnett's multiple comparison test to the siNT control. **b** Protein-protein interaction networks for candidate proteins (see methods) were plotted by % of interacting proteins belonging to each highlighted compartment, value in brackets represents total number of interacting proteins. **c** siRNA treatment with indicated oligos for 48 h prior to 24 h treatment  $\pm$  1 mM DFP and subsequent analysis of citrate synthase activity levels. Values were normalised to the siNT control and plotted  $\pm$  SEM for n=4 independent experiments. Significance was determined by two-way ANOVA followed by Sidak's multiple comparison test. **d** U2OS cells treated  $\pm$  1 mM DFP for 24 h were enriched from a post-nuclear supernatant (PNS) for mitochondria followed by western blotting for the indicated proteins. **e** U2OS IMLS cells treated  $\pm$  1 mM DFP for 24 h followed by PFA fixation and staining for endogenous PRKCD (Alexa Fluor-647). Images were obtained by 20x objective using a Zeiss AxioObserver. Scale bar = 10  $\mu$ m, insets = 1  $\mu$ m. **f** U2OS cells treated  $\pm$  1 mM DFP for 24 h  $\pm$  50 nM BafA1 for the final 16 h and blotted for the indicated proteins. **g** Quantitation of PRKCD and TIM23 levels to  $\beta$ -actin in **f** from n=3 independent experiments  $\pm$  SEM. Significance was determined by two-way ANOVA followed by Dunnett's multiple comparison test to the control. \* = p < 0.05, \*\* = p < 0.01, \*\*\* = p < 0.001, \*\*\*\* = p < 0.0001 and n.s = not significant in all relevant panels.

# Figure 4

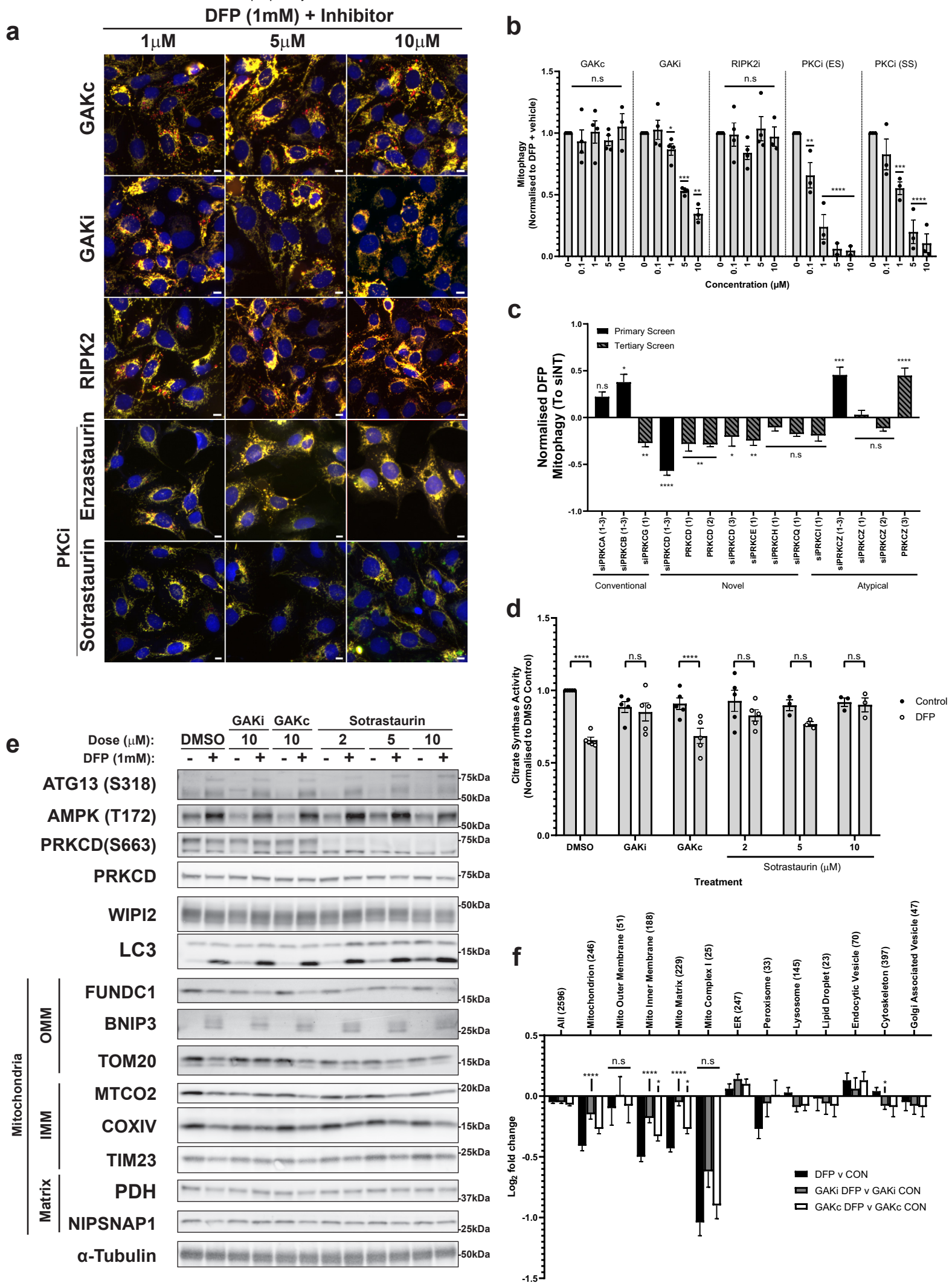
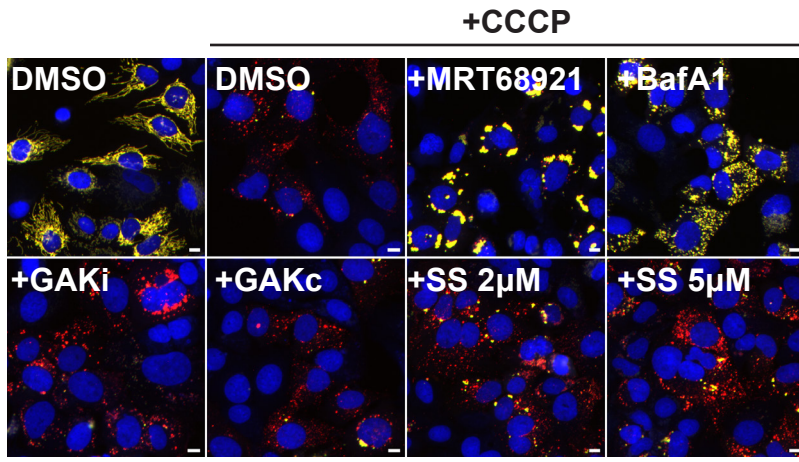


#### Figure 4 – GAK and PRKCD kinase activity regulates DFP-induced mitophagy

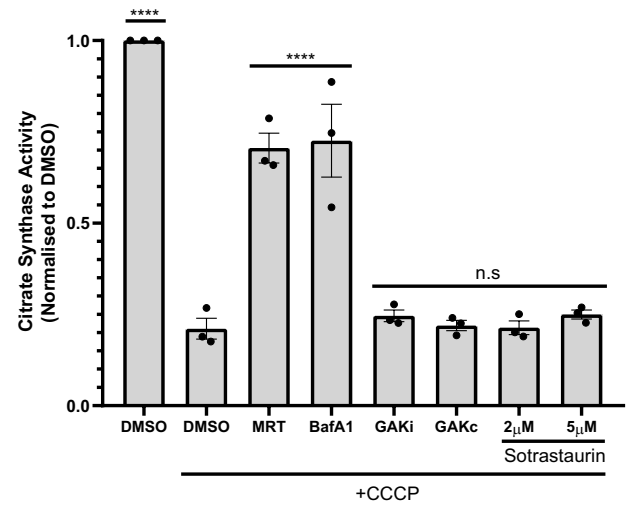
**a** Fluorescence images of U2OS IMLS cells treated with 1 mM DFP for 24 h in the presence of indicated inhibitors at stated concentrations (1-10  $\mu$ M). Scale bar = 10  $\mu$ m **b** Quantitation of cells red only structures normalised to DMSO + DFP control treatment. Significance was determined by two-way ANOVA followed by Dunnett's multiple comparison test to the DMSO + DFP control from a minimum of n=3 independent experiments. **c** U2OS IMLS cells treated with siRNA against indicated PKC isoforms (Primary screen = 7.5 nM, Tertiary = 15 nM) for 48 h prior to induction of mitophagy with 1 mM DFP for 24 h. Value in brackets represents oligonucleotide # used. Values represent mean fold change in mitophagy relative to the siNT control  $\pm$  SEM from n=3 independent experiments. Significance was determined by one-way ANOVA to the relevant siNT control. **d** Citrate synthase activity of U2OS cells treated 24 h  $\pm$  1 mM DFP in combination with 10  $\mu$ M GAKi, GAKc or 2-10  $\mu$ M Sotrastaurin. Values represent mean citrate synthase activity normalised to DMSO control and plotted  $\pm$  SEM from n=3 (Sotrastaurin 5/10 $\mu$ m) or n=5 independent experiments. Significance was determined by two-way ANOVA followed by Sidak's multiple comparison test. **e** U2OS cells were treated  $\pm$  1 mM DFP 24 h with GAKi or GAKc (10  $\mu$ M), Sotrastaurin (2-10  $\mu$ M) or DMSO control and western blotted for indicated proteins, including outer mitochondrial membrane (OMM), inner mitochondrial membrane (IMM) or Matrix proteins. **f** Cellular protein abundance was determined by mass spectrometry. U2OS cells were treated  $\pm$  1 mM DFP for 24 h in addition to DMSO, GAKi or GAKc (both 10  $\mu$ M) and analysed by mass spectrometry. Comparison of mean abundance of GO annotated proteins between control and DFP treated samples for each GAKi, GAKc and DMSO control are shown  $\pm$  SEM, value in brackets represent number of proteins classified in group by GO analysis. Significance was determined by two-way ANOVA followed by Dunnett's post-test to the DFP v CON sample. Significance is denoted in figure where: \* = p < 0.05, \*\* = p < 0.01, \*\*\* = p < 0.001, \*\*\*\* = p < 0.0001 and n.s = not significant in all relevant panels.

# Figure 5

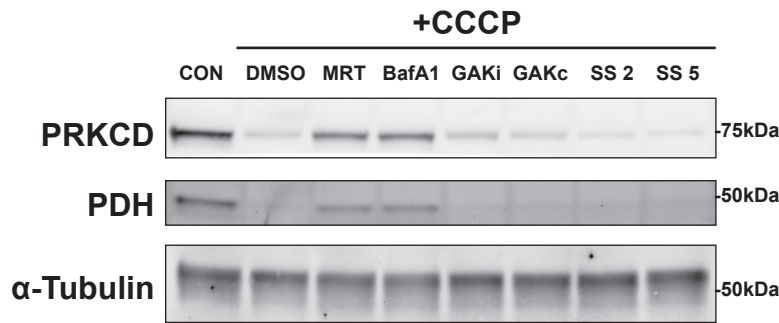
**a**



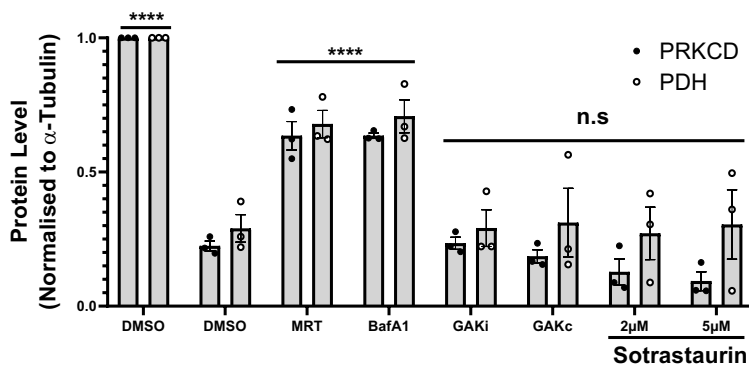
**b**



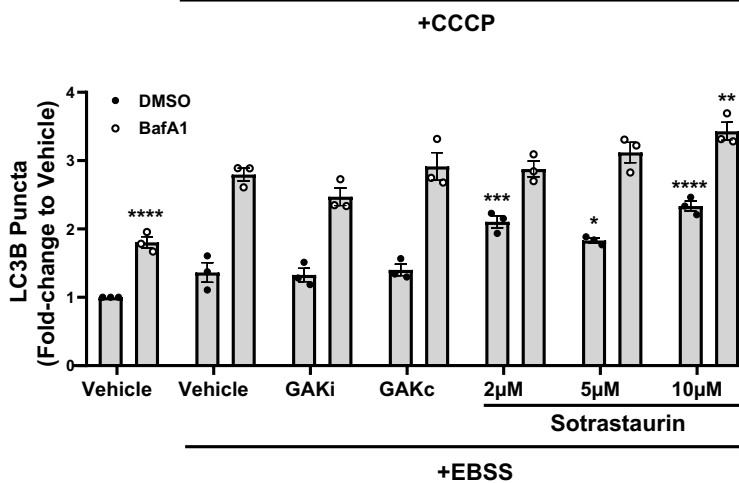
**c**



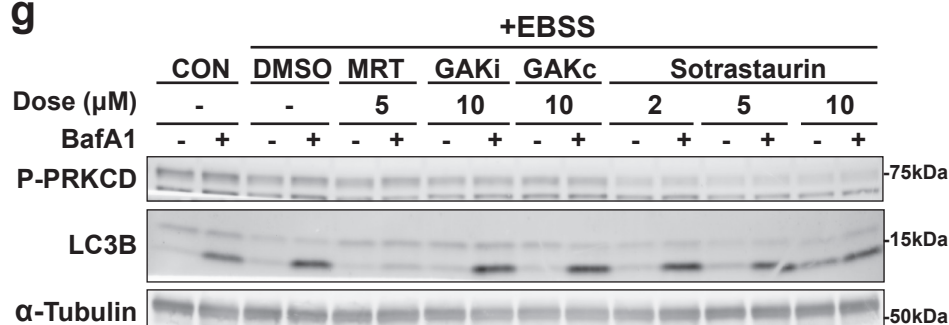
**d**



**f**



**g**



**e**

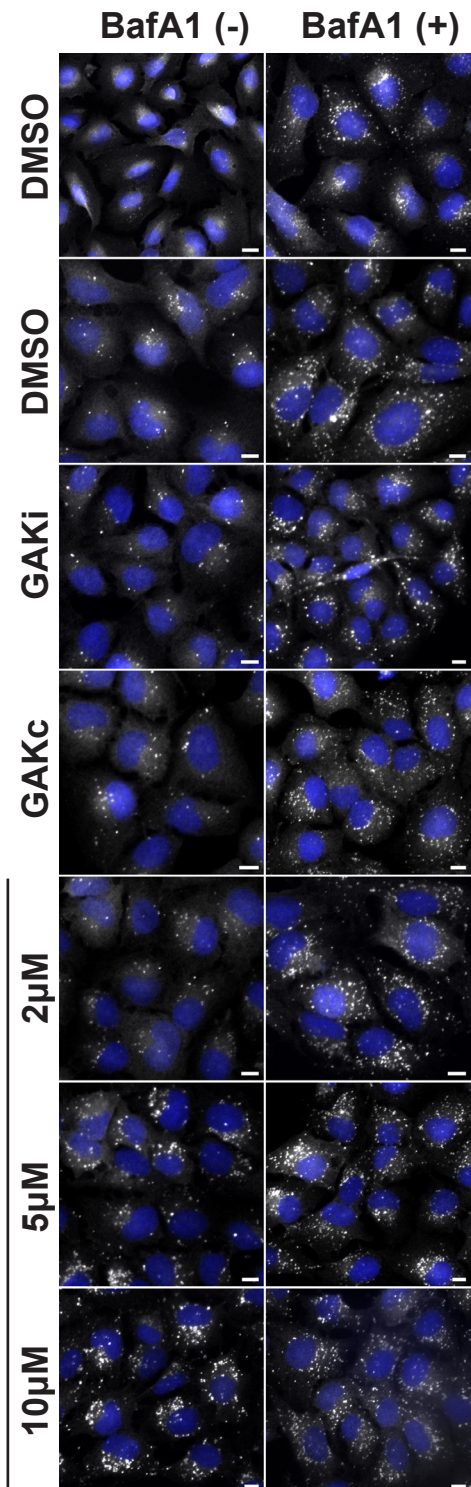
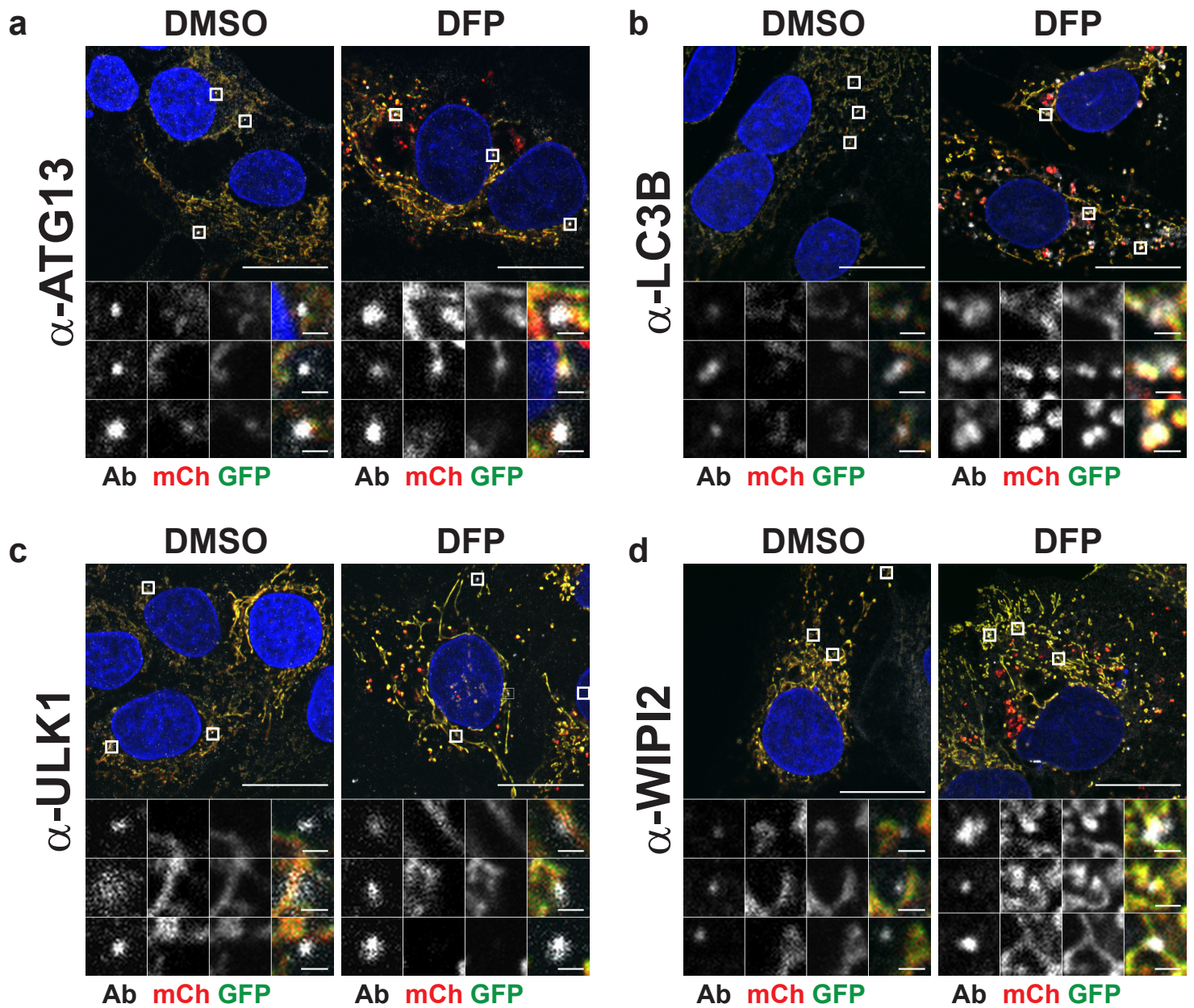


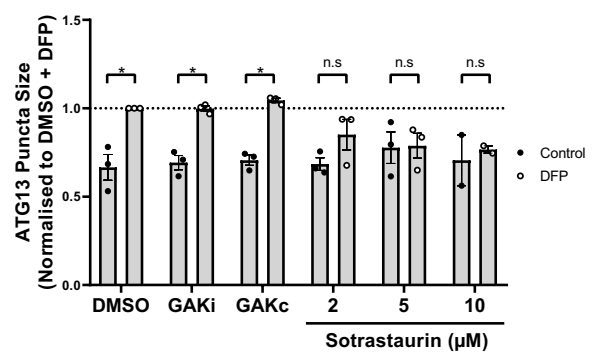
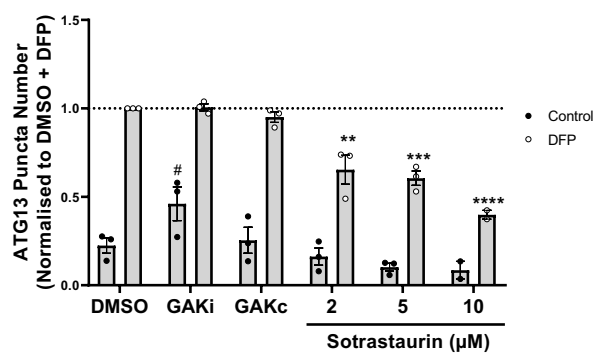
## Figure 5 – GAK and PRKCD kinase activity are dispensable for PRKN-dependent mitophagy

**a** Representative fluorescence images of U2OS IMLS-PRKN cells treated for 16 h  $\pm$  20  $\mu$ M CCCP and including 10  $\mu$ M QVD-OPh to promote cell survival in addition to either MRT68921 (5  $\mu$ M), BafA1 (50 nM), GAKi (10  $\mu$ M), GAKc (10  $\mu$ M) or Sotrastaurin (2-5  $\mu$ M). Scale bar = 10 $\mu$ m **b** Cells treated as in **a** and assayed for citrate synthase activity and normalised to DMSO control. Mean value plotted  $\pm$  SEM from n=3 independent experiments and significance determined by one-way ANOVA followed by Dunnett's multiple comparison to the CCCP+DMSO control. **c** Representative example of western blots from cells treated as in **a** and blotted for indicated proteins. **d** Quantitation of PRKCD and PDH levels from western blots in **c** from n=3 independent experiments  $\pm$  SEM. Values represent protein level normalised first to  $\alpha$ -Tubulin and subsequently normalised to the DMSO control. Significance was determined by two-way ANOVA followed by Dunnett's multiple comparison test to the DMSO control. **e** Representative 20x immunofluorescence images of U2OS cells stained for endogenous LC3B and nuclei (DAPI, blue). Cells were grown in complete media or EBSS (starvation) media for 2 h with addition of GAKi (10  $\mu$ M), GAKc (10  $\mu$ M) or Sotrastaurin (2-10 $\mu$ M)  $\pm$  50 nM BafA1, scale bar = 10  $\mu$ m. **f** Quantitation of LC3B puncta from **e**. The average LC3 puncta per cell was normalised to that of the complete media control and represents the mean  $\pm$  SEM from n=3 independent experiments. Significance was determined by two-way ANOVA followed by Dunnett's multiple comparison test to the EBSS vehicle treated sample. **g** Representative western blot of cells treated as in **e** and blotted for indicated proteins. \* = p < 0.05, \*\* = p < 0.01, \*\*\* = p < 0.001 and \*\*\*\* = p < 0.0001 and n.s = not significant in all relevant panels.

# Figure 6



**e**



**f**

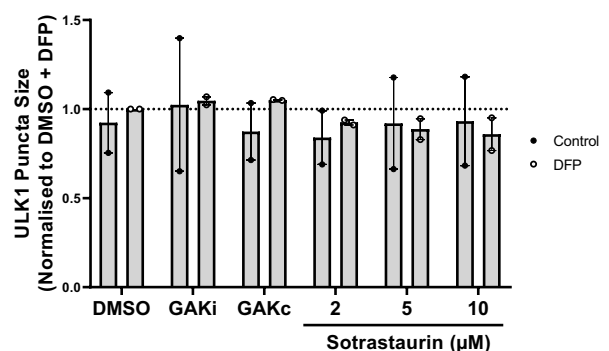
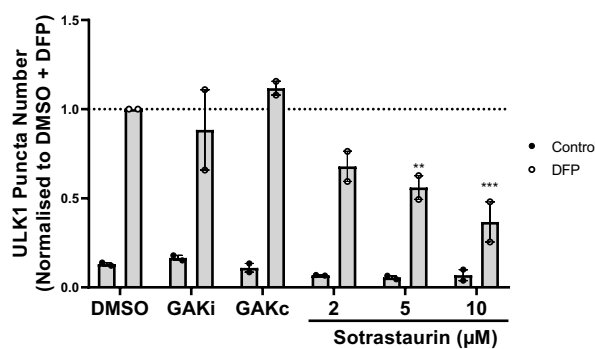


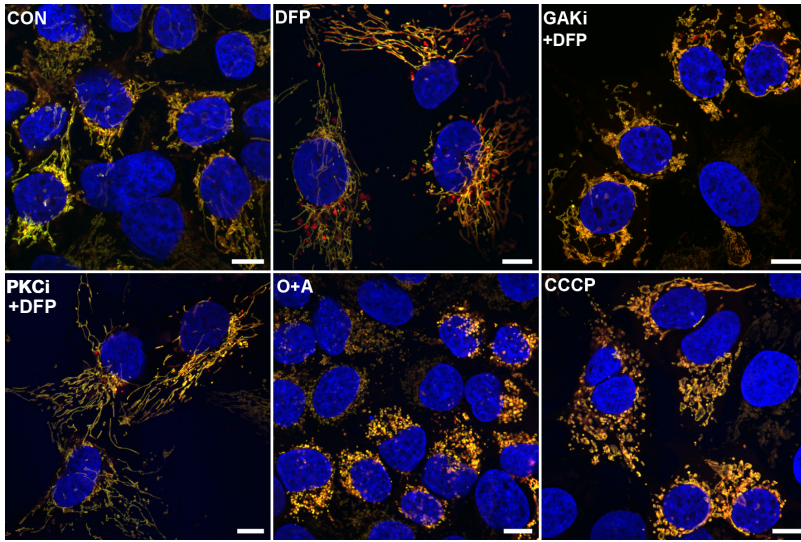


## Figure 6 – Early autophagy protein recruitment is defective upon PKCi

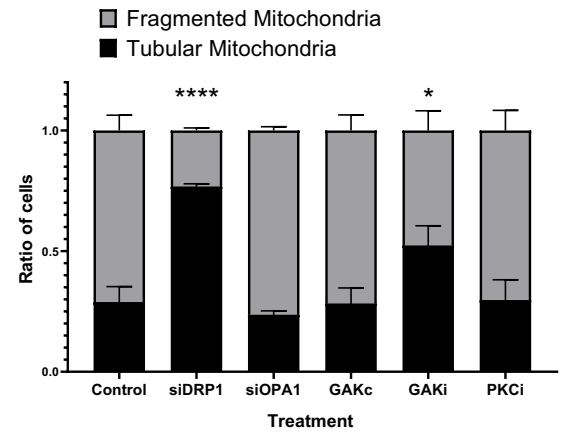
**a-d** U2OS IMLS cells were treated  $\pm$  1 mM DFP for 24 h, fixed and stained for nuclei (DAPI) and the indicated endogenous autophagy markers; **a** ATG13, **b** LC3B, **c** ULK1 or **d** WIPI2. Representative 63x images of cells taken by Zeiss LSM 710 are shown, scale bar = 10  $\mu$ m. **e-f** U2OS cells were treated  $\pm$  1 mM DFP for 24 h together with GAKi (10  $\mu$ M), GAKc (10  $\mu$ M) or Sotrastaurin (2-10  $\mu$ M), then fixed in PFA before staining for nuclei (DAPI) and the indicated endogenous early autophagy markers; **e** ATG13, **f** ULK1. The number and size of puncta formed for each marker was analysed and values obtained were normalised to the DMSO + DFP control. Mean values were plotted from n=3 independent experiments  $\pm$  SEM. Significance was determined by two-way ANOVA and Dunnett's multiple comparisons test to the DMSO+DFP control sample where \* =  $p < 0.05$ , \*\* =  $p < 0.01$ , \*\*\* =  $p < 0.001$ , \*\*\*\* =  $p < 0.0001$ , n.s = not significant and # =  $p < 0.05$  (to the DMSO Control).

# Figure 7

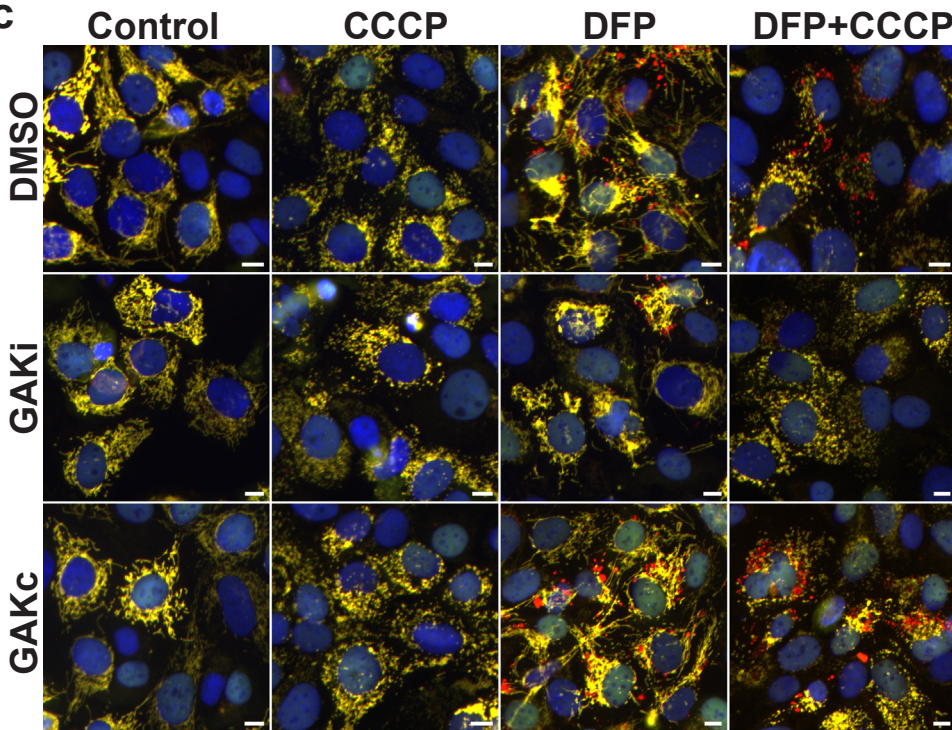
**a**



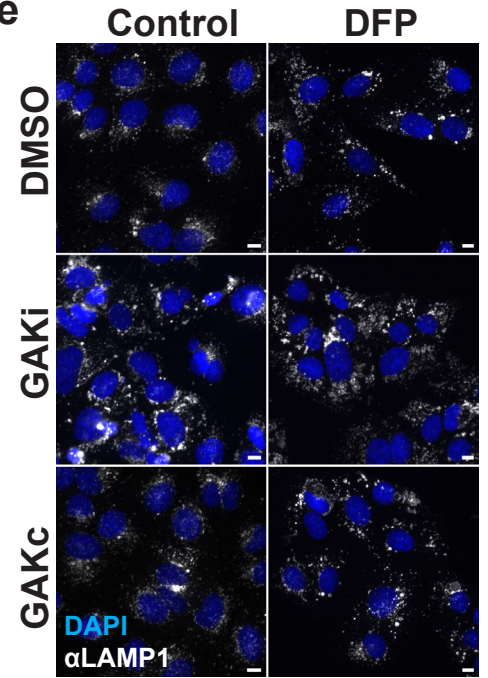
**b**



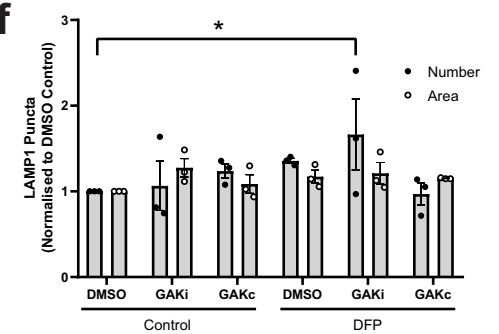
**c**



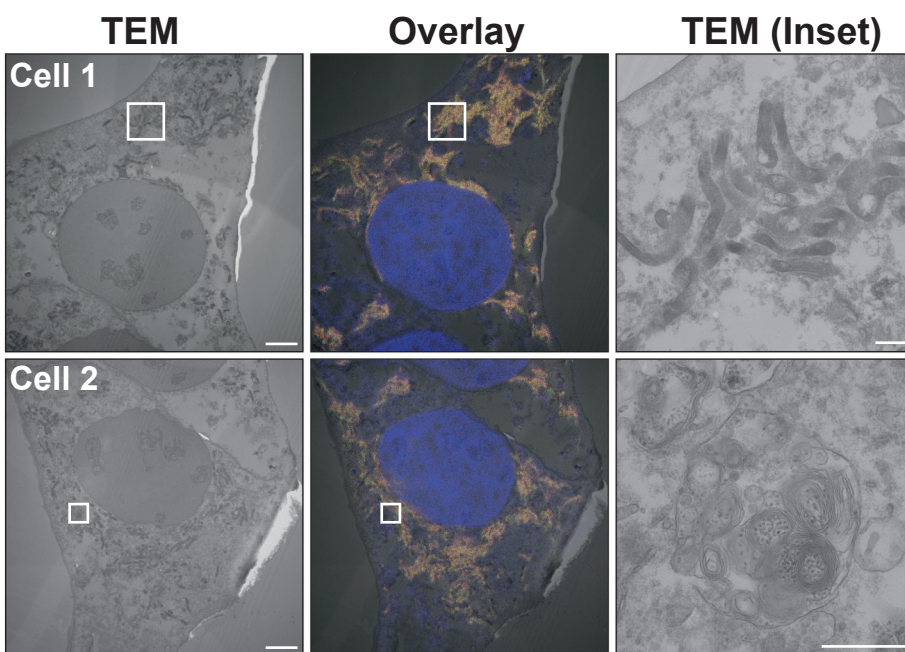
**e**



**f**



**d**



**g**

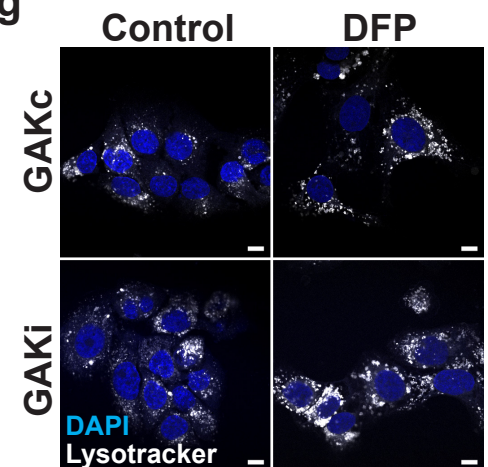


## Figure 7 – GAKi induces abnormal mitochondrial and lysosomal morphology

**a** Representative 63x images of U2OS IMLS cells taken by Zeiss LSM 710 confocal microscopy. Cells were treated  $\pm$  1 mM DFP 24 h in addition to GAKi (10  $\mu$ M), Sotrastaurin (PKCi – 2  $\mu$ M), Oligomycin and Antimycin A (O+A – 10  $\mu$ M and 1  $\mu$ M respectively) or CCCP (20  $\mu$ M), scale bar = 10  $\mu$ m. **b** Machine learning classification of U2OS IMLS cell mitochondrial network as fragmented or tubular (utilising EGFP images, see methods) after 24 h treatment with GAKi (10  $\mu$ M), GAKc (10  $\mu$ M) or Sotrastaurin (PKCi – 2 $\mu$ M) compared to 72 h knockdown of non-targeting control, siDRP1 or siOPA1. Significance was determined by two-way ANOVA followed by Dunnett's post-test to the control treatment. **c** U2OS IMLS cells were treated as indicated with DMSO, GAKi or GAKc (10  $\mu$ M each) for 24 h in addition to either DFP (24h, 1 mM), CCCP (20  $\mu$ M, 12 h) or in combination. Images obtained by 20x objective, scale bar = 10 $\mu$ m. **d** U2OS IMLS cells were treated with 1 mM DFP + 10  $\mu$ M GAKi for 24h prior to fixation for CLEM analysis. EM images demonstrate mitochondrial clustering (Cell 1) and an increase in autolysosome structures (Cell 2) induced by GAKi treatment, scale bar = 10  $\mu$ m, inset = 1  $\mu$ m. **e** U2OS cells treated  $\pm$  1 mM DFP 24 h in addition to DMSO, GAKi (10 $\mu$ M) or GAKc (10 $\mu$ M) were PFA fixed and subsequently stained for endogenous LAMP1. Images acquired by widefield microscopy on a Zeiss AxioObserver microscope, scale bar=10  $\mu$ m. **f** Quantitation of LAMP1 structures identified in **e** for size and number from n=3 independent experiments and plotted as mean  $\pm$  SEM. Significance was determined by two-way ANOVA followed by Dunnett's multiple comparisons test to the DMSO control. **g** U2OS cells were treated for 24 h  $\pm$  1 mM DFP with either GAKc (10  $\mu$ M) or GAKi (10  $\mu$ M) and then stained for lysosomes using lysotracker red DND-99 at 50 nM. Representative images taken by Zeiss LSM710, scale bar = 10  $\mu$ m. Significance was denoted where \* =  $p < 0.05$ , \*\*\*\* =  $p < 0.0001$  and n.s = not significant.

# Figure 8

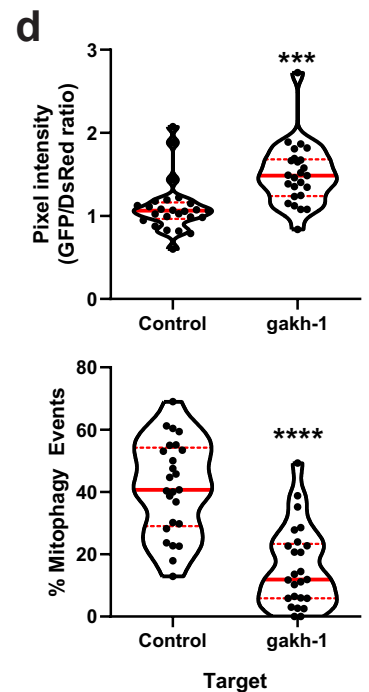
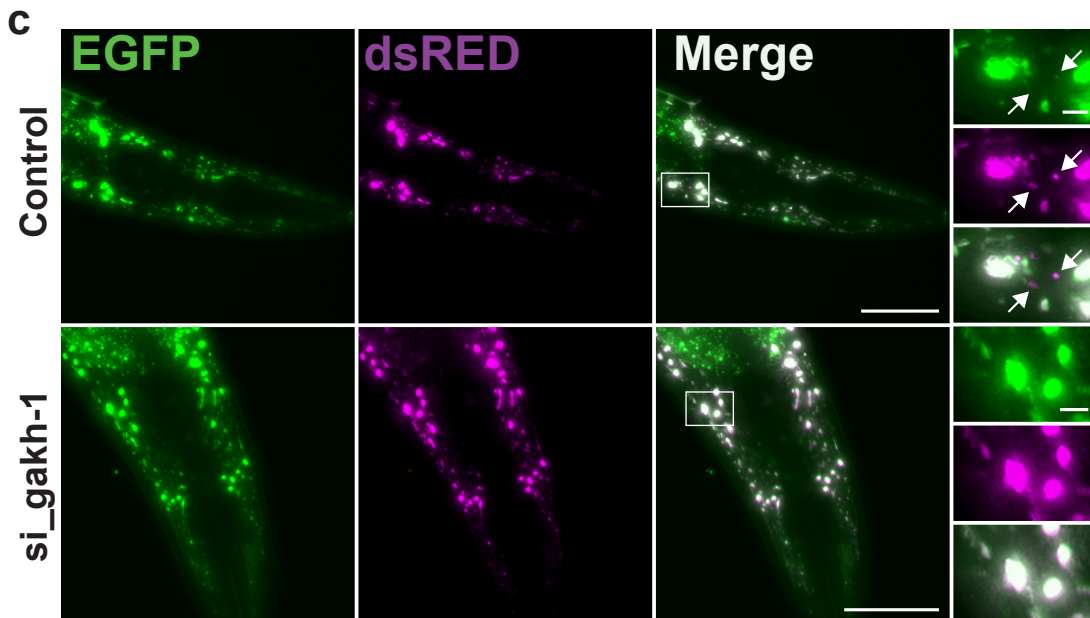
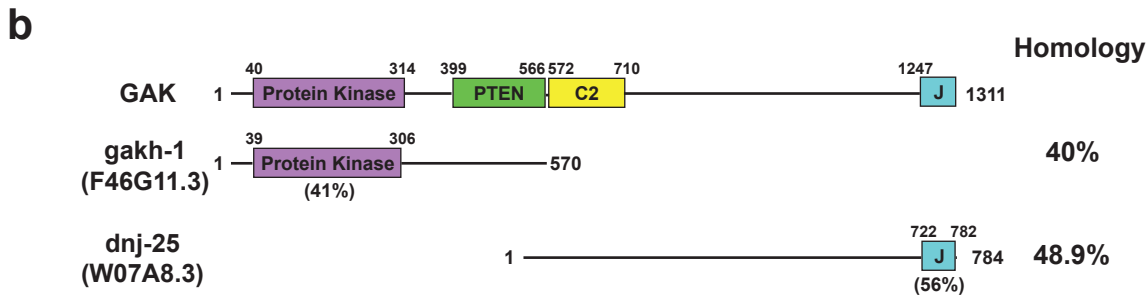
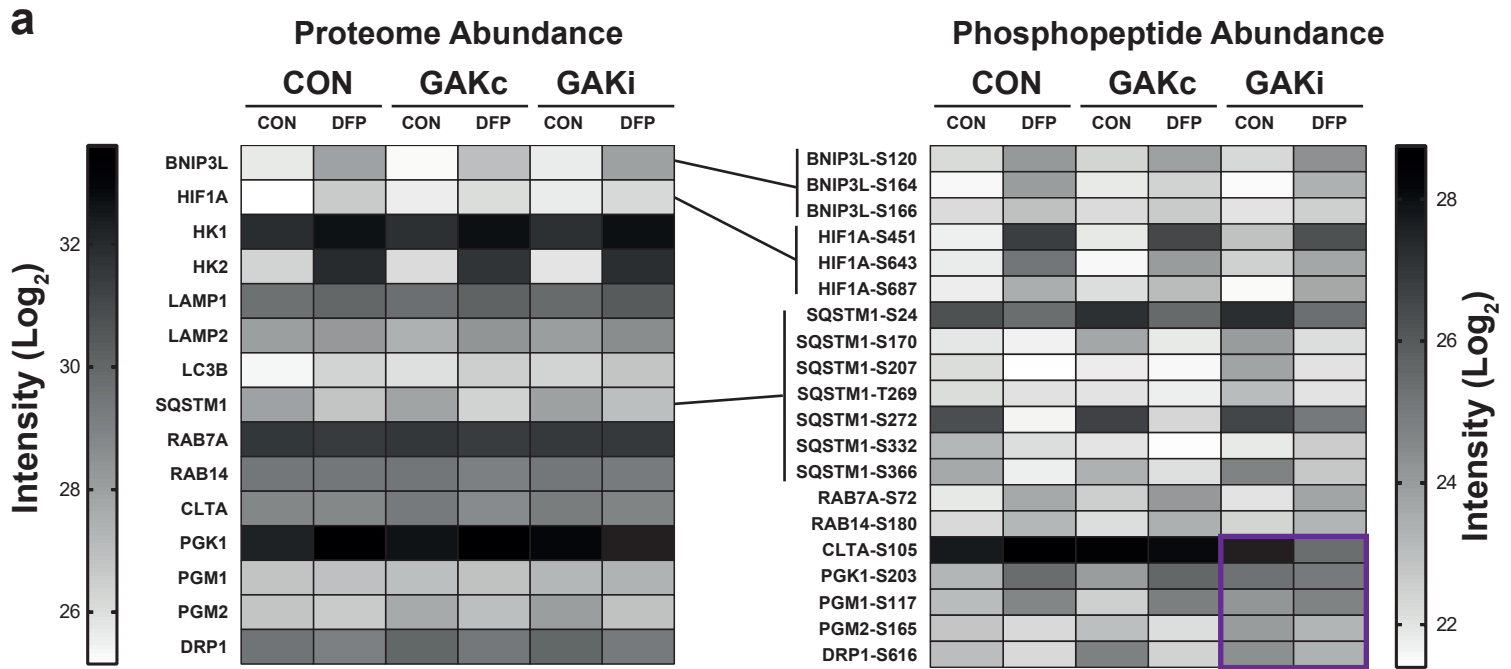


## Figure 8 – gakh-1 regulates mitophagy in vivo

**a** Mass spectrometry of DFP and GAKi regulated proteins/phospho-peptides. U2OS cells were treated  $\pm$  1 mM DFP for 24 h in combination with DMSO vehicle, GAKi or GAKc (both 10  $\mu$ M). Cell pellets were collected and split between proteome and phospho-peptide analysis (see methods). Data represents average intensity from n=2 independent experiments. **b** Schematic representation of GAK domain structure and orthologues gakh-1 and dnj-25 present in *C.elegans*. Homology values were obtained by protein blast alignment. **c** In vivo detection of mitophagy in *C. elegans*. Transgenic nematodes expressing mtRosella in bodywall muscle cells were treated with gakh-1 RNAi or pL4440 control vector. dsRED only structures represent mitochondria in acidic compartments (arrowheads). Scale bar = 50  $\mu$ m, inset = 5  $\mu$ m. **d** Mitophagy stimulation signified by the ratio between pH-sensitive GFP to pH insensitive dsREd (n= 25, upper panel). Quantification of the frequency of mitochondria undergoing mitophagy (dsREd puncta lacking EGFP co-localisation) are expressed as percentage of total mitochondria detected (n= 25, lower panel). The data is presented as violin plots of individual values with median (red, solid line) and quartiles (red, dashed line) shown. Significance was determined by unpaired two tailed t-test from n=2 independent experiments, where \*\*\* =  $p < 0.001$  or \*\*\*\* =  $p < 0.0001$ .

# Figure 9

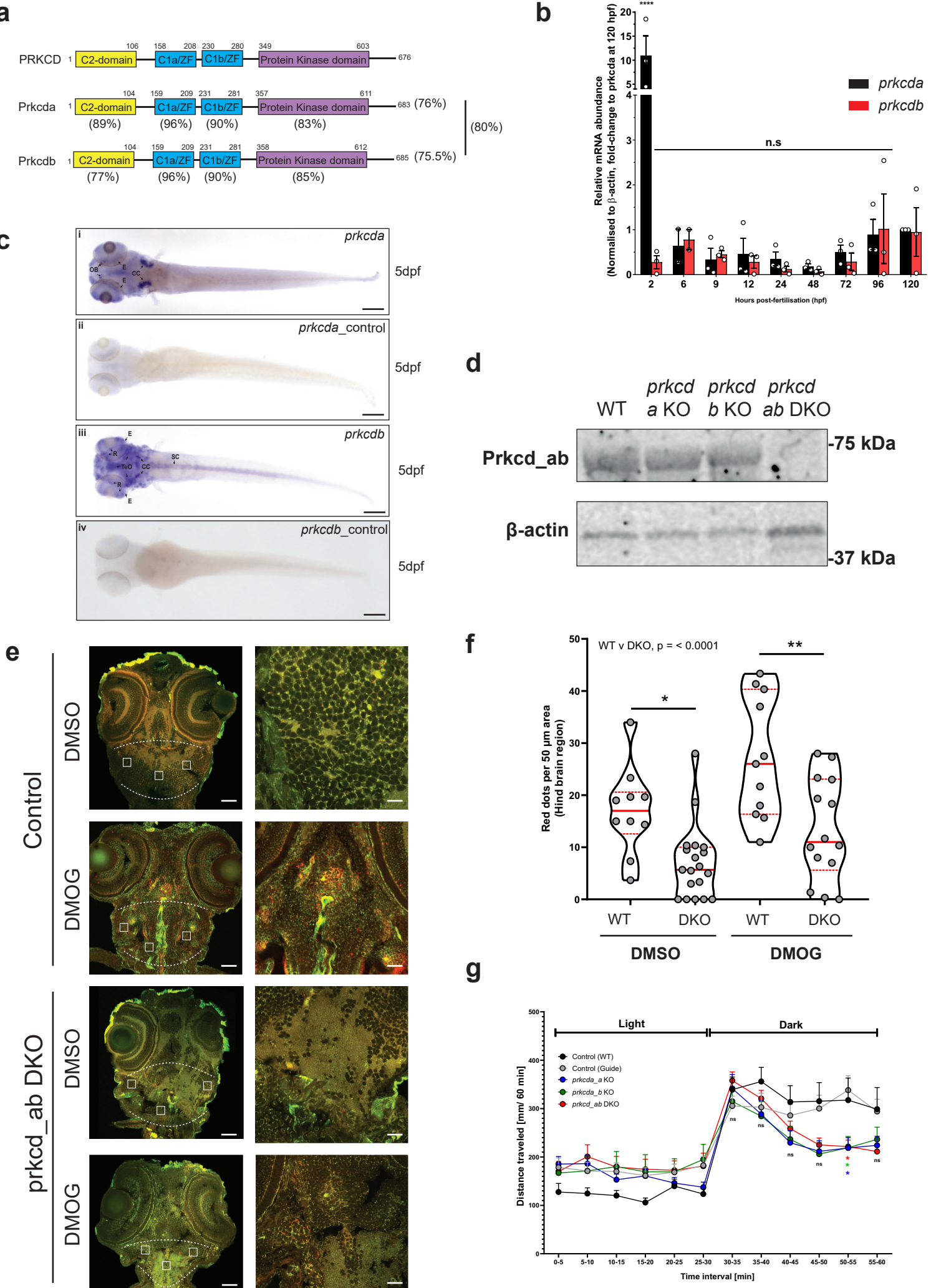


## Figure 9 – prkcda and prkcdb regulate mitophagy in vivo

**a** Overview and schematic diagram of human PRKCD, zebrafish prkcda and prkcdb proteins. Percentage identity of respective domains on comparison with human counterpart shown below the zebrafish domains. Also shown is the percentage identity of the protein amongst each other. **b** Temporal expression pattern of prkcda and prkcdb. The graph shows the mean relative transcript abundance in whole zebrafish embryos from 2 hpf to 5 dpf from n=2 (6 hpf) or n=3 (all others) independent experiments **c** Spatial expression pattern of prkcda and prkcdb at 5 dpf as demonstrated by whole mount in situ hybridisation at the indicated stage using a 5'UTR probe. Both the larvae are in dorsal view. Scale bar = 200  $\mu$  m. **d** Representative immunoblots of Prkcd and  $\beta$ -actin on whole embryo lysates from wild-type and single or double prkcda/prkcdb KO (DKO) animals. **e** Representative confocal images of cryosections taken from control (guide only) and prkcd\_ab DKO transgenic tandem-tagged mitofish larvae treated with DMSO only or with DMOG at 3 dpf. Images are from the hind brain region of the respective larvae as marked. Scale bars = 50  $\mu$ m (left), 20  $\mu$ m (right). **f** The graph shows the average number of red puncta from three 50  $\mu$ m hind brain region (as marked in e) from each of 10-19 larvae for control and prkcd\_ab DKO tandem-tagged mitofish larvae. Significance was determined by two-way ANOVA followed by Tukey's post-test to compare all groups. **g** Motility analysis of zebrafish embryos at 5 dpf using the "ZebraBox" automated videotracker (Viewpoint). Assay was carried out during daytime, and consisted of one cycle of 30 min exposure to light followed by 30 min of darkness. Data represents mean distance moved  $\pm$  SEM. Each group consisted of 43-124 larvae from n= 9 independent experiments. Significance was determined by two-way ANOVA followed by Dunnett's post-test to the Control (WT). Significance are denoted where \*p < 0.05, \*\*p < 0.01, \*\*\*p < 0.001, \*\*\*\*p < 0.0001, n.s = not significant.